Lehrstuhl für Steuerungs- und Regelungstechnik
Technische Universität München
Univ.-Prof. Dr.-Ing./Univ. Tokio Martin Buss

Haptic Telepresence in Packet Switched Communication Networks

Sandra Hirche

Vollständiger Abdruck der von der Fakultät für Elektrotechnik und Informationstechnik der Technischen Universität München zur Erlangung des akademischen Grades eines

Doktor-Ingenieurs (Dr.-Ing.)

genehmigten Dissertation.

Vorsitzende:	Univ.-Prof. Dr.rer.nat Doris Schmitt-Landsiedel
Prüfer der Dissertation:	
1.	Univ.-Prof. Dr.-Ing./Univ. Tokio Martin Buss
2.	Univ.-Prof. Dr.-Ing. Dirk Abel Rheinisch-Westfälische Technische Hochschule Aachen

Die Dissertation wurde am 04.05.2005 bei der Technischen Universität München eingereicht und durch die Fakultät für Elektrotechnik und Informationstechnik am 30.06.2005 angenommen.

Preface

This thesis has emerged from three years of work at two different labs. The preliminaries have been established between 2002 and 2003 at the Control Systems Group, Technische Universität Berlin. Following the change of affiliation of my doctoral advisor Prof. Martin Buss I have found a very creative, intensive and fruitful working environment at the Institute of Automatic Control Engineering, Technische Universität München where I stayed from 2003 until now.

First of all, I would like to thank my doctoral advisor Prof. Martin Buss, you have been a deep source of inspiration and of indispensable help in the numerous discussions we had. Your ideas and general advice along with the freedom of research you have given to me are invaluable.

I am grateful to my colleague and friend Kolja Kühnlenz (LSR, TU München), I never want to miss our fruit- and joyful discussions. I want to thank Peter Hinterseer (LKN, TU München) and Bartlomiej Stanczyk (LSR, TU München) for our great collaboration, and of course all my other team mates at our Institute. To all my students, Katharina Klank, Andrea Bauer, Martin Kuschel, Philipp Kremer, Chih-Chung Chen, and Robert Schuster, I thank you very much for your dedication and the fruitful cooperation.

In deep gratitude I want to thank my parents, for all your patience and encouragement, for your deep love. Very special thanks to my brother and all my friends for your empathy and enduring support.

Munich, 2005. Sandra Hirche

my parents

...

Abstract

Multi-modal telepresence systems allow the human to be present and to actively perform complex manipulation tasks in remote environments without physically being there. Application areas reach from tele-surgery over tele-maintenance and tele-manufacturing to tele-edutainment applications. The haptic feedback system, as part of the multi-modal telepresence system, enables the haptic (motion and force) coupling between the human, in contact with the human system interface, and the robot (teleoperator), which interacts with the remote environment. The telepresence system is transparent if the human may not distinguish between direct and tele-interaction.

Packet switched communication networks, as e.g. the Internet, are very attractive for the transmission of haptic information between the operator and the teleoperator side. As a result of the haptic coupling a global control loop is closed through the packet switched communication network with the human and the environment being part of it. Without further control measures the intrinsic communication unreliabilities render the haptic telepresence system unstable. Similar challenges arise in the closely related field of networked control systems (NCS), however, in haptic telepresence systems extended stabilization methods are required due to the largely unknown human/environment dynamics. Human factors play a major role in the evaluation of the control performance in terms of transparency.

This thesis focuses on stability and transparency of haptic telepresence systems in packet switched communication networks. So far unique is the methodical approach that conjointly considers control theoretic, communication related, and human haptic perception aspects. Based on the passivity framework methods to stabilize the system with time delay and packet loss are developed and systematically analyzed. The emphasis lies on the passive reconstruction of lost packets. With regard to the limited communication resources in packet switched communication networks the reduction of network traffic in haptic telepresence systems without impairing transparency is addressed by a novel approach based on deadband control. Exploiting the Quality-of-Service (QoS) concept, well-known in the network community, a very innovative approach targeting the simultaneous control of the haptic telepresence system and the QoS communication network is considered. This QoS control is studied and discussed here for the first time. The transparency for all the considered control approaches is evaluated by a novel transparency measure taking human haptic perception into account. The obtained results are validated in experiments. Further insights with focus on human factors are gained in experimental user studies.

Zusammenfassung

Multi-modale Telepräsenzsysteme ermöglichen dem Menschen die Anwesenheit und das Ausführen von komplexen Manipulationsaufgaben in entfernten Umgebungen ohne physikalisch vor Ort zu sein. Die vielfältigen Anwendungsmöglichkeiten derartiger Systeme erstrecken sich von der Tele-Chirurgie, über Tele-Wartung und Produktion, bis hin zur Tele-Lehre und Unterhaltung. Durch das haptische (kraftrückkoppelnde) Teilsystem werden dem Menschen Berührungseindrücke der enfernten Umgebung über die Mensch-System-Schnittstelle vermittelt. Gleichzeitig vermag er mittels des entfernten Roboters (Teleoperator) aktiv mit der Umgebung zu interagieren. Wenn der Mensch nicht mehr zwischen der direkten und der Tele-Interaktion mit einer Umgebung unterscheiden kann, dann ist das haptische Telepräsenzsystem transparent.

Paketvermittelnde Kommunikationsnetze, wie z.B. das Internet, sind äußerst attraktiv für die Übermittlung haptischer Information zwischen der Bedienstation und dem Teleoperator. Der globale Regelkreis, welcher den Menschen und die enfernte Umgebung als Teilsystem beinhaltet, wird über das Kommunikationsnetzwerk geschlossen. Ohne weitere regelungstechnische Maßnahmen destabilizieren die inhärenten Kommunikationsunsicherheiten das Gesamtsystem. Ähnliche Herausforderungen entstehen im Umfeld der bekannten Netzwerkregelsysteme; für haptische Telepräsenzsysteme sind jedoch wegen der weitestgehend unbekannten Dynamik von Mensch und Umgebung erweiterte Analyse- und Synthese-Methoden erforderlich. Im Unterschied zu traditionellen Regelungssystemen spielt das menschliche Empfinden bei der Bewertung der Regelgüte (Transparenz) eine wesentliche Rolle.

Diese Dissertation befasst sich mit grundlegenden Fragen der Stabilität und Transparenz haptischer Telepräsenzsysteme in paketvermittelnden Kommunikationsnetzen. Bisher einzigartig in der Literatur ist die methodische Herangehensweise, bei der regelungstechnische, kommunikationstechnische und wahrnehmungsbezogene Aspekte berücksichtigt werden. Basierend auf dem Passivitätsansatz werden erweiterte Methoden zur Stabilisierung des Systems in der Gegenwart von Zeitverzögerungen und Paketverlusten entwickelt. Durch einen neuartigen Tote-Zone-Regelungsansatz wird eine essentielle Reduktion des Datenverkehrs in haptischen Telepräsenzsystemen erreicht. Äußerst innovativ ist die Idee einer simultanen Regelung von haptischem Telepräsenzsystem und Kommunikationsnetz, ermöglicht durch das aus der Kommunikationstechnik bekannte Quality-of-Service (QoS)-Konzept. Eine derartige QoS-Regelung wird hier zum ersten Mal im Kontext von haptischen Telepräsenzsystemen untersucht und diskutiert. Die Transparenz der entwickelten Regelungsansätze wird durch eine im Rahmen dieser Dissertation entwickelte Transparenz-Analyse-Methode evaluiert, wobei der Schwerpunkt auf der Interpretierbarkeit bezüglich der menschlichen haptischen Wahrnehmung liegt. Sämtliche Ansätze werden in Experimenten und experimentellen Studien mit Testpersonen abschließend bewerted.

Contents

Notations

Abbreviations

DiffServ	Differentiated Services
DoF	Degree of Freedom
HLS	Hold Last Sample
HSI	Human System Interface
IntServ	Integrated Services
IP	Internet Protocol
NCS	Networked Control System
QoS	Quality of Service
QoS/OL	QoS approach - OffLine
QoS/TC	QoS approach - Transparency Control
TCP	Transmission Control Protocol
TO	TeleOperator
UDP	User Datagram Protocol

Conventions

Scalars, Vectors, and Matrices

Scalars are denoted by upper and lower case letters in italic type. *Vectors* are denoted by lower case letters in boldface type, as the vector $\boldsymbol{x}$ is composed of elements x_i. *Matrices* are denoted by upper case letters in boldface type, as the matrix $\boldsymbol{M}$ is composed of elements M_{ij} (i-th row, j-th column).

x	scalar
$\boldsymbol{x}$	vector
$\boldsymbol{X}$	matrix
$f(\cdot)$	scalar function
$\boldsymbol{f}(\cdot)$	vector function
$\dot{\boldsymbol{x}}$, $\ddot{\boldsymbol{x}}$	equivalent to $\frac{\mathrm{d}}{\mathrm{d}t}\boldsymbol{x}$ and $\frac{\mathrm{d}^2}{\mathrm{d}t^2}\boldsymbol{x}$
$\overline{x}$	mean of x

Subscripts and Superscripts

$u_r,\ u_l$	wave variable, referring to right or left
x_{hu}	value x associated with the human operator
x_h	value x associated with the HSI
x_t	value x associated with the teleoperator
x_e	value x associated with the environment
x_c	value x associated with the communication subsystem
x_u	value x associated with the incident wave
x_v	value x associated with the reflected wave
x^d	desired value of x, set value for the control loop
$x_{\max}$	maximum value of x
$x_{\min}$	minimum value of x
x_1	value x associated with the forward communication path
x_2	value x associated with the backward communication path
x^{app}	approximated value of x
x_0	reference value of x

Symbols and Abbreviations

b	wave impedance
$b_{(\cdot)}$	damping coefficient
D_1	communication time delay in the forward path as number of sample intervals
D_2	communication time delay in the backward path as number of sample intervals
Δ	absolute deadband value
Δ_c	constant deadband value
ΔZ	impedance error norm
$E_{(\cdot)}$	energy
E_{store}	storage function
E_{in}	energy balance
$E_{cf,in}$	energy balance of the communication forward path
$E_{bf,in}$	energy balance of the communication backward path
$E\{\cdot\}$	expected value of a stochastic quantity
e_x	position error
E_x	integrated squared position error
ε	relative deadband value
f	force
k	independent variable in discrete time
k^*	sampling instance when most recent packet was received
$k_{(\cdot)}$	stiffness coefficient
l	packet loss indicator
$m_{(\cdot)}$	mass
ω	frequency
Ω	event indicator 'packet sent'
P	power
P_{diss}	dissipated power
$\boldsymbol{p}$	mechanical parameters of impedance
P_l	packet loss probability
Φ	phase
R	reflection factor
s	independent variable in Laplace domain
S	scattering operator
t	time. independent variable in time domain
T	roundtrip communication time delay
T_1	communication time delay in the forward path
T_2	communication time delay in the backward path
T_A	sampling time interval
u	wave variable, incident wave
v	wave variable, reflected wave
$\boldsymbol{x}$	position
$\dot{\boldsymbol{x}}$	velocity
$\ddot{\boldsymbol{x}}$	acceleration
Z	mechanical impedance
ζ	data reconstruction operator

List of Figures

List of Tables

1 Introduction

Telepresence ("teleoperation") is the extension of a person's sensing and manipulation capability to a remote location.

Sheridan, 1989

In order to locate the fictional origin of the concept of telepresence, one may look at Robert Heinlein's short novel "Waldo," [47] written in 1942. He tells the tale of Waldo F. Jones, a genius who suffered from a disabling disease and who built for himself a zero-gravity home in orbit around Earth. Using his impotent muscles without the constraints of gravity he developed hardware ("waldoes") that allowed him to perform teleoperations on Earth. He built waldoes with robotic hands of different sizes, from half an inch to several feet across their palms, which responded to the command of his arms and fingers. "The same change in circuits which brought another size of waldoes under control automatically accomplished the change in sweep of scanning to increase or decrease the magnification, so that Waldo always saw before him in his stereo receiver a "life-size" image of his other hands."

With nowadays technology this fictional concept has become reality in the form of telepresence systems. Today's telepresence systems allow the interaction with environments at a distance and can also scale human force and motion to achieve stronger, bigger, or smaller telepresence. Inaccessible, too dangerous or scaled environments become accessible to the human. Applications range from classical nuclear/toxic/explosive material handling and disposal [76], space exploration [59, 115, 130], rescue applications in dangerous environments [57], minimally invasive surgery [41], tele-nanorobotics [131] to training, education [18], and entertainment applications, see also [23] for an overview.

The user of a telepresence system is able to interact with remote objects or humans and to execute tasks without being there [128]. In order to make the user *feel* like being there, the telepresence system provides the user with the multi-modal sensor information on the remote enviroment. At the same time the user may multi-modally interact with the remote object by a robotic system. Multi-modal refers to the perceptual modalities of human beings, such as the visual, the auditory, and the haptic modality. Haptics, as an extension to classical multimedia, refers to the feeling of force, motion, and vibration and is accordingly divided into the kinesthetic, the proprioreceptive, and the tactile submodality. In the following, haptics is refered to as the kinesthetic and proprioreceptive submodalities.

A typical multi-modal telepresence system architecture is depicted in Fig. 1.1. The human operator, equipped with a headmounted display and headphones, manipulates a human system interface (HSI), a robot equipped with motion and force sensors, and thereby commands the remote executing robot, the teleoperator. While the teleoperator interacts with the remote environment, the multi-modal sensor data are fed back and displayed to the operator. A communication network realizes the transmission of the command and sensor signals between the operator and the teleoperator side.

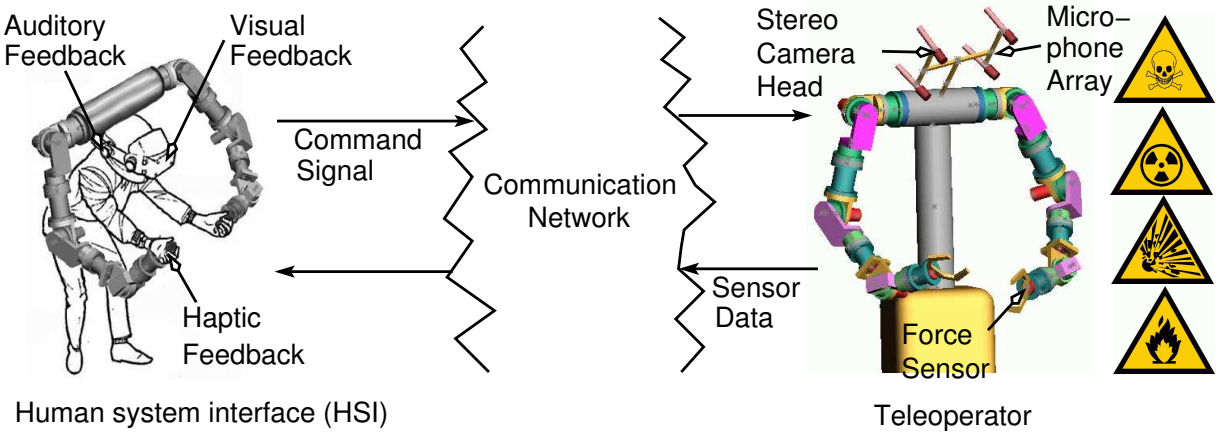

Figure 1.1: Multi-modal telepresence system.

Remark 1.1 The terms of telepresence, teleoperation, telemanipulation, and telerobotics are generally used in an interchangeable manner in the engineering community, however, they have a slightly different flavor. While the latter ones clearly set their emphasis on the technological aspects, telepresence [96], as we will call it throughout this thesis, additionally brings in the human factor.

Haptic feedback, which is in the focus of interest in this thesis, is recognized to be an indispensable part of telepresence systems. It provides the operator with more complete information and increases the sense of being present in the remote environment, thereby, improving the ability to perform complex tasks [129]. Even if there is a significant time delay of up to one second due to communication between operator action and the corresponding haptic feedback, it is beneficial for the task completion [59, 80].

The haptic feedback system is highly challenging from the control point of view. Through the command and feedback signals energy is exchanged between the HSI and the teleoperator, thereby, closing a global control loop through the communication network. Naturally, the transmission of the signals is afflicted with time delay. Without further control measures the telepresence system is unstable [36] resulting in a severe hazard for the human and the environment.

In the late 90's, researchers started to consider the Internet as a communication channel for telepresence systems. In fact, the Internet is the most attractive communication medium as it provides low cost, easy access, worldwide coverage and high flexibility. However, it introduces further destablizing effects such as time-varying time delay and in most cases the possibility of data loss. Therefore early tele-applications did not consider force feedback [39]; most currently realized experiments work on a tele-programming level and supervisory control. There is an enormous demand and potential for control architectures, that allow bilateral haptic telepresence in packet switched networks, the general class of networks the Internet also belongs to. The main challenges faced by the control design of haptic telepresence systems in packet switched networks are summarized in the following.

1.1 Challenges

The control design for telepresence systems faces multiple interdisciplinary challenges in the intersection of the fields robot control, human-machine interaction, and communication systems. Some of the key issues targeted in this thesis are summarized as follows:

Control Issues
A haptic telepresence system can be considered a robotic system consisting basically of the HSI and the teleoperator. Through the command and feedback signals, energy is exchanged between the HSI and the teleoperator, thereby, closing a global control loop. The human, which is in contact with the HSI, and the environment manipulated by the teleoperator are also part of this control loop. Naturally, stability is a major issue for the development of the control design. For the stability analysis and the control design not only the robots (typically multi-degree-of-freedom with non-linear dynamics) but also the largely unknown dynamics of the human operator and the environment have to be considered. If a packet switched communication network is utilized for the transmission of the command and feedback signals, this control loop is affected by unpredictable time-varying time delay and other communication unreliabilities such as packet loss. It is well-known that already constant time delay destabilizes a closed loop system. In summary, the stabilization requires sophisticated approaches beyond the traditional control methods accounting for these difficulties.

Human related Issues
The human is the 'supervising' component in the telepresence system. His/her subjective feeling of presence and interaction with the remote environment is essential for the evaluation of the performance. Ideally, he/she should feel directly interacting with the remote environment; the telepresence system is then called transparent. However, generally a trade-off between (robust) stability and transparency must be made in the control design. Human perception and action characteristics can be used to find this trade-off in a human perception/action appropriate sense. Clearly, traditional performance evaluation methods fail here.

Communication related Issues
The packet switched communication network, part of the global control loop in the haptic telepresence system, introduces destabilizing effects such as time-varying delay and data loss. Due to the complexity of packet switched communication networks, such as e.g. the Internet, these effects are difficult to model. In fact, they are unpredictable in general. Additionally, communication constraints in terms of data rate limitations further complicate the telepresence system control design. Lately developed communication architectures with Quality-of-Service incorporate enhanced real time capabilities and allow the control of the communication network. The simultaneous control of the telepresence system and the communication network is a very innovative research direction that requires the development of novel control methodologies.

1.2 Main Contributions and Outline of the Thesis

The presented work focuses on the design of stable and transparent control for haptic telepresence systems in packet switched communication networks. An important issue

is the consideration of human perception characteristics for the performance evaluation of the considered control approaches. In the sequel of the thesis the integration of the communication network into the control concept rises with each chapter. In each individual chapter the developed methods are evaluated using transparency measures, that allow a human perception oriented interpretation. The experimental validation in hardware environments comprises objective and subjective (in terms of experimental user studies) elements. With the pervading focus on the control design, these two orthogonal research aspects, the communication and the human oriented design, give the structure to this thesis, as highlighted in Fig. 1.2. The combined consideration of control theoretic, communication related, and human oriented aspects for haptic telepresence systems, not yet performed in this depth in the known literature, is a source of inspiration for the development of novel concepts and the revelation of new insights on telepresence system control design. The main contributions of this work together with an outline are presented in the following. Supplementary information, especially videos and publications, can be found on the author's web page[1].

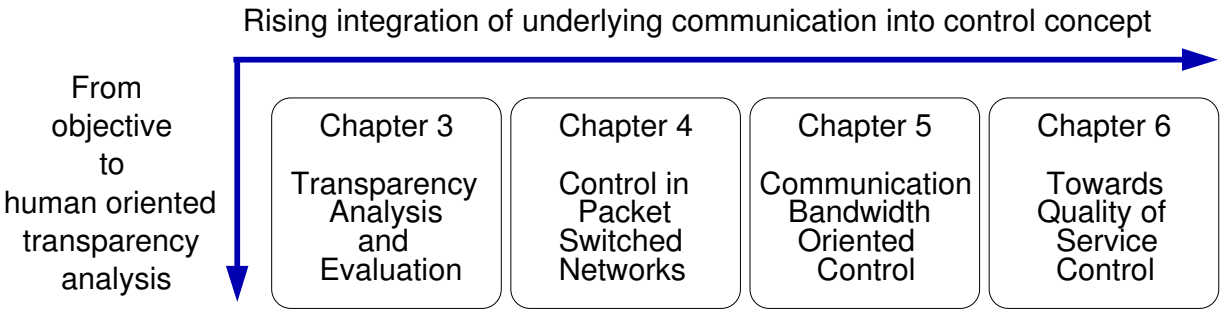

Figure 1.2: Outline of the thesis.

Human Oriented Evaluation

It is well-known *that* unreliabilities in the communication subsystem of a haptic telepresence system deteriorate the realistic impression of the remote environment. The important question to answer is *how* this degradation is *perceived by the human* in order to determine the limits of sensitive tele-applications. Therefore, a transparency measure is introduced in Chapter 3 based on arguments of psychophysical studies on human haptic perception. Due to the complexity of telepresence systems and the stochastic nature of the communication unreliabilities, an analytical description of their impact on transparency is often difficult to obtain. In Chapter 3 two novel transparency analysis tools are developed, an analytical and an optimization based numerical approach. Using these tools an extensive transparency analysis is performed for haptic telepresence systems with *constant delay*. The results are validated in objective experiments and experimental user studies. In fact, the developed optimization based tool is not only well suited for the transparency analysis, but also for the optimal design of transparent, so-called impedance matched, control architectures as discussed in Appendix A.

[1] `http://www.lsr.ei.tum.de/~hirche` or `http://shirche.de`

Communication Oriented Control

Communication over packet switched networks introduces destabilizing effects into the closed control loop, such as *time-varying time delay* and *loss of data*. Only a few researchers considered the implicitely arising challenges for the stabilization of telepresence systems under these circumstances; a transparency analysis is not reported in the known presented literature. In Chapter 4 a systematic consideration of haptic telepresence in packet switched networks is presented. The focus is on reconstruction of lost data and data that due to time-varying delay arrive too late. Stability conditions provide a general framework for the design of data reconstruction strategies. The few existing approaches are classified therein, and novel strategies are introduced. With the transparency evaluation tool developed in Chapter 3 a transparency analysis is carried out and validated in objective experiments and experimental user studies.

Another challenge associated with haptic telepresence in unreliable communication environments is the position tracking of the HSI and teleoperator, which is not guaranteed for the standard control architectures based on the communication of velocity and force signals. A novel position feedforward control architecture to achieve position transparency is introduced in Appendix A.

A packet switched network as a shared medium of multiple users has limited communication resources. No approach is reported in the known literature that considers data rate constraints in haptic telepresence systems. Driven by well-known human perception limits an innovative deadband control approach is proposed in Chapter 5 targeting this challenge. As a result a substantial *network traffic reduction of up to 95%* is achieved *without impairing transparency*. In order to guarantee stability, novel reconstruction strategies are developed using the framework of stability conditions from Chapter 4. The combined performance in terms of transparency and network cost associated with induced traffic is evaluated in simulations and experiments. Experimental user studies are conducted to validate the deadband control approach.

Novel impulses for further development of haptic telepresence systems control architectures are gained by the lately emerging Quality-of-Service (QoS) communication architectures that allow the control of the communication network. A novel concept for the simultaneous control of the haptic telepresence system and the QoS communication network, not yet considered in the known literature, is studied in Chapter 6. Two different control architectures are introduced and compared with respect to their benefits in simulation. Open problems, expected to direct future research in this area of QoS control as well as the ongoing research on QoS network architectures are discussed.

Generalization of the Methods

Looking at the closed loop structure of a haptic telepresence system its strong relation to the general class of networked control systems (NCS), see [145, 155] for an overview, becomes evident. The human together with the HSI can be interpreted as the controller, while the teleoperator together with the environment act as the plant. The controller and the plant are connected over a communication network, being exactly the definition of a NCS. In fact, due to the known (or assumed to be known) dynamics of controller and plant in most NCS, they can be interpreted as a special class of networked telepresence systems.

In consequence, the control methods developed for haptic telepresence systems have a very general character paving the way for novel NCS control methods potentially relaxing model assumptions. First results [92] indicate that haptic telepresence system control methods can be generalized to networked control systems opening very new aspects especially for robust control.

2 State-of-the-Art Control and Evaluation Methods

In recent years, the Internet has given a big impulse for the promotion of existing and the development of novel tele-applications. This is mainly due to the development of the Internet towards real-time capability resulting from the extensive propagation of multimedia applications, such as voice-over-IP [95] and video-conferencing. Nevertheless, in its current state the Internet communication characteristics pose numerous challenges for the deployment of control applications over such networks.

The main challenges from a control theoretic point of view are the communication unreliabilities, such as time-varying delay, packet loss, or even the complete loss of the connection. It is well-known that without appropriate control measures already constant time delay in a closed loop causes instability. While control theory for linear systems with constant time delay is well developed, the research on general time-varying delay systems is still ongoing; only few reserachers have considered systems with loss of data. Current research mainly focuses on networked control systems (NCS), i.e. control systems with the loop closed over a communication network. Most approaches, see [145, 155] for an overview, rely on strong assumptions for controller and plant model, and they cannot directly be carried over to networked telepresence systems. This is mainly due to the largely unknown dynamics of the human and the environment that are part of the closed loop telepresence system. Consequently, extended methods for the analysis and synthesis of telepresence over packet switched communication networks are required. This statement not only holds for the stability property but also for the performance evaluation.

In telepresence systems performance metrics from NCS such as tracking errors are applicable to some extent only; the main factor in performance evaluation is the human 'feeling'. Accordingly, performance measures are necessary that take human perception into account.

This chapter introduces the general control architecture of haptic telepresence systems along with the notations used in the sequel of this thesis. State-of-the-art telepresence control architectures are reviewed with the focus on stabilizing control architectures for time-varying delay and packet loss. Finally, state-of-the-art performance evaluation measures and methods are introduced and discussed.

2.1 System Architecture

In a haptic telepresence system the operator interacts with a force feedback capable interface, the human system interface (HSI), and thereby commands the executing robot, the teleoperator, to follow the desired trajectory. The teleoperator interacts with the remote environment, the haptic sensory data (motion, force) are fed back and displayed to the operator on the HSI. As the haptic information flows in both directions this scheme is called bilateral; it is the type of haptic telepresence considered in this thesis.

Telepresence System Components

The basic components, interconnected as depicted in Fig. 2.1, are described in the following with respect to their functionality, the assumed dynamic models, and notations:

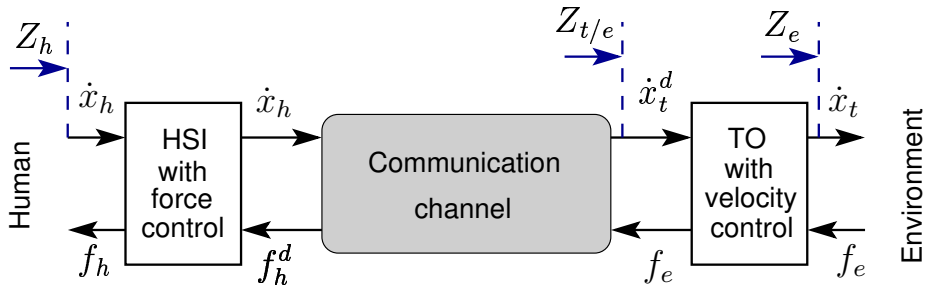

Figure 2.1: Haptic telepresence system with velocity/force architecture.

- Human operator - manipulates the HSI and perceives the force information from the remote environment via this interface. He/she moves his/her arm holding on to the HSI with the velocity $\dot{x}_h$ and applies the force f_h. The human's dynamics is largely unknown as it depends on intentional and physiological aspects [60], and varies from operator to operator.

- HSI - also called haptic display or master manipulator, is a robot used to display the environment interaction force. An appropriately chosen local controller assures that the HSI follows the desired trajectory, for instance the desired force f_h^d, received from the teleoperator. Non-linearities are assumed to be compensated by a feedback linearization. As the impact of communication is of main interest, in the following for simplicity a 1DoF mass-damper-system is assumed

$$m_h \ddot{x}_h + b_h \dot{x}_h = \tau_h + f_h, \tag{2.1}$$

with the mass m_h, the damping b_h, and τ_h the motor torque as the control input from the controller. The human holds on to the HSI, such that the velocities of the HSI and the human are equal, denoted by $\dot{x}_h$. The force f_h measured at the HSI is equal to the force applied by the human. The mechanical impedance, the mapping from velocity to force, is used to describe the perceived dynamics by the human

$$f_h = Z_h(\dot{x}_h). \tag{2.2}$$

Assuming a time-invariant, linear or linearized dynamics the impedance can also be described in the Laplace domain by the transfer function

$$Z_h(s) = \frac{f_h(s)}{v_h(s)}, \tag{2.3}$$

where $v_h(s)$ represents the velocity of the HSI in the Laplace domain ($\dot{x}_h$ in time domain).

- Communication channel - performs the transmission of the motion and force information between the operator and the teleoperator side and thereby induces a constant or time-varying delay, possibly packet loss. Specific details on the characteristics are introduced in the corresponding chapters.

- Teleoperator - is the executing robot that interacts with the environment. By appropriate local control it follows the desired trajectory, for instance the desired velocity $\dot{x}_t^d$, received from the HSI. Non-linearities are assumed to be compensated by feedback linearization. In the most general case the teleoperator has a different kinematics than the HSI. Again for simplicity a similar kinematics as the HSI, a mass-damper-system

$$m_t\ddot{x} + b_t\dot{x}_t = \tau_t - f_e, \tag{2.4}$$

  is assumed with the mass m_t, the damping b_t, and τ_t the motor torque as the control input from the controller, f_e represents the force resulting from interaction with the environment.

- Remote environment - is composed of various objects the human manipulates by means of the teleoperator. Typically, no a priori knowledge exists about the environment (unstructured); in some applications at least some knowledge about the environment is available (structured). In this thesis unstructured environments are assumed. Further, it is mostly assumed that the teleoperator is in contact with the environment, such that the positions of the teleoperator and the environment are equal $x_t = x_e$ as well as the measured force and the environment force. The environment dynamics is assumed to be approximately linear, the mechanical environment impedance is defined by

$$Z_e(s) = \frac{f_e(s)}{v_e(s)},$$

  where $v_e(s)$ represents the Laplace transformed of the environment/teleoperator velocity $\dot{x}_e$. The impedance $Z_{t/e}$ describing the dynamics of the controlled teleoperator with the environment together is also assumed to be approximately linear, its transfer function is represented by

$$Z_{t/e}(s) = \frac{f_e(s)}{v_t^d(s)}, \tag{2.5}$$

  where $v_t^d(s)$ represents the Laplace transformed of the desired teleoperator velocity $\dot{x}_t^d$.

Closed Control Loop

Interpreting the haptic telepresence system as a traditional control loop, see Fig. 2.1, the human together with the HSI act as the controller, the teleoperator together with the remote environment as the plant. The controller and plant are seperated by a communication network showing the close relation to NCS. Compared to traditional control loops the main challenges in the control design are:

- Both, the controller and the plant are largely unknown.

- The control goal, defined by the task related human intention, is largely unknown.

Considering a packet switched communication network for the data transmission the global closed loop is afflicted by communication unreliabilities such as time-varying delay and packet loss. Without appropriate control measures the system is unstable. Sophisticated control methods are required to stabilize the networked haptic telepresence system. Due to the previously mentioned differences the control methods for NCS, see e.g. [145, 150, 155], cannot directly be carried over to telepresence systems. Vice versa, developed telepresence systems control approaches hold great promise for the application in NCS, as we have preliminarily shown in [92].

Besides stability, which is the fundamental requirement for every control system, transparency is the principal goal in telepresence system control design. Transparency is achieved, if the human feels directly interacting with the remote environment [118].

In the following state-of-the-art summary haptic telepresence systems control methods to cope with constant time delay and recently also with time-varying time delay and packet loss are reviewed with respect to their applicability conditions and transparency.

2.2 Control Methods

The instability of haptic telepresence systems in presence of communication delay has been shown in [36]. In recent years several methods to stabilize haptic telepresence systems with *constant* time delay have been presented, for an overview on the control challenges and a survey on current approaches see [20, 23, 35, 122], and [3, 4] for a comparison of control schemes. The control architectures can be categorized based on the number and the type of signals transmitted between the operator and the teleoperator side.

Early approaches consider a position/force architecture [36, 37], where the position is sent to the teleoperator, the environment force is transmitted back to the HSI. This approach is extended to improve the contact stability by position error based force feedback [33, 70] and compliance control at the teleoperator [69, 71]. In four channel architectures, see [81] for the generic definition, velocity and force information is transmitted in both directions. Ideal transparency is achieved by dynamic filters [44], but only for zero delay. By proper definition of the control parameters this control scheme can be simplified to a three channel architecture [44]. In order to cope with the changing environment dynamics, adaptive schemes are considered in [84, 163, 164], based on a position/force four channel architecture. A robust control based scheme using μ-synthesis is reported in [86].Variable structure control with an impedance controller at the HSI, and a sliding mode controller to obtain robust stability is applied in [114].

The underlying general control principle of most mentioned approaches can be stated as follows: by appropriate control design the gain of the open loop system is adopted, such that with the delay induced phase lag the stability margins are still preserved, i.e. stability with time delay can only be achieved when the bandwidth of the closed loop system is severely reduced [149]. The considered approaches have to assume a maximum time delay; some even assume bounded environment parameters or bounds on the deviation from a nominal environment model.

However, in packet switched communication networks the assumption of a bound on the delay is not reasonable. Limiting the range of possible environments is not desired. Further, the design rules of most approaches are frequency domain based making the consideration of time-varying time delay and packet loss difficult. Clearly, the reviewed

approaches are not appropriate for the analysis and synthesis of telepresence systems over packet switched communication networks.

The well-known passivity paradigm [34] has the potential to target these challenges. From current approaches it is the most powerful concept in telepresence systems analysis and synthesis. Being the underlying approach in this thesis, it is discussed in detail in the following.

2.2.1 Passivity based Approach

The passivity formalism represents a mathematical description of the intuitive physical concepts of power and energy, see [34, 68, 132, 148] for a compendium, and is related to the more general framework of dissipative systems [157]. It provides a simple, robust, and powerful tool to analyze the stability of a system, solely based on input-output properties, hence without the exact knowledge of the system model. Passivity is well suited for application in linear or non-linear, time-invariant or time-varying, continuous or discrete time, and distributed systems. These generalities make passivity approaches very valuable for haptic telepresence systems analysis and synthesis.

Background: Passive Systems

Intuitively, a system is passive if it absorbs more energy than it produces. To formalize this, define the power input P_{in} (also referred to as power balance), which is positive when entering the system, as the scalar product between the input vector $\boldsymbol{f}$ and the output vector $\dot{\boldsymbol{x}}$

$$P_{in} = \dot{\boldsymbol{x}}^T \boldsymbol{f}. \tag{2.6}$$

Note, that this power does not necessarily correspond to physical power. The input power should either be stored or dissipated in the system. Define a lower bounded energy storage function $E_{\text{store}} \geq E_{min}$ and a non-negative power dissipation function $P_{\text{diss}} \geq 0$. Without loss of generality we may set $E_{min} = 0$ as the energy storage can always be shifted by an additive constant. A system is passive, if it obeys

$$P_{in} = \frac{\mathrm{d}}{\mathrm{d}t} E_{\text{store}} + P_{\text{diss}}.$$

The system is called strictly passive if $P_{\text{diss}} > 0$, and energetically lossless if $P_{\text{diss}} = 0$.

A passive system can not generate energy and provide only as much as initially was stored, as the passivity condition expressed in the integral form shows

$$\int_0^t P_{in}\,\mathrm{d}\tau = E_{\text{store}}(t) - E_{\text{store}}(0) + \int_0^t P_{\text{diss}}\,\mathrm{d}\tau \geq -E_{\text{store}}(0) \quad \forall t > 0,$$

for all admissible inputs $\boldsymbol{f}$ and outputs $\dot{\boldsymbol{x}}$.

Without loss of generality, in the sequel of this thesis it is assumed that zero energy is initially stored $E_{\text{store}}(0) = 0$, the passivity condition is then

$$\int_0^t P_{in}\,\mathrm{d}\tau = E_{in}(t) \geq 0 \quad \forall t > 0, \tag{2.7}$$

with E_{in} representing the energy balance that can easily be computed from the input and output signals.

Generally, the energy storage function E_{store} can be used as a Lyapunov-like function. This becomes evident setting the input $\boldsymbol{f} = 0 \rightarrow P_{in} = 0$ for the autonomous system: the power dissipation function forces a non-positive derivative of E_{store}. Further assuming that all system state variables are represented in the energy storage function, such that bounded energy will also bound all states, passivity implies stability in the sense of Lyapunov.

One of the nicest features of passivity is its ability to connect to passive elements into a passive unit. This occurs if the interconnection is either made in feedback or parallel configuration (or as interconnected n-ports in the network circuit analogon). The resulting total energy storage is the sum of the individual storage functions, the same holds for the power dissipation.

Remark 2.1 As passivity is a system input-output related concept, the passivity property is not invariant to the choice of the output. As an example lets assume a simple mechanical mass-spring-damper system in serial connection excited by an external force, which is the input to the system. The system is passive with respect to the velocity, but not passive with respect to the position.

Passive Haptic Telepresence

The passivity concept has been firstly applied to haptic telepresence systems in [1], and has in the sequel emerged as one of the most preferred tools in haptic telepresence control, for constant and recently also for time-varying delay and packet loss [2, 8, 11, 15, 27, 43, 45, 48–58, 73, 79, 80, 83, 90, 97, 98, 100, 103, 106, 107, 117, 125, 126, 133, 135, 136, 160, 161].

In order to apply the passivity concept to haptic telepresence systems, it is decomposed into the interconnected subsystems human, HSI, communication channel, teleoperator, and environment, as visualized in Fig. 2.1. The human and the environment are represented by one-ports, the HSI, the bilateral communication channel and the teleoperator by two-ports.

Following the stability arguments from [1, 103] the subsystem of interconnected HSI, communication channel and teleoperator has to be passive as well as the environment. Note, that according to [32] the passivity of the system in contact with an arbitrary, passive environment is not only a sufficient, but also a necessary condition for stability. The human operator naturally produces energy to interact with the system, however, the input energy is assumed to be bounded, and the above passivity arguments remain intact. In fact, it has been shown that the human passively interacts [60] with passive environments.

For passivity reasons the appropriately locally controlled HSI and teleoperator exchange the power variables velocity and force [1] (flow and effort in a system theoretic context). The mapping from velocity to force is generally passive, further the local control laws can easily be designed, such that passivity property of HSI and teleoperator is always preserved [1, 2, 103, 107].

The bilateral communication channel can be modeled as a time delaying two-port for constant delay, with the time-delays T_1, T_2 in the forward and the backward path, respectively. It is shown in [1] that the scattering operator S (B.1) of the time-delaying two-port has a singular value larger than one, in fact, the supremum is unbounded. Thereby the passivity condition (B.3) is violated, the two-port is active, i.e. destabilizes the haptic telepresence system.

Passivity for Constant Time Delay by Wave Variable Transformation

The scattering transformation, introduced in [1], and extended in [103, 107] referring to it as wave variable transformation, maps the time delaying two-port on a long, energetically lossless transmission line in an electrodynamical sense. As a result the communication subsystem is passified for arbitrarily large *constant* delays. The wave variable transformation, as it is referred to in the sequel of this thesis, is a bijective transformation. The transformation equations are given by

$$\begin{aligned} u_l &= \frac{f_h^d + b\dot{x}_h}{\sqrt{2b}}\,; & u_r &= \frac{f_e + b\dot{x}_t^d}{\sqrt{2b}}\,; \\ v_l &= \frac{f_h^d - b\dot{x}_h}{\sqrt{2b}}\,; & v_r &= \frac{f_e - b\dot{x}_t^d}{\sqrt{2b}}\,, \end{aligned} \tag{2.8}$$

with the design parameter b, a positive definite matrix or scalar for single degree of freedom systems, representing the wave impedance of the emulated transmission line. No longer the power variables are transmitted over the communication two-port, but the wave variables u_l (forward path) and v_r (backward path), which arrive time delayed at the corresponding receiver

$$u_r(t) = u_l(t - T_1) \qquad v_l(t) = v_r(t - T_2), \tag{2.9}$$

as depicted in Fig. 2.2. Assuming the 1DoF system as described in Section 2.1 and visu-

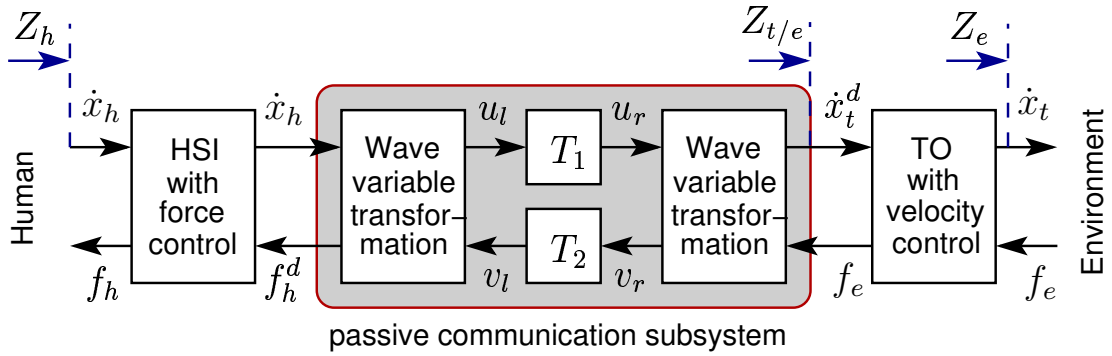

Figure 2.2: Velocity/force haptic telepresence system architecture with the wave variable transformation for passivity of the communication subsystem with constant time delay.

alized in Fig. 2.2 the power input (2.6) into the communication subsystem with the input vector $\boldsymbol{f^T} = [f_h^d \;\; f_e]^T$, and the output vector $\dot{\boldsymbol{x}}^{\boldsymbol{T}} = [\dot{x}_h \;\; -\dot{x}_t^d]^T$ at any point in time is

$$P_{c,in} = \dot{x}_h\, f_h^d - \dot{x}_t^d\, f_e. \tag{2.10}$$

Integrating (2.10) with the power variables substituted by the appropriately reformulated equations from (2.8) yields the energy balance $E_{c,in}(t)$ in the wave domain as

$$E_{c,in}(t) = \int_0^t P_{c,in}(\tau)\,\mathrm{d}\tau = \int_0^t \frac{1}{2}(u_l^2 - u_r^2) + \frac{1}{2}(v_r^2 - v_l^2)\,\mathrm{d}\tau, \tag{2.11}$$

where the time dependency of the wave variables is omitted for the sake of clear notation. By inserting (2.9) and assuming zero initial energy storage $E_{\text{store}}(0) = 0$ the expression (2.11) reduces to

$$E_{c,in}(t) = \frac{1}{2}\int_{t-T_1}^{t} u_l^2 \,\mathrm{d}\tau + \frac{1}{2}\int_{t-T_2}^{t} v_r^2 \,\mathrm{d}\tau \geq 0. \tag{2.12}$$

As both terms under the integrals are positive the passivity condition (2.7) is satisfied. The communication subsystem including the wave variable transformation is passive according to the condition (2.7). In fact, the wave energy in the wave variables u_l and v_r is temporarily stored for the corresponding transit times T_1 and T_2. The communication subsystem is energetically lossless.

Note, that according to the latter equation in (2.11) the energy balance can be separately considered for the forward and the backward path. Passivity of the communication subsystem is guaranteed if

$$E_{cf,in}(t) = \int_0^t (u_l^2 - u_r^2) \,\mathrm{d}\tau \geq 0, \tag{2.13}$$

and

$$E_{cb,in}(t) = \int_0^t (v_r^2 - v_l^2) \,\mathrm{d}\tau \geq 0. \tag{2.14}$$

Remark 2.2 The introduced passivity based approach is also referred to as passive communication approach in the literature [80]. A similar approach embedded into the formal framework of port-Hamiltonian systems leading to an intrinsically passive controlled (IPC) system can be found in [135, 138]. Other passivity related approaches are based upon Llewellyns [89] stability criterion for absolute stability in [45, 117], time domain passivity in [43] and similarily using fictious energy storage elements in [83].

Remark 2.3 In the original approaches [1, 103, 107] the coordinated torque, i.e. the controller output at the teleoperator, is fed back as a measure for the environment interaction force f_e. As a result, though, the operation in free space motion feels 'sluggish'. Here, the directly measured environment interaction force is used as feedback improving the transparency. Without further control measures, there may exist teleoperator/environment configurations showing a non-passive behavior. In Appendix A it is indicated that the passivity can be preserved by approriate low pass filtering in the wave domain, also referred as wave compensators in [103, 107, 143].

Impedance Matching

As the wave variable transformation is a concept originating from network theory, some of the effects well-known in network theory can also be interpreted in the context of haptic telepresence systems.

Looking at the teleoperator side, the wave variables can be interpreted as an incident wave u and the reflected wave v. As well-known from network theory, the reflected wave contains the energy, that is reflected at an impedance discontinuity. This phenomenon - called wave reflection - occurs if the teleoperator/environment impedance $Z_{t/e}$ (2.5) of the remote system is not matched to the wave impedance b of the transmission line, hence a impedance discontinuity appears at the transition from the transmission line to the teleoperator/environment impedance. Wave reflections include the information of the reflected force signal, but they also carry useless information deteriorating transparency [103, 105]. In particular, high frequency components of the reflected wave disturb the perception of the remote environment as they are reflected back and forth within the energetically lossless communication subsystem resulting in oscillatory behavior of HSI and teleoperator with a frequency of T^{-1}, the reciprocal of the round-trip time delay $T = T_1 + T_2$.

The wave reflection is characterized by the wave transfer function from (B.4), the so-called reflection factor R well-known from network theory

$$R = \frac{v_r}{u_r} = \frac{Z_{t/e} - b}{Z_{t/e} + b}, \tag{2.15}$$

with the Laplace variable s being omitted. The dynamics of the wave reflection v_r is determined by the wave impedance b which can be chosen arbitrarily and the terminating impedance $Z_{t/e}$. The wave reflection is suppressed, i.e. $v_r = 0$, only if the teleoperator/environment impedance matches the wave impedance $Z_{t/e} = b$, hence a pure damper environment is encountered with the damping coefficient $b_e = b$. Generally though, the impedances do not match.

The impedance matching technique proposed in [103, 105] uses an appropriately tuned controller at the teleoperator achieving reduced wave reflections at the cost of the tracking performance. Impedance matching based on dynamic filters and thereby achieving high transparency is proposed in [10]. The filter design is heuristic [9] or available only for special cases [11]. A generic method for the filter design is proposed in [50] and discussed in Appendix A.

The bilateral control of haptic telepresence in packet switched communication networks, such as the Internet, faces the additional challenges of time-varying delay, packet loss and limited bandwidth. A short overview on the state-of-the-art approaches is given in the following, a more detailed discussion follows in the corresponding chapters. Almost all state-of-the-art approaches are based on the wave variable formalism, and such is the focus in the following section.

2.2.2 Control in Packet Switched Communication Networks

The Internet belongs to the more general class of packet switched communication networks that are considered in this thesis for data transmission in haptic telepresence systems. The data are transmitted in data packets that are afflicted by time-varying delay and may even get lost. Further, the limited communication capacity has to be considered. The resulting control challenges for haptic telepresence systems, see also [100, 110–112], are summarized as follows:

- non-deterministic, unbounded time-varying delay

- non-deterministic, unbounded packet loss
- limited communication bandwidth (data rate)
- packet oriented character

Passivity with Time-Varying Delay

Time-varying delay leads to distorted wave variable signals; as a result the passivity of the communication subsystem can no longer be guaranteed [106]. Only few approaches exist, that may cope with the time-varying delay problem. In [73] a maximum delay is assumed and all data with a lower than the maximum delay are virtually delayed resulting in unnecessarily poor performance; further an upper delay bound can not be given in packet switched communication networks in general. The approach from [106] is based on the transmission of the wave integral instead of the wave variables and additionally the input energy allowing arbitrarily large delay. The wave variable output, however, might non-smoothly fluctuate deteriorating transparency. Targeting position tracking in [160], the distorted wave variable is compensated by the use of time stamps. The energy balance is monitored from the reconstructed input energy value at the receiver side to guarantee passivity. Packet loss and the packet oriented nature are not incorporated. In [161] additionally the problem of communication blackouts is considered in continuous time, however, it is difficult to be applied to the packet loss problem. The introduction of time-varying gains in [90] targets the regulation of the power content of the wave variable signals, it is adusted depending on the delay variation, therefore the knowledge of the delay variation is required. In [97, 99, 100] the wave variable approach is combined with prediction in order to cope with the time-varying delay problem. The mentioned approaches are formulated in continuous time and cannot directly be carried over to packet switched communication networks.

Passivity in Packet Switched Communication Networks

One of the main features of packet switched communication networks is their packet oriented character. As the mechanical systems in the haptic telepresence systems are continuous time systems, a consideration of the communication subsystem in discrete time consequently leads to a sampled data system. The passivity preserving transition from the continuous time system to the discrete time system, i.e. passive sampling, is non-trivial as indicated in [85]. Passivity preserving sampling within the formal framework of port-Hamiltonian systems is investigated in [126, 137] applying the wave variable transformation in discrete time. As a result the haptic telepresence system with constant delay can be considered a passive sampled data system. Based on this formulation the communication subsystem with time-varying delay is investigated in discrete time [136], a similar passivity argument as in [73], using send and receive queues, is applied.

Packet loss results in empty sampling instances at the receiver side; the packet loss problem is adressed by data reconstruction algorithms. Implicitely, there is the possiblity of energy generation rendering the communication subsystem including data reconstruction non-passive. An energy conserving, i.e. passive, interpolation algorithm is proposed in [125] assuming that maximal n consecutive packets are lost, and further introducing an additional delay of $(n + 2)$ sample time intervals by buffering at the receiver side. The

communication signal management introduced in [15] accounts for time-varying delay and packet loss by passive interpolation, signal compression and expansion. The additional delay introduced by buffering is a tuning parameter related to the smoothness of the interpolated signal. Both reconstruction strategies dissipate energy, i.e. render the communication subsystem strictly passive, and are likely to be overly conservative therefore.

Remark 2.4 Aside from the wave variable based approaches there are only a few other telepresence control architectures considering the challenges in packet switched networks. In [112] the position error force feedback scheme [33, 70] is modified with the proper adjustments of gains to cope with the time-varying delay problem and a quasi-optimal estimator for small data loss. For stability the delay must be bounded here, further an approximate model of the human together with the HSI is required. In the event-based approach proposed in [159] a data sample is only transmitted after receiving a data sample from the opposite site, comparable to a move-and-wait strategy. The resulting (likely poor) closed loop performance is not discussed.

Remark 2.5 The problem of packet loss with resulting empty sampling instances and the necessity of data reconstruction also arises in Networked Control Systems (NCS). A number of estimation algorithms have been proposed for application in NCS guaranteeing stability of the closed loop system. In [109] two classes of compensation schemes for the treatment of the empty sampling instances are defined: keeping the old control (Hold Last Sample, HLS) or generating new control with estimated data. The HLS algorithm for data reconstruction in NCS is also proposed in [88]. Generally, event based considerations of NCS as [150] assume the HLS as the underlying algorithm. Estimation techniques for NCS based on recursive and Kalman filters have been suggested in [6, 142].

Another characteristic of packet switched communication network is the limited communication bandwidth. Multiple user run their network applications at the same time sharing the limited resources of the physical links in terms of bandwidth. The aggregate network traffic induced by the applications determines the communication quality for each network application. Higher network traffic load results in a higher probability of congestion and thereby in higher delay and packet loss, impairing the performance of each network application. From this point of view it is of high interest to minimize the network traffic in network applications in general. In addition, high packet transfer rates as they occur in haptic telepresence systems are hard to maintain over long distance packet switched communication networks.

Recently, a number of researchers considered the stability of networked control systems (NCS) under communication constraints, see [63, 116] and the references therein. Aiming at network traffic reduction in NCS the deadband control approach is proposed [62, 87, 113]. A data packet is send only, if the current value has changed more than a given threshold. To the best knowledge of the author, packet rate reduction in haptic telepresence systems has not been considered yet in the known literature. Due to the previously mentioned differences, see Section 2.1, the approaches from NCS cannot be generalized to haptic telepresence systems. In this thesis for the first time a packet rate reduction approach is considered for haptic telepresence systems.

Position Tracking

The standard wave variable approach does not imply explicit position tracking between the HSI and the teleoperator due to the encoding of velocity and force signals. If the wave variable signal is changed during the transmission due to time-varying delay or approximate reconstruction at the receiver in the case of packet loss, a non-recoverable position drift between the HSI and the teleoperator occurs.

In [103] an outer position feedback loop is closed adding a drift correction term to the wave variable signal. This correction is possible only at time instances when no energy is generated by this correction. In [106, 160] position tracking is achieved by the transmission or reconstruction of the integrated wave variable that contains position and force information; energy monitoring ensures the passivity of the communication subsystem. However, both the approaches based on the wave integral may not recover an initial position drift. An alternative approach [27] forwards the HSI position to the teleoperator in addition to the wave variables; an appropriately tuned controller ensures the passivity of the teleoperator, see Appendix A for details. In order to obtain position tracking in [50], not the velocity, but the position signals are encoded into the wave variable. Passivity is ensured by appropriately designed dynamic filters. This architecture modification together with a novel filter design methodology is discussed in detail in Appendix A.

Control in Future Packet Switched Communication Networks

The existing approaches consider the communication subsystem as a black box associated with the communication quality parameters time delay and very few also with packet loss. Future Internet will offer the possibility of requesting a certain level of communication quality. In fact, there are strategies developed in the networking community ready to be implemented in local area networks. This concept, called Quality-of-Service (QoS), allows the control of the communication subsystem in terms of the received communication quality. As far as known to the author, the simultaneous control of the haptic telepresence system and the communication subsystem has not been considered in the known literature yet. In this thesis this is discussed for the first time.

2.3 Transparency Evaluation

The performance objective for the telepresence system design is discussed in terms of transparency.

Definition 2.1 *Telepresence is called transparent if the human is unable to distinguish between direct and tele-interaction with a (remote) environment.*

Naturally, there is a trade-off between transparency and robust stability in all control schemes, i.e. perfect transparency is not achievable in practice [42, 45, 81]. Consequently, the question arises how close a certain system design is to the transparency requirement or how to quantitatively measure the transparency level.

In the following several known objective transparency criteria and the corresponding measures are reviewed. The notion of "objective" criteria and measures is derived from traditional control engineering in terms of measurable quantities.

2.3.1 Objective Transparency Criteria and Measures

Transparency according to [162] requires the equality of the positions and forces at the HSI and the teleoperator/environment

$$x_h = x_e \qquad \text{and} \qquad f_h = f_e. \tag{2.16}$$

A performance index in terms of a maneuverability measure is derived from this criterion comprising two values based on the integral norm in the frequency domain for the transfer functions in operator force to position error and operator force to force error, respectively. The upper integral bound is determined by the human perceptual bandwidth. Small values indicate low position and force error, hence a good level of transparency. Comparative statements about the relative quality can be made by this measure. However, absolute statements are hardly derivable. Further, a direct relation of the obtained values to psychophysical findings, discussed later in this chapter, is difficult to find and such the interpretation using human factors is difficult.

Another criterion requires for transparency the equality of the impedance displayed to the human and the environment impedance [81]

$$Z_h = Z_e. \tag{2.17}$$

Measures derived from this criterion are integral impedance error norms in the frequency domain as applied in [75, 153]. Following the argumentation above, again, the value of such a measure does not allow an intuitive interpretation. The Z-width, another derived transparency measure borrowed from the haptic literature [21, 31], is used in [46] to express the dynamic range of the impedance transmitted to the operator as a measure for the level of transparency. However, it is quantified for the two extreme values of environment impedance $Z_e = 0$ (free space motion) and $Z_e \to \infty$ (contact with an infinitely stiff wall) only. Accordingly, transparency is good if $Z_h \to 0$ and $Z_h \to \infty$, respectively. This measure is appropriate for qualitative comparisons of control schemes. Human perception limits are not considered. Well suited instead is the evaluation on the basis of a comparison between the mechanical parameters of the impedances [3, 4] as numerous psychophysical studies on the perception of such material characteristics exist.

Aiming at the evaluation of transparency in medical telepresence applications, where the detection of compliance differences in soft environments is essential, another transparency (named fidelity by the authors) criterion is introduced in [24]. Fidelity is defined as the sensitivity of the perceived impedance to the change in the environment impedance. Transparency is achieved if a change in the environment impedance results in an equal change in the perceived impedance

$$\frac{\mathrm{d}Z_h}{\mathrm{d}Z_e} = 1.$$

The derived fidelity measure, an integral norm on the weighted impedance change error, incorporates by its weighting filter results from human compliance discrimination studies. However, it is very specific for relative changes of impedances in soft environments.

2.3.2 Evaluation considering Human Factors

The level of transparency, according to the transparency Definition 2.1, can be interpreted as the human perceived performance. Hence the 'feel' of the human is essential for transparency evaluation. To measure this 'feel' depending on physical stimuli is the goal of psychophysics, which is the branch of psychology concerned with the quantitative relation between physical stimuli and the sensations and perceptions evoked by these stimuli.

It is wellknown that the human may not discriminate arbitrarily small differences in a physical quantity, expressed by the just noticeable difference (usually abbreviated as JND), the smallest difference in a sensory input that is perceivable by a human being. For many sensory dimensions the JND is an increasing function of the base level of input. For most force-related physical properties the ratio of the two is roughly constant over a large range [22] and can therefore be represented by Weber's law [154]

$$\frac{\Delta I}{I} = c, \tag{2.18}$$

where I is the original intensity of stimulation, ΔI is the addition to it required for the difference to be perceived (the JND), and c is the Weber fraction. Discrimination thresholds for mechanical parameters such as stiffness, inertia, and viscosity and for quantities, such as position, velocity, and force, are in most literature, see e.g. [14, 64–67, 119, 120, 140], given as the percentual change with respect to the original intensity of stimulation (therein also called JND or JND% or differential threshold). In this thesis we will follow most of the literature, where the percentual discrimination threshold is referred to as JND. Some of the most relevant JNDs for haptic telepresence systems are summarized in Table 2.1.

Table 2.1: Overview on perceptual discrimination thresholds for haptics related properties reported in the literature.

Physical property	JND [%]		Experimental conditions
Force	7 ± 1 %	[64]	arm/forearm, cross-limb-matching
	ca. 15 %	[65, 120]	arm, static force
	7 %	[139]	pinch-fingers, at 2.5-10 N
	ca. 10 %	[22, 134]	arm/forearm
Movement	8 ± 4 %	[64]	arm/forearm, cross-limb-matching
Position	8 ± 2 %	[64]	arm/forearm, cross-limb-matching
Stiffness	23 ± 3 %	[64, 66]	arm/forearm, cross-limb-matching
	8 %	[139]	pinch-fingers, work/maximum force applied
Viscosity	34 ± 5 %	[67]	arm/forearm, cross-limb-matching, > 20 Ns/m
	13.6 ± 3 %	[14]	pinch-fingers, at 120 Ns/m
Mass	21 ± 5 %	[14]	pinch-fingers, at 12 kg
	113 %	[119]	
Compliance	$15 - 99$ %	[140]	pinch-fingers

Remark 2.6 It is wellknown that the experimental conditions have a significant influence on the results gained in psychophysical experiments. The experimental condition comprise e.g. the considered limbs and their configuration. Further, most JND results are based on a static consideration. The impact of the temporal rate of change of a physical stimuli or parameter is not considered in the known literature as far as known to the author. The different experimental conditions explain the in some cases wide variation for JNDs. Additionally, some parameters, as e.g. inertia, are suspected of not [64] following Weber's law (2.18). As the results are empirically obtained they generally represent some statistical quantity. Still, these results give a good indicator for the human perceivable performance.

Another interesting result is on the limitations of stiffness perception. The results obtained in [82] indicate that the human operator cannot haptically perceive a difference between a wall with a stiffness coefficient of 10000N/m and an infinitely stiff wall. The average where subjects reported the wall feels no longer rigid is found to be 24200N/m [141].

Aside from the perception limits there exist similar psychophysical studies on the action limits referring to the maximum realizable forces, accelerations, and velocities by the human. Further, the control range is of interest. Generally, a control bandwidth of 20-30Hz is assumed [141]. According to [20] a bandwidth of 4-10Hz is required for the normal operation of a haptic telepresence system.

There are other evaluation approaches not based on the human perception and action characteristics. A very common experimental measure of transparency is the task completion time. Typically, visual feedback is additionally provided, such that the evaluation includes more than the haptic modality. A relation between the perceived dynamics and the task completion time is reported in [20], where it is stated that the task completion time doubles, if the stiffness is reduced by 66%. Other experimental measures are based on the peak force, the sum of squared forces, or the number of error trials. Another tool for transparency evaluation are self reports (surveys) on the subjective feel of the haptic telepresence system. The rating is performed by the test person after the experiment; rating scales such as Likert-type scales are commonly used therefore. However, the latter methods using task performance metrics or surveys for a human oriented evaluation of transparency give a good indicator but are very difficult to generalize from an engineering point of view.

2.4 Discussion

In this chapter the known control architectures for haptic telepresence systems are reviewed. Most of them aim at the stabilization in the presence of constant time delay. Basically all existing control methods to cope with (time-varying) time delay and packet loss are based on the passivity paradigm and use the wave variable transformation. Very few researchers considered the typical effects of a packet switched communication network; the few known approaches are likely to be overly conservative or use too strong assumptions for the communication network characteristics. The transparency of these approaches has not been evaluated. Obviously, there is a demand for less conservative approaches, and for tools to evaluate the transparency. One goal of this thesis is to develop transparent control approaches for telepresence systems in packet switched communication networks. For the first time a systematic transparency analysis of telepresence systems in packet switched communication networks is presented.

Approaches that explicitly consider the required bandwidth for data transmission, hence the network cost from the communication point of view, are not reported in the known literature for haptic telepresence systems. The recently developed methods from the closely related field of networked control systems cannot directly be carried over because of the largely unknown models of the human and the environment. An innovative approach to reduce the network traffic in haptic telepresence systems without impairing the transparency is considered in this thesis.

The telepresence system control approaches in the known literature are based on the phenomenological description of the packet switched communication network in terms of parameters such as time delay and packet loss; in some approaches the observation of these parameters is considered. However, the Quality-of-Service concept allows the control of the communication parameters. Telepresence control concepts considering the additional control of the communication network have not been investigated yet in the known literature. For the first time the simultaneous control of the haptic telepresence system and the packet switched communication network is proposed in this thesis.

The transparency evaluation is mostly carried out without the consideration of the human haptic perception as discussed in this chapter. However, human perception and action characteristics can be used to find the appropriate trade-off between robust stability and transparency in the control design. Known human perception limits, expressed for example in the notion of the just noticeable difference, give a good and well quantifiable indicator for the level of transparency, hence on the closeness of some haptic telepresence system control design to perfect transparency from a human perception point of view. One goal of this thesis is to develop measures and tools for the transparency evaluation, where such perception limits are incorporated in order to advance the transparency evaluation to a more human oriented view. In this context experimental user studies are seen to be an indispensible instrument.

In summary, the goal of this thesis is the systematic analysis and the further improvement of control strategies for haptic telepresence systems in packet switched communication networks. Main emphasis in the methodical approach lies on the conjoint consideration of control theoretic, communication related, and human haptic perception aspects, which is so far unique in this depth in the known literature.

3 Transparency Analysis and Evaluation

It is well-known *that* communication induced disturbances such as time delay and packet loss deteriorate the transparency of a haptic telepresence system. Widely open is the question *how* it influences the human perception of the remote environment. This knowledge is absolutely necessary in order to determine the limits of tele-applications over packet switched communication networks. It would be desirable to have analysis methods that quantify the level of transparency depending on the communication parameters. The obtained measure should allow an interpretation incorporating human factors.

Many of the transparency measures known from the literature [24, 46, 75, 153, 162], refer to Section 2.3.1 for a detailed discussion, give a good relative valuation for qualitative comparisons. However, they are difficult to interpret using known human perception characteristics. The evaluation on the basis of physical parameters of the impedance perceived by the human operator, as performed in [3, 4], is superior. A mapping from the parameter time delay on the perceived stiffness and inertia is studied in [3, 4] for special cases of control schemes and for the wave variable approach in [103, 104, 108]. However, the time delay has to be assumed constant for the analysis, the latter approach is limited to steady state considerations. The resulting implications of time delay effects on the human perception have not been investigated yet. No approach exists in the literature to evaluate the effect of packet loss on transparency.

The innovation in this chapter is the development of tools for the systematic analysis of the transparency of haptic telepresence systems. As transparency measure serves the set of mechanical parameters to describe the perceived impedance. This is motivated by the fact, that many results from psychophysical studies on the detection and discrimination of mechanical parameters exist, see Section 2.3.2 for an overview. An analytical approximation method extends the steady state consideration on time delay effects from [103, 104, 108] to a low frequency consideration. A generic optimization based analysis uses known parameter identification methods and is applicable for an impact analysis of general communication effects such as time delay, packet loss, network sampling rate, etc. In this chapter its effectiveness for the constant time delay case is demonstrated, thereby verifying the special results from [103, 104, 108]. The relevant implications of the obtained results are discussed and validated in objective experiments and experiments considering human factors.

In fact, the optimization-based transparency analysis tool, further applied in the following chapters, is not only well suited for analysis, but also for the systematic design of impedance matched haptic telepresence systems [50, 51], see Section 2.2.1 for details on impedance matching and a review on existing techniques. The proposed approach allows a systematic design for impedance matching architectures as exemplarily shown in Section A.3.

The remainder of this chapter is organized as follows: Starting from the problem definition for the constant delay case, the analytical method to obtain an approximation of the perceived impedance is introduced in Section 3.1.1, and the generic impedance approximation approach in Section 3.1.2. These methods are applied for the time delay transparency

analysis followed by a discussion of the results and their consequences with respect to human haptic perception in Section 3.2. Objective experiments and experimental user studies in Section 3.3 validate the obtained results.

3.1 Analysis Method

The general goal is to evaluate the influence of communication effects on the transparency of the haptic telepresence system on the basis of the transparency criterion requiring the equality of the perceived and the environment impedance [81] given by (2.17). Here, the perceived impedance Z_h (2.3) is compared to the real teleoperator/environment impedance $Z_{t/e}$ (2.5) instead of the pure environment impedance Z_e (2.17). This addresses the fact, that only the communication effects should be evaluated, and not the influence of the teleoperator control. In order to allow an interpretation considering human perception characteristics, we compare the impedances in terms of their physical parameters, such as mechanical stiffness, mass, and damping. It is desirable to find a mapping from the communication parameters $\boldsymbol{p_c}$ and the teleoperator/environment parameters $\boldsymbol{p_e}$ on the set of mechanical parameters $\boldsymbol{p_h}$ describing the perceived impedance.

Special Case: Constant Time Delay

In the following the constant delay case $\boldsymbol{p_c} = [T_1 \; T_2 \; b]^T$ is considered, the underlying control architecture is depicted in Fig. 2.2. The perceived impedance can be computed depending on the teleoperator/environment impedance $Z_{t/e}(s, \boldsymbol{p_e})$ using the notion of the reflection factor $R = R(s, \boldsymbol{p_e}, b)$ (2.15) and the reformulated wave variable transformation equations (2.8) together with (2.9) in the Laplace domain

$$Z_h(s, \boldsymbol{p_h}) = Z_h(s, \boldsymbol{p_c}, \boldsymbol{p_e}) = b\frac{1 + R\, e^{-sT}}{1 - R\, e^{-sT}}, \quad \text{with} \quad T = T_1 + T_2. \tag{3.1}$$

Actually, the right hand term represents the impedance seen by the HSI. With the argument on the exclusive investigation of the communication effects, the HSI dynamics is assumed to be negligible due to sufficient control bandwidth, such that the displayed force at the HSI is equal to the desired force $f_h = f_h^d$, i.e. the impedance perceived by the human (2.3) is equal to the impedance displayed to the HSI. However, the HSI dynamics can, if necessary, easily be incorporated into the analysis.

Note that due to the assumption of LTI impedances, the perceived impedance depends on the round-trip delay T only. For the analysis the delays T_1 in the forward path and T_2 in the backward path can be accumulated to the overall delay, i.e. $\boldsymbol{p_c} = [T \; b]^T$. For vanishing round-trip delay $T = 0$ the perceived impedance is equal to the environment/teleoperator impedance.

The main challenge for an intuitive physical interpretation of the perceived impedance parameters is the complexity of the transfer function (3.1). Due to the delay element this transfer function has an infinite number of poles and zeros, hence has infinite order, i.e. is transcendent. Accordingly, the parameter vector $\boldsymbol{p_h}$ is of infinite dimension.

In order to obtain a finite order approximation of the perceived impedance, we propose two methods: an analytical and an optimization-based numerical approach. The parameters of the approximated perceived impedance are then used for the transparency analysis.

3.1.1 Low Frequency Approximation for Constant Time Delay

The approximation of the perceived impedance transfer function is computed using a Padé series of finite order to approximate the delay transfer functions in (3.1). The order of the perceived impedance approximation depends on the order N of the Padé approximation. In order to simplify the analysis, here, the delay elements are approximated by a first order Padé series

$$e^{-sT} \approx \frac{1 - \frac{T}{2}s}{1 + \frac{T}{2}s}. \tag{3.2}$$

Generally, a Padé approximation of order N is valid for frequencies $\omega < \frac{N}{3T}$. Consequently, the first order approximation is valid for frequencies $\omega < \frac{1}{3T}$. Inserting (3.2) and (2.15) in (3.1) the approximated perceived impedance Z_h^{app} is computed by

$$Z_h(s) \approx Z_h^{\text{app}}(s) = b\frac{2Z_{t/e} + bTs}{2b + TZ_{t/e}s} \quad \text{for} \quad \omega < \frac{1}{3T}. \tag{3.3}$$

As the approximation is valid for limited frequency range only, for further analysis this transfer function is split into a low frequency component $Z_{h,lf}^*$ and a high frequency component F_{hf}

$$Z_h^{\text{app}}(s) = Z_{h,lf}^*(s, \boldsymbol{p_{h,lf}^*})F_{hf}(s), \tag{3.4}$$

with $|F_{hf}(s)| \approx 1$ at low frequencies $\omega < \frac{N}{3T}$. In order to obtain similar results as in [103, 104, 108], hence a static consideration, $|F_{hf}(0)| = 1$ is required.

The component $Z_{h,lf}^*$ represents a good approximation of the low frequency behavior of the perceived impedance. The advantage of this method is that the mechanical parameters $\boldsymbol{p_{h,lf}^*}$ of the approximated perceived impedance can analytically be derived as a function $\boldsymbol{p_{h,lf}^*} = \boldsymbol{f}(\boldsymbol{p_c}, \boldsymbol{p_e})$ of the communication and environment parameters. The approximation, though, is valid only for frequencies $\omega < \frac{1}{3T}$, a restriction governed by the Padé delay approximation. Accordingly, the parameters $\boldsymbol{p_{h,lf}^*}$ describe the low frequency behavior of the perceived impedance. Validity for higher frequencies can easily be obtained by the use of a higher order Padé approximation.

Generally, this approach of low frequency approximation is applicable if the perceived impedance can be analytically represented as a function of the communication parameter of interest. This is possible for constant time delay, but difficult for general communication effects such as packet loss. A more generic approach that targets this challenge and that additionally extends the frequency range of validity of the approximation is introduced in the following.

3.1.2 Generic Impedance Approximation by Optimization

The goal of the following optimization-based approach is to find an optimal approximation Z_h^* of the perceived impedance (3.1) with respect to an impedance error norm.

We define the impedance error ΔZ, visualized in Fig. 3.1, between the real impedance Z_h and the approximated impedance Z_h^* in the frequency domain according to

$$\Delta Z(j\omega, \boldsymbol{p_h^*}, \boldsymbol{p_c}, \boldsymbol{p_e}) = |Z_h(j\omega, \boldsymbol{p_c}, \boldsymbol{p_e})|_{\text{dB}} - |Z_h^*(j\omega, \boldsymbol{p_h^*})|_{\text{dB}}, \tag{3.5}$$

with the approximated impedance Z_h^* assumed to be a stable, minimal phase system with the parameter vector $\boldsymbol{p}_h^*$. Note that the structure of the approximated impedance can be chosen according to the desired accuracy of the result that should be governed by psychophysical arguments. Higher order, however, generally increases computational cost.

In order to get an approximation of the impedance Z_h, the impedance error has to be minimized. Consequently, we define the cost function to be minimized as the integral over the squared impedance error computed in the frequency domain

$$J(\boldsymbol{p}_h^*, \boldsymbol{p_c}, \boldsymbol{p_e}) = \int_{\omega_{\min}}^{\omega_{\max}} \left[G_h(j\omega)\Delta Z(j\omega, \boldsymbol{p}_h^*, \boldsymbol{p_c}, \boldsymbol{p_e})\right]^2 \, \mathrm{d}\omega \rightarrow \min_{\boldsymbol{p}_h^*}, \tag{3.6}$$

where $[\omega_{\min},\ \omega_{\max}]$ represents the frequency window for optimization and G_h a tunable filter in order to weigh frequency bands of interest.

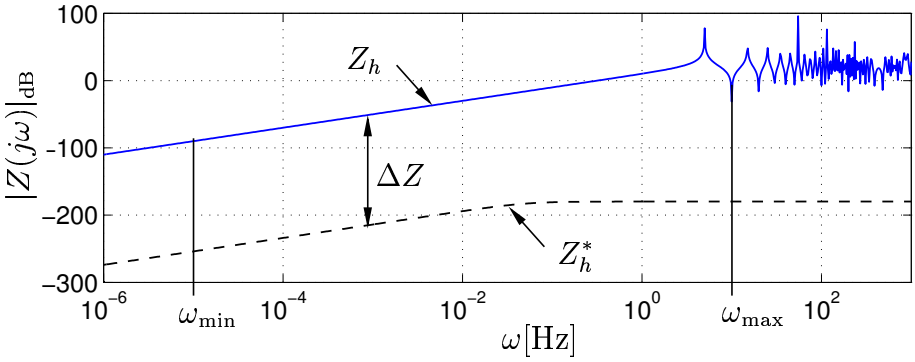

Figure 3.1: Definition of the impedance error ΔZ.

Optimization Procedure

In the most general case no analytical representation of the dependency of the perceived impedance from the communication parameters exist. In fact, they may be of stochastic nature. In such cases, the frequency response of the perceived impedance Z_h is estimated from a cross-correlation analysis. Therefore, the numerical model is excited by a sinusoidal signal with a small amplitude around some working point of interest for fixed environment parameters $\boldsymbol{p_e}$ and communication parameters $\boldsymbol{p_c}$. The gain and phase relation between the exciting HSI velocity signal and the resulting HSI force signal is computed using standard cross-correlation method [61]. If the communication parameter is of stochastic nature such as a packet loss probability, Monte Carlo simulations are performed for numerous realizations of the stochastic parameter $\boldsymbol{p_c}$ with the subsequent cross-correlation analysis. The resulting mean magnitude and phase for a certain communication parameter probability setting and a dedicated exciting frequency $\omega_i,\ i = 1, 2, ..., N$ represent one point of the frequency response of the corresponding perceived impedance. The procedure is performed for numerous exciting frequencies within the window of optimization $[\omega_{\min},\ \omega_{\max}]$. The obtained mean of the frequency response $Z_h(j\omega_i, \boldsymbol{p_c}, \boldsymbol{p_e})$ of the perceived impedance is used for the computation of the impedance error (3.5). The cost function (3.6) is then computationally realized as the sum of the weighted impedance errors $Z_h(j\omega_i, \boldsymbol{p_c}, \boldsymbol{p_e})$ at the discrete frequencies ω_i

$$J(\boldsymbol{p}_h^*, \boldsymbol{p_c}, \boldsymbol{p_e}) = \sum_{i=1}^{N} \left[G_h(j\omega_i)\Delta Z(j\omega_i, \boldsymbol{p}_h^*, \boldsymbol{p_c}, \boldsymbol{p_e})\right]^2, \qquad \omega_1 = \omega_{\min};\quad \omega_N = \omega_{\max}.$$

The optimal parameter $\boldsymbol{p}_{\boldsymbol{h}}^{*}$ can be computed depending on the communication parameter $\boldsymbol{p}_{\boldsymbol{c}}$ and the environment parameter set $\boldsymbol{p}_{\boldsymbol{e}}$. Especially in the considered general case, an analytical mapping $\boldsymbol{p}_{\boldsymbol{h}}^{*} = \boldsymbol{\Phi}(\boldsymbol{p}_{\boldsymbol{c}}, \boldsymbol{p}_{\boldsymbol{e}})$ is difficult to find. There is a chance to find such a mapping or at least an approximation if the optimization is performed for multiple sets of environment and communication parameter values.

In contrast to the proposed analytical approach this optimization-based method represents a generic approach to obtain the approximated perceived impedance. This approach is not only well suited for the transparency analysis but also for the design of transparency oriented impedance matched architectures, as follows.

Impedance Matching by Optimization

In [103, 105] wave reflections as a result of mismatching impedances are recognized to deteriorate the transparency, see also Section 2.2.1 for details on impedance matching and a review on existing techniques. The goal is to match the impedances of the transmission line and the teleoperator/environment. Therefore, several techniques are available. An appropriately tuned controller for the teleoperator is proposed in [103, 105], appropriately tuned dynamic filters in [10, 11].

By means of the proposed optimization methods the optimal tuning parameters with respect to the cost function (3.6) for both the impedance matching techniques can be found. Here, the impedance error ΔZ is defined between the transmission line impedance b and the teleoperator/environment impedance $Z_{t/e}$ similarily to (3.5). The determined tuning parameters optimally match the teleoperator/environment impedance to the transmission line impedance. The proposed approach allows a systematic design of impedance matched architectures [50, 51], and is studied in detail in Appendix A.

3.2 Transparency Analysis for Constant Delay

For the following transparency analysis the teleoperator/environment impedance is represented by a LTI mass-spring-damper system of the form

$$Z_{t/e}(s) = m_e s + b_e + \frac{k_e}{s}, \tag{3.7}$$

with the environment mass m_e, the damping coefficient b_e, and the spring coefficient k_e representing the environment parameter set $\boldsymbol{p}_{\boldsymbol{e}}$. Note that these assumptions are not necessary, more complex dynamics can easily be considered in the proposed analysis method.

3.2.1 Perceived Impedance for Different Environment Dynamics

An analysis of the perceived impedance is exemplarily carried out in detail for the prototypical cases 'free space motion' and 'contact with a stiff wall'. For all other possible combinations of environment impedances given by (3.7) only the results are presented.

Free Space Motion

In free space motion no environment force is exerted on the teleoperator $f_e = 0$. The environment mass, the damping, and the stiffness coefficient in (3.7) are zero $m_e = b_e = k_e = 0$, i.e. the terminating impedance is $Z_{t/e} = 0$. Inserting the resulting reflection factor (2.15) $R(s) = -1$ in (3.1) yields the perceived impedance in free space motion

$$Z_h(s) = b\frac{1 - e^{-sT}}{1 + e^{-sT}}. \tag{3.8}$$

Inserting the teleoperator/environment impedance for free space motion $Z_{t/e} = 0$ into (3.3) gives the analytically derived approximation of the perceived impedance for low frequency

$$Z_h^{\text{app}}(s) = m_h s\frac{1}{T_h s + 1} \quad \text{for} \quad \omega < \frac{1}{3T}, \tag{3.9}$$

with

$$m_h = \frac{bT}{2} \quad \text{and} \quad T_h = \frac{T}{2}. \tag{3.10}$$

Note, that the left hand factor in (3.9) represents the low frequency component $Z^*_{h,lf}$ in (3.4). The righthand factor is the high frequency component F_{hf}.

Thus, at low frequencies the perceived impedance equals an inertia with the mass m_h. In order to obtain a reliable high frequency approximation, the optimization proposed in the previous section is applied.

Therefore, the optimization based on the cost function (3.6) is performed in the frequency range $[\omega_{\min}, \omega_{\max}] = [10^{-6}, 10^3]$Hz. A typical Bode plot of the perceived impedance (3.8) and the impedance approximated by optimization is depicted in Fig. 3.2 showing that the transfer function

$$Z_h^*(s) = m_h s\frac{1}{T_h s + 1}, \tag{3.11}$$

with the optimization variables $\boldsymbol{p_h} = [m_h\, T_h]^T$ approximates the perceived impedance well. Note that the structure of the numerical approximation (3.11) is equal to the analytical low frequency approximation (3.9), which is not the general case. At low frequency ($\omega < \frac{1}{3T} \approx 3$Hz) the inertia characteristics as analytically derived in (3.9) is observed, see the left factor of the approximated transfer function (3.11). For higher frequencies the infinite number of poles and zeros in (3.9) resulting from the delay elements e^{-sT} becomes obvious.

As a result of multiple numbers of optimizations for combinations of the communication parameters T and b the values of the parameters m_h and T_h of the approximated perceived impedance are derived, validating the analytical result from (3.10).

Contact

In contact with a stiff wall environment a force proportional to the penetration depth with the stiffness coefficient $k_e > 0$ is applied to the teleoperator. The teleoperator/environment impedance given by the transfer function $Z_{t/e} = \frac{k_e}{s}$ yields a reflection factor (2.15) of

$$R(s) = \frac{k_e - bs}{k_e + bs}.$$

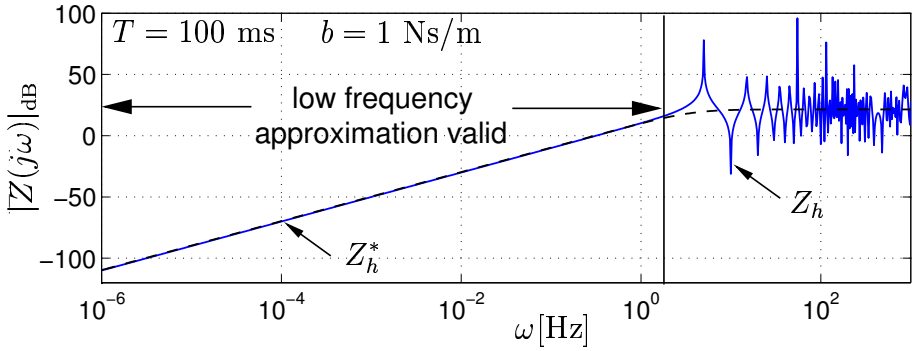

Figure 3.2: Amplitude/frequency characteristics of the perceived and the approximated impedance in free space motion.

With this reflection coefficient the perceived impedance (3.1) is given by

$$Z_h(s) = b\frac{k_e + bs + (k_e - bs)e^{-sT}}{k_e + bs - (k_e - bs)e^{-sT}}\,.$$

The low frequency approximation given by (3.3) for the contact case yields

$$Z_h^{\mathrm{app}}(s) = \frac{k_h}{s}(1 + \frac{bT}{2k_e}s^2) \quad \text{for} \quad \omega < \frac{1}{3T}, \tag{3.12}$$

with

$$k_h = \frac{2bk_e}{2b + Tk_e}. \tag{3.13}$$

The left hand factor is the low frequency component $Z_{h,lf}^*$ from (3.4). The right hand factor in (3.12) exhibits high pass behavior with a cut-off frequency of $\sqrt{2k_e/(bT)}$ that is possibly higher than the allowed frequency, hence only the integrating characteristics can be taken as a good approximation of the low frequency behavior. As a result the perceived impedance in contact at low frequency has a spring like behavior but with a lower stiffness k_h than the environment stiffness k_e.

The numerically approximated perceived impedance has a spring-damper characteristics

$$Z_h^*(s) = \frac{k_h}{s} + b_h, \tag{3.14}$$

as shown in Fig. 3.3. Similarily to the low frequency approximation (3.12) a stiffness is apparent, and additionally a damping. The value of the stiffness coefficient (3.13) is validated, the damping is computed to $b_h = b$. In contact with a stiff wall (spring characteristics) the operator perceives a spring-damper behavior.

General Environment Impedances

The proposed approximation method for the perceived impedance is applied to various environment impedances with only the results given here.

The following environment impedances are considered:

- damper: $k_e = 0$, $b_e > 0$, $m_e = 0$,

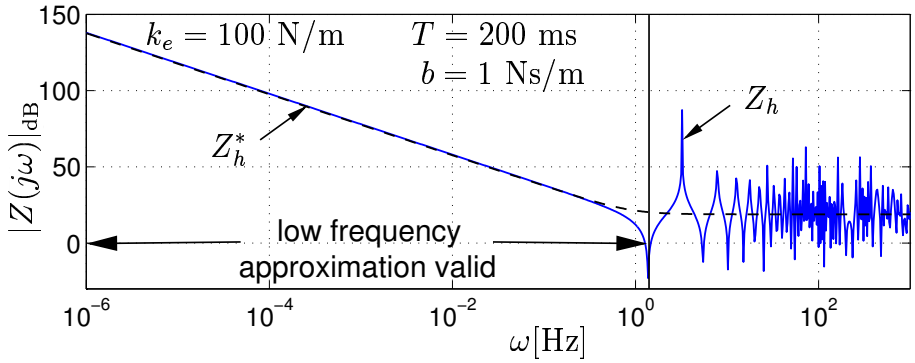

Figure 3.3: Bode plot of the perceived and the approximated impedance in contact.

- mass: $k_e = 0$, $b_e = 0$, $m_e > 0$,
- spring-damper: $k_e > 0$, $b_e > 0$, $m_e = 0$,
- mass-damper: $k_e = 0$, $b_e > 0$, $m_e > 0$,
- spring-mass-damper: $k_e 0$, $b_e > 0$, $m_e > 0$.

Low frequency analytical approximation and optimization for high frequency approximation are performed analogously to the described free space motion and the contact case. The results are summarized in Table 3.1.

Generally, for all environment impedances exhibiting stiffness characteristics $k_e \neq 0$ the low frequency approximation yields an equivalent result with the same parameter dependency of the stiffness coefficient as the contact case; except for a varying high frequency component. Also the damping coefficient for the damper environment and the mass for the inertia environment are analytically derived.

In order to find the remaining parameter, the optimization with the cost function described by (3.6) is performed in the frequency range $[\omega_{\min},\ \omega_{\max}] = [10^{-6},\ 10^{3}]$Hz. In all cases except for the damper environment the parameter b_h as well as T_h were observed to react very sensible to the frequency window for optimization.

Remark 3.1 The obtained results for the time delay analysis are for low frequencies equivalent to the results from the steady state consideration in [103, 104, 108], thereby verifying the validity of the approach.

3.2.2 Interpretation of the Results

The interpretation of the results focuses on the most interesting results, the communication induced perceived inertia and the reduced perceived stiffness of a stiff environment.

Communication Induced Inertia Perception

In free space motion as well as with a damper and spring-damper environment (cases 1, 3, and 5 in Table 3.1) an inertia is perceived even though no inertia is contained in the environment. In all cases where an inertia is already contained in the environment (cases 4, 6, 7, and 8 in Table 3.1) the perceived inertia is increased. Consequently,

Table 3.1: Results of perceived impedance approximation, parameters marked by * are analytically derived by low frequency approximation, all others by optimization, parameters marked by ** could not be computed by the proposed methods .

Case	Environment	$Z_{t/e}(s)$	$Z_h^*(s)$	Parameters
1	Free space	0	$\frac{m_h s}{T_h s+1}$	$^*m_h = \frac{bT}{2}$ $T_h = \frac{T}{2}$
2	Contact (spring)	$\frac{k_e}{s}$	$\frac{k_h}{s} + b_h$	$^*k_h = \frac{2bk_e}{2b+Tk_e}$ $^{**}b_h$
3	Damper	b_e	$\frac{m_h s+b_h}{T_h s+1}$	$m_h = \frac{T(b_e+b)}{2}$ $T_h = \frac{T}{2}$ $^*b_h = b_e$
4	Mass	$m_e s$	$\frac{m_h s}{T_h s+1}$	$^*m_h = m_e + \frac{Tb}{2}$ $T_h = \frac{T}{2}$
5	Spring-damper	$b_e + \frac{k_e}{s}$	$\frac{m_h s+b_h+\frac{k_h}{s}}{T_h s+1}$	$^*k_h = \frac{2bk_e}{2b+Tk_e}$ $m_h = \frac{T(b_e+b)}{2}$ $T_h = \frac{T}{2}$ $b_h \in [b, b_e]$
6	Spring-mass	$m_e s + \frac{k_e}{s}$	$\frac{m_h s+b_h+\frac{k_h}{s}}{T_h s+1}$	$^*k_h = \frac{2bk_e}{2b+Tk_e}$ $m_h = m_e + \frac{Tb}{2}$ $T_h = \frac{T}{2}$ $^{**}b_h$
7	Mass-damper	$m_e s + b_e$	$\frac{m_h s+b_h}{T_h s+1}$	$^*m_h = m_e + \frac{T(b_e+b)}{2}$ $T_h = \frac{T}{2}$ $b_h \in [b, b_e]$
8	Spring-mass-damper	$m_e s + b_e + \frac{k_e}{s}$	$\frac{m_h s+b_h+\frac{k_h}{s}}{T_h s+1}$	$^*k_h = \frac{2bk_e}{2b+Tk_e}$ $m_h = m_e + \frac{T(b_e+b)}{2}$ $T_h = \frac{T}{2}$ $b_h \in [b, b_e]$

the inertia characteristics is induced by the wave variable transformation and the communication delay. The mass mainly depends on the delay and the wave impedance. With increasing round-trip delay the mass proportionally grows as shown in Fig. 3.4 for the free space motion case. The perceived inertia also increases with the wave impedance b.

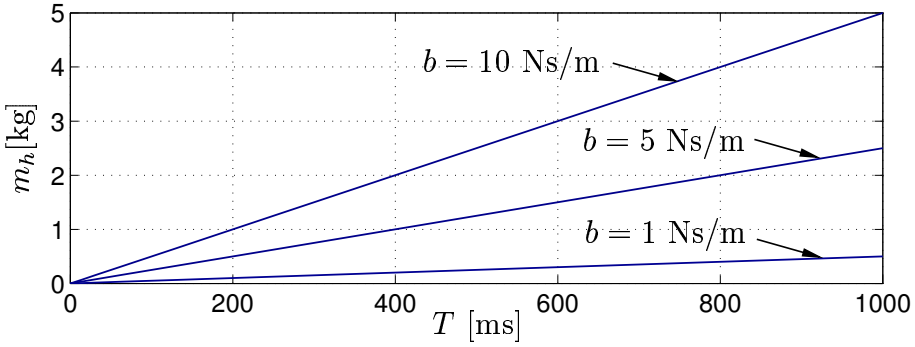

Figure 3.4: Perceived inertia in free space motion depending on delay.

Example: Lets assume free space motion of the teleoperator, a communication round-trip delay $T = 200$ ms, typical for the communication over the Internet, and the wave impedance tuned to $b = 1$ Ns/m. Then the operator perceives an inertia with $m_h = 0.1$ kg. If the wave impedance is chosen $b = 10000$ Ns/m then the perceived mass is increased to $m_h = 1000$ kg.

Result: At high delay environments without spring characteristics are transparent only if the wave impedance is tuned to a very small value, otherwise an inertia proportional to the time delay is perceived.

Communication Induced Stiffness Reduction

If the environment exhibits spring characteristics (cases 2, 5, 6, and 8 in Table 3.1) the operator perceives a substantially reduced stiffness. The environment feels softer.

An interesting result is the nonlinear dependency of the perceived stiffness coefficient (3.13) of the communication delay and the environment stiffness as shown in Fig. 3.5. In fact, the communication subsystem together with the environment behave like a serial connection of mechanical impedances. In contact with a stiff environment a stiffness of $T/2b$ is associated to the communication subsystem verifying the results from [143]. At high environment stiffness any additional delay substantially decreases the perceived stiffness, percentually more than with low environment stiffness. With high communication delay the same additional delay has less impact on the perceived stiffness. Higher values of the wave impedance result in less impact of the communication delay on the percentual reduction of the perceived stiffness, see Fig. 3.6.

Example: Consider a stiff wall with $k_e = 30000$ N/m, and the wave impedance tuned to $b = 1$ Ns/m. Already a very small round-trip delay of $T = 1$ ms substantially decreases the perceived stiffness to $k_h = 1875$ N/m, a reduction by 94%. At a delay of $T = 200$ ms the operator perceives only a stiffness of $k_h = 10$ N/m, hence 0.03% of the environment

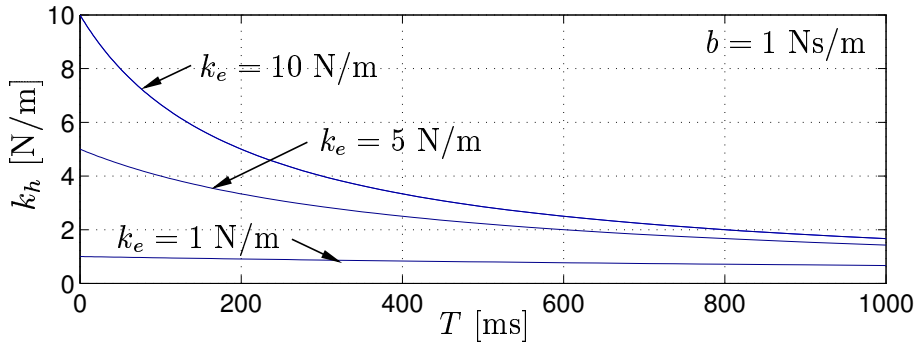

Figure 3.5: Perceived stiffness in contact depending on delay for different environment stiffness coefficients.

stiffness. Contacting a soft environment with $k_e = 10$ N/m, see Fig. 3.5 and Fig. 3.6, the perceived stiffness at $T = 1$ ms is still $k_h = 9.95$ N/m, at $T = 200$ ms still $k_h = 5$ N/m.

Increasing the wave impedance for the hard wall to $b = 10000$ Ns/m at $T = 1$ ms the perceived stiffness is $k_h = 23700$N/m. Still a wall characteristics is perceived as according to psychophysic studies [141] a wall feels like a wall above 24200 N/m. Recall that the inertia in free space from the previous example is increased with these values.

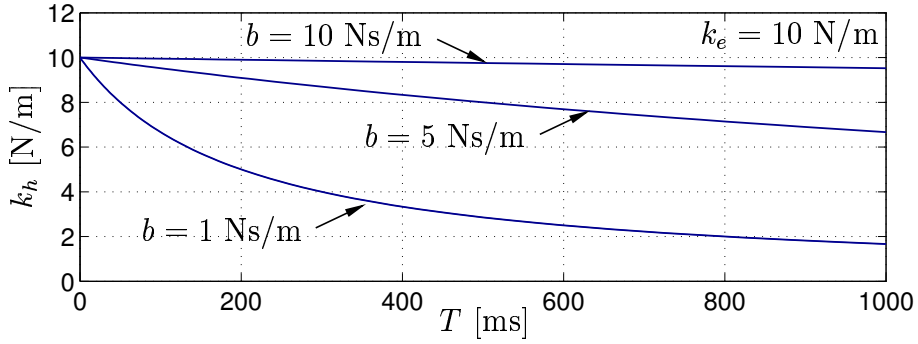

Figure 3.6: Perceived stiffness in contact depending on delay for different wave impedances and constant environment stiffness.

Result: Soft environments are generally more transparent than hard environments. Any additional delay results in higher percentual reduction of the perceived stiffness at low than at high delay. At high delay the spring characteristics of the environment is transparent only with a high wave impedance value. This contradicts the design rule for environments without spring characteristics.

Communication Induced Stiffness Bound

Another interesting result from the stiffness analysis for spring environments (cases 2, 5, 6, and 8 in Table 3.1) is that the perceived stiffness can never exceed a certain value $k_h \leq k_{h,\max}$. This result is indicated in Fig. 3.7 by the asymptotic behavior of the perceived stiffness for increasing environment stiffness. Independent of the environment stiffness the perceived stiffness (3.13) is never higher than

$$k_{h,\max} = \lim_{k_e \to \infty} k_h = \frac{2b}{T}, \tag{3.15}$$

determined by the communication delay T and the wave impedance b. The maximum perceivable stiffness is depicted in Fig. 3.8.

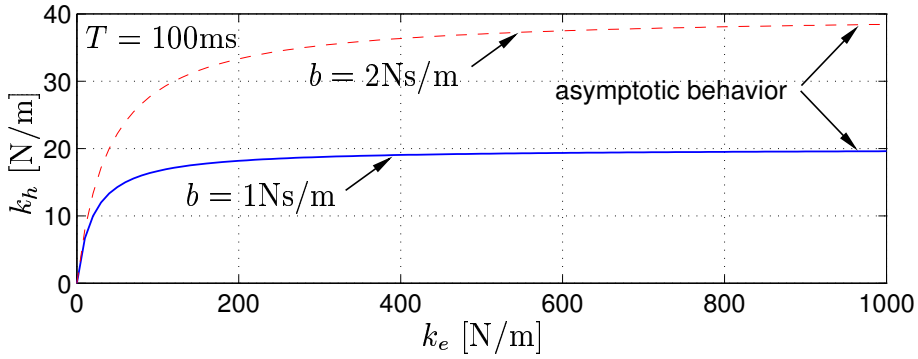

Figure 3.7: Perceived stiffness depending on environment stiffness.

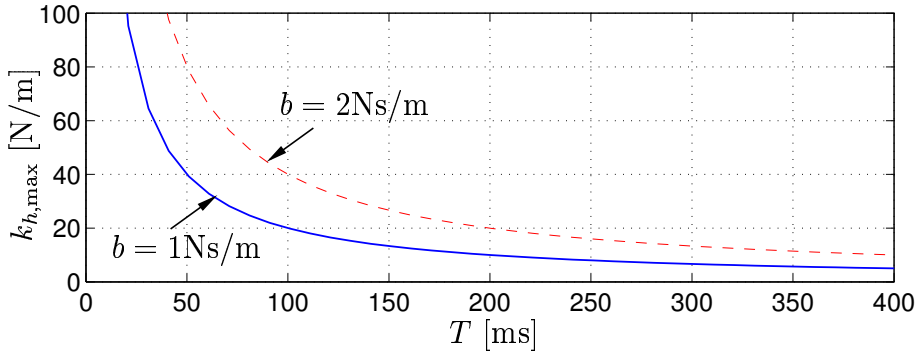

Figure 3.8: Maximum displayable stiffness depending on communication delay.

Example: Assuming a communication delay $T = 200$ ms with a wave impedance tuned to $b = 1$ Ns/m the maximum displayable stiffness is only $k_{h,\max} = 10$ N/m. Any stiff environment feels much softer.

Result: At high delay the stiffness, especially in case of hard walls, is not transparent. Appropriate tuning (high values) of the wave impedance increases the transparency in terms of the maximal displayable stiffness.

Bounded Perceivable Environment Stiffness Change

In some tasks not only the absolute value of the perceived stiffness is important but also the possibility to distinguish between differently stiff environments. This is especially important for soft environments (e.g. in tele-surgery), where different characteristics have to be distinguished.

As indicated by the asymptotic behavior of the perceived stiffness in Fig. 3.7 at higher values of the environment stiffness any stiffness change in the environment results in a very small change in the perceived stiffness. This is also observable in the mapping from the percentual change in the environment stiffness Δk_e on the change in the perceived

stiffness Δk_h

$$\Delta k_h = \frac{2b\Delta k_e}{2b + T(1+\Delta k_e)k_e^0} \quad \text{with} \quad \Delta k_i = \frac{|k_i - k_i^0|}{k_i^0}, \quad i \in \{h, e\},\ k_i^0 \neq 0. \tag{3.16}$$

The values denoted by ^{0} represent the reference values, with $k_h^0 = k_h(k_e^0)$ according to (3.13). The change of perceived and environment stiffness is equal only for the marginal cases of zero delay or infinite wave impedance. At high delay and high environment stiffness a large change in the environment stiffness may result in a very small change of the perceived stiffness.

From psychophysical studies it is well-known that the human may not distinguish between stiffnesses if the difference is smaller than a certain threshold, the just noticeable difference (JND), see Section 2.3.2. Note, that the definition of the percentual stiffness change Δk in (3.16) is equal to the definition of the JND (2.18), hence the results from psychophysics can directly be carried over. The interesting question in this context is, in which range of the environment stiffness the perception of its change is possible. Due to the asymptotic behavior of the perceived stiffness over the environment stiffness the upper bound clearly defines the constraint. As the upper bound we define the highest value $k_{e,\max}$ of the environment stiffness at which a human is able to detect the change to a very large (mathematically infinite) value of environment stiffness. According to the boundness result of the perceived stiffness the value $k_{e,\max}$ corresponds to the perceived stiffness $(1 - JND)k_{h,\max}$. As the JND for stiffness reported in literature highly varies depending on experimental conditions (23% in [66] for cross-limb, 8% in [139] in the context of work/maximum force applied) the upper bound for the environment stiffness is depicted in Fig. 3.9 depending on the delay for two JND assumptions.

Example: Let us assume the wave impedance is $b = 1$ Ns/m and the communication delay is $T = 200$ ms. If the environment stiffness coefficient is larger than $k_{e,\max} = 40$ N/m than a positive change is not perceptable under the 23%-JND assumption, for a JND of 8% the bound is at $k_{e,\max} = 130$ N/m.

Result: At high delay a change in the environment stiffness may not be perceivable anymore, especially at high environment stiffness values. Appropriate tuning (high values) of the wave impedance increases the transparency in terms of the range of environment stiffness where a change is perceptable.

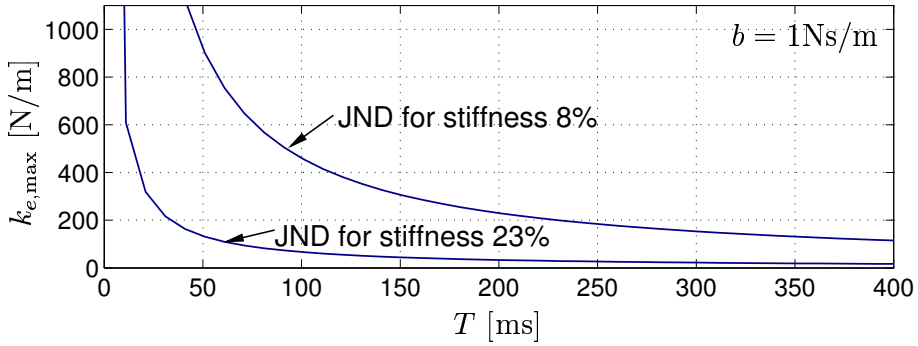

Figure 3.9: Maximum allowable environment stiffness depending on communication delay.

Remark 3.2 As investigated before, transparency can be increased in a limited range by the proper adjustment of the wave impedance b. This can be interpreted as matching the wave impedance to the environment impedance in a very limited frequency range. We have investigated methods that allow the impedance matching over a broad frequency range by the introduction of appropriately designed dynamic filters resulting in a substantially increased transparency. This approach together with a novel design method for the so-called impedance matching filters is introduced in Section A.3.

3.3 Experiments

The first goal of the experiments is the validation of the theoretically obtained dependency of the perceived impedance parameters from the round-trip time delay. Therefore, an objective transparency evaluation is performed, see Section 3.3.1.

Given the analytical relation between the time delay and the perceived impedance parameters the question arises, whether the transparency with time delay can be evaluated based on the numerous evaluation results from psychophysical studies in terms of discrimination thresholds for mechanical parameters, see Section 2.3.2. The second goal of the experiments is to give a first indicator for answering this question. Therefore, psychophysical experiments are conducted, see Section 3.3.2. In both experiments, the prototypical cases of free space motion and contact with a stiff wall are investigated seperately.

Experimental Setup

For the experiments the experimental haptic telepresence system described in Appendix C is used. In order to seperately consider the prototypical cases, especially in the experiments performed with test persons, the real teleoperator including environment, shown in Fig. C.1 is here replaced by a virtual environment. In free space motion the environment force to be fed back is $f_e = 0$, in contact with the stiff wall the environment force is proportional to the penetration depth $f_e = k_e x_t$ with $k_e = 12500\,\mathrm{N/m}$. The communication subsystem, shown in Fig. C.1 consists of the communication line with constant delay and the wave variable transformation with the wave impedance set to $b = 125\,\mathrm{Ns/m}$.

3.3.1 Objective Transparency Evaluation

The perceived inertia m_h in free space motion and the perceived stiffness coefficient k_h in contact with the wall are determined depending on the round-trip delay that is varied within the interval $T \in [5,\ 400]$ms. The parameters m_h and k_h are determined by a least squares identification from the measured HSI position and HSI force signals.

Results

The results for the perceived inertia in free space motion are shown in Fig. 3.10 (a), and for the perceived stiffness in contact in Fig. 3.10 (b). The theoretically obtained dependencies of these parameters from the round-trip delay given by (3.10) and (3.13) are convincingly validated. The slightly reduced stiffness and higher inertia compared to the theoretical result from the limited bandwidth of the conservative force control loop at the HSI and from possible saturation of the motor current.

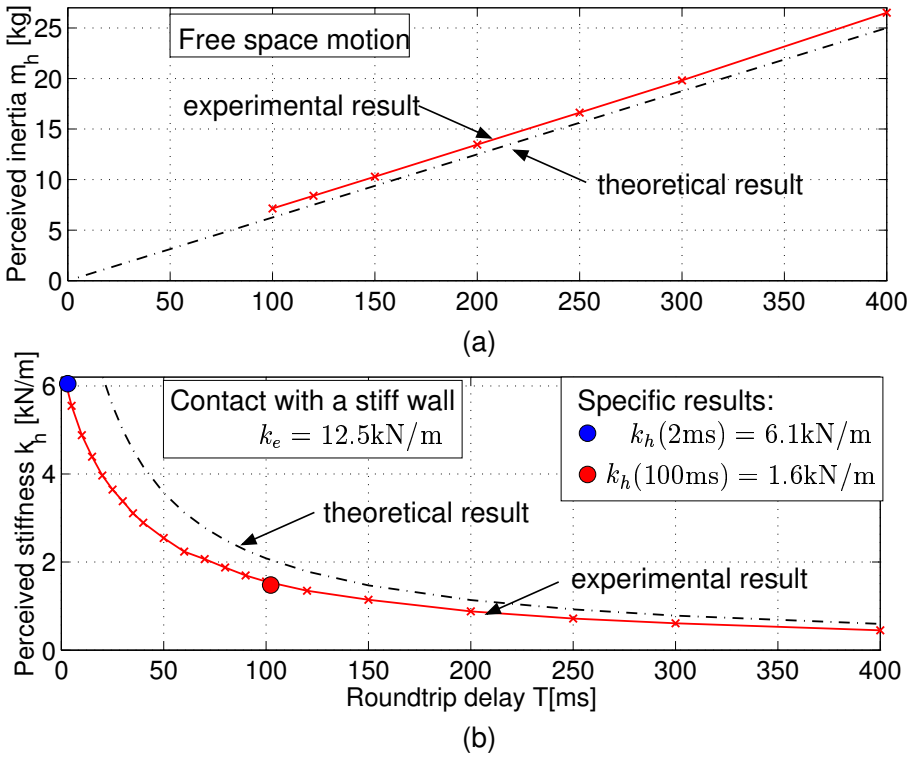

Figure 3.10: Experimentally obtained perceived inertia m_h (a) and stiffness coefficient k_h (b) depending on the round-trip delay T, comparison to theoretical results.

3.3.2 Evaluation considering Human Factors

The inspirational question is, whether widely known discrimination thresholds for the mechanical parameters such as inertia and stiffness can be used to estimate the influence of the time delay by using the results of this chapter. Aiming at the answer of this question preliminary experiments are conducted to evaluate the hypothesis from Section 3.2.2:

Hypothesis 3.1 A certain additional delay degrades the transparency more at low time delay than at high time delay.

The discrimination thresholds for the time delay $\Delta T = T - T_0$ are determined, where T_0 represents a reference round-trip delay. Four experiments with test persons are performed for two different reference round-trip delays $T_0 = 2\text{ms}$ and $T_0 = 100\text{ms}$ for each of the considered prototypical cases 'free space motion' and 'contact with a wall' using the same parameters as in the foregoing experiment. Therefore, the well-known three interval forced choice (3IFC) paradigm is applied.

Background on the Three Interval Forced Choice (3IFC) Paradigm

The 3IFC paradigm is a common experimental tool in psychophysics to determine discrimination or detection thresholds in human haptic perception, see [38]. The main feature is that the subjects are presented three time intervals, two with a reference value of the interesting parameter, one with the reference parameter value changed. The subject then has to tell which of the intervals felt different.

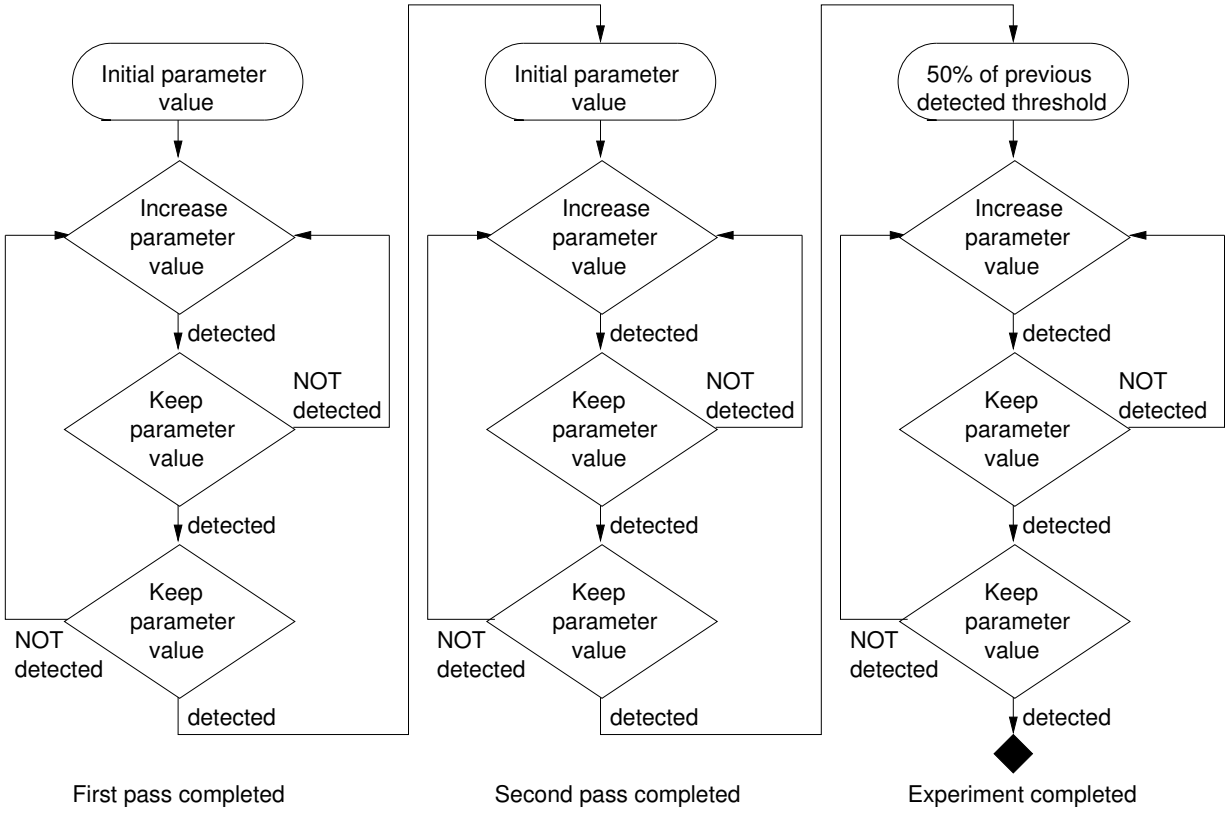

Figure 3.11: Visualization of the 3IFC paradigm.

In order to obtain reliable results, the procedure visualized in Fig. 3.11 is followed. In an initial familiarization phase the subjects perform the experiment with the reference value. Then the first pass starts with the smallest initial value of the interesting parameter. This value has to be chosen, such that a detection is very unprobable. The subjects are presented with the three consecutive intervals in which they perform the experiment. The interval with the changed parameter is chosen randomly out of the three. Every three intervals the subject have to tell which of the intervals felt different than the other two. The deviation from the reference parameter value is increased after every incorrect answer. When an answer was correct, the same value was used again until 3 consecutive right answers were given, completing the first of three passes. From the corresponding parameter value the discrimination/detection threshold for this pass is computed. The initial value for the second pass is the same as in the first, in the third pass the initial value is 50% of the most recent detected threshold value. The subjects are not told when a new pass starts.

The average of the discrimination/detection thresholds of the three passes is taken as the detection threshold for the specific subject.

Conditions

Altogether 7 subjects (aged 20–30, 3 female, 4 male, 2 with prior contact to the experimental system). The subjects were told to operate with their preferred hand. They were equipped with earphones to mask the sound the device motors generate. Visual feedback was not provided.

In order to determine the discrimination thresholds for the time delay difference, the three interval forced choice (3IFC) paradigm was applied, see above for more details on the experimental procedure. The reference round-trip delay was applied in two of the three intervals, in the other interval, which was randomly determined, the round-trip delay was increased. Each interval had a length of 20s. The experiment started with a delay of $T_{2\text{ms}} = 3\text{ms}$ ($T_{100\text{ms}} = 103\text{ms}$), i.e. a delay difference of $\Delta T_{2\text{ms}} = 1\text{ms}$ ($\Delta T_{100\text{ms}} = 3\text{ms}$), where the subscript $_{2\text{ms}}$ indicates a reference round-trip delay of $T_0 = 2\text{ms}$, and accordingly $_{100\text{ms}}$ $T_0 = 100\text{ms}$.

Results

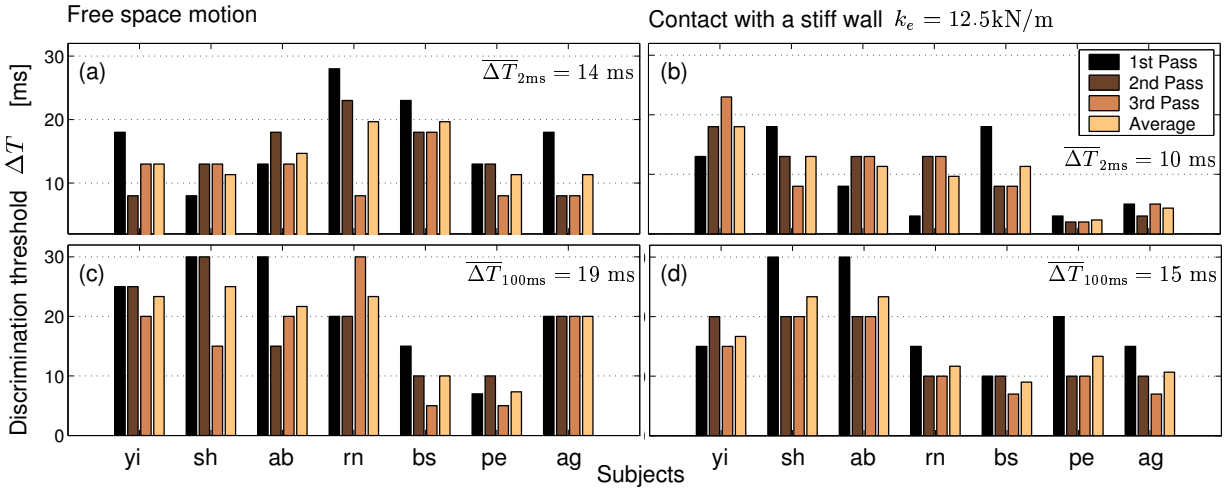

Figure 3.12: Results of psychophysical experiment: discrimination thresholds for delay ΔT at reference delays $T_0 = 2\text{ms}$ (a), (b) and $T_0 = 100\text{ms}$ (c), (d) for free space motion (a), (c) and contact with a stiff wall (b), (d).

The specific results for the subjects for all four experiments are shown in Fig. 3.12, including the average for each subject, which is taken as specific discrimination threshold, and the average $\overline{\Delta T}$ over all subjects.

The gain between the specific discrimination thresholds $\Delta T_{2\text{ms}}/\Delta T_{100\text{ms}}$ is computed for both situations, 'free space motion' and 'contact with the wall'. In both situations 5 out of the 7 subjects, i.e. 81% of the test persons, detected a lower delay difference for the low delay reference as indicated by the gain lower than one in Fig. 3.13.

For further analysis the Student's test (also called T-test) is performed giving a statement about the statistical significance of the average discrimination thresholds difference $\Delta T_{2\text{ms}} - \Delta T_{100\text{ms}}$. For 'contact with the wall' the mean discrimination threshold for low reference delay is statistically significant (95%) smaller than for high reference delay $\overline{\Delta T}_{2\text{ms}} < \overline{\Delta T}_{100\text{ms}}$, for 'free space motion' it is not significant (90%) in a statistical sense. However, a more significant result is to be expected for more test persons.

In fact, for 'contact with the wall' the detected average delay differences correspond to percentual stiffness differences (3.16) that are in the range of the percentual stiffness JND results of 8% [139] and 23% [66], see Table 3.2. The percentual stiffness difference is computed from the experimentally determined, perceived stiffness in Section 3.3.1, see Fig 3.10.

The average discrimination threshold $\overline{\Delta T}_{2\text{ms}} = 10\text{ms}$ corresponds to a change in the perceived stiffness of 20%, and $\overline{\Delta T}_{100\text{ms}} = 15\text{ms}$ to a change of 10%. In free space motion the percentual change in mass[1] of 17% corresponding to the average discrimination threshold $\overline{\Delta T}_{100\text{ms}} = 19\text{ms}$ is below the reported values in literature (21% [14] to 113% [119]), but mass is anyway suspected of not [64] following Weber's law (2.18), see also [154].

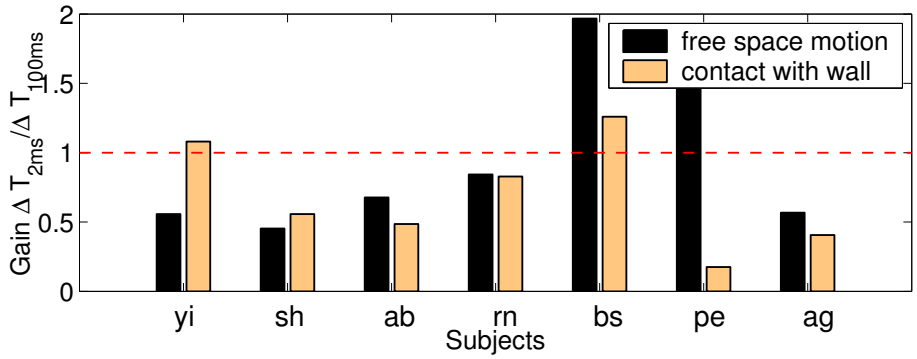

Figure 3.13: Results of psychophysical experiment: Gain between specific detection thresholds $\Delta T_{2\text{ms}}/\Delta T_{100\text{ms}}$; gains lower than one are as expected from theory, i.e. indicate the validity of Hypothesis 3.1.

Table 3.2: Results of psychophysical experiment: Average detected delay differences and corresponding percentual parameter changes for different reference time delays T_0.

		Free space $T_0 = 2\text{ms}$	Free space $T_0 = 100\text{ms}$	Contact $T_0 = 2\text{ms}$	Contact $T_0 = 100\text{ms}$
$\overline{\Delta T}$	[ms]	14	19	10	15
$\lvert m_h^0 - m_h \rvert$	[kg]	n.a.[1]	0.048		
Δm_h	[%]	n.a.[1]	17		
$\lvert k_h^0 - k_h \rvert$	[kN]			1.2	0.16
Δk_h (3.16)	[%]			20	10

As a result, the discrimination threshold for time delay is lower for low round-trip delay, in contact with a wall as well as in free space motion. Using the obtained mapping on the mechanical parameters, the contact feels earlier softer, and the perceived inertia larger at low reference time delay. This validates the Hypothesis 3.1. ■

Discussion

This result is highly interesting with respect to haptic telepresence in packet switched networks. It gives directions for the design of data buffering strategies that naturally introduce additional delay, see Section 2.2.2 for an overview and Chapter 4 for detailed investigations.

[1] The mass for low reference delay $T_0 = 2\text{ms}$ could not be identified from the sensor signals in Section 3.3.1. Accordingly, the corresponding percentual changes in mass are not available (n.a.) in Table 3.2.

Further, the results indicate that the effect of the time delay on the transparency of the haptic telepresence system to some extend can be evaluated by the easily computable mechanical parameters of the perceived impedance, at least the discrimination thresholds for the contact case correspond to the known discrimination threshold for stiffness.

Clearly, the conducted psychophysical experiments have a preliminary character and represent a first step towards a psychophysical evaluation of the time delay influence on transparency. Due to the low number of persons tested a generalizable statement is not possible, but a direction is indicated. For the targeted mapping of discrimination thresholds for mechanical parameters on the discrimination threshold for the time delay further reference experiments under the same conditions without time delay and the variation of the mechanical parameters, instead, are necessary. Visual feedback would extend the scope of the time delay transparency influence analysis to a performance analysis in multi-modal telepresence.

3.4 Discussion

The transparency of a haptic telepresence system is generally deteriorated by communication effects such as time delay. Generic approaches to evaluate the transparency from a human perception point of view are not available in the known literature. Therefore, the goal of this chapter is to develop measures and tools to quantify the degradation induced by communication effects from a human perception point of view.

In this chapter a generic method for the systematic evaluation of the influence of communication induced disturbances on the transparency is developed. In order to apply well-known results from psychophysical studies on human haptic perception limits, the transparency is measured based on the mechanical parameters of the perceived impedance, such as stiffness, inertia, and damping. However, these parameters are in most cases difficult to derive analytically. Therefore, two approximation methods are proposed. The developed low frequency approximation leads to an analytical mapping from the communication and environment parameters to the perceived impedance parameters, but this method requires an analytical representation of the perceived impedance as a function of the communication and environment parameters. Such a function is not always available, for instance for stochastic packet loss; therefore, a more generic optimization-based approximation of the perceived impedance is proposed, also valid for higher frequencies.

With the developed tools the transparency analysis is performed for the special case of constant time delay for a one-degree-of-freedom system. Similar results are expected for multi-degree-of-freedom systems under the reasonable assumption that the degrees of freedom are independent from each other, i.e. decoupled, e.g. by computed torque or other control. The interpretation of the results reveals interesting insights, not yet reported in the known literature, with implications for the control design in packet switched communication networks and the range of tele-applications with regard to the allowable time delay. The most important results are summarized:

- There exists a maximum perceivable stiffness, which depends on the round-trip delay and the wave impedance.
- Higher delay and higher environment stiffness makes the differentiation between differently stiff environments harder.

- Additional delay results in higher transparency degradation for low reference delay.

The results obtained from the transparency analysis are validated in objective experiments. Experimental user studies indicate that the proposed transparency measure give a very good insight about for the human perceived transparency. In order to determine, whether detection thresholds for communication parameters such as time delay can be *directly* computed from the known detection thresholds for mechanical parameters using the obtained mapping, further psychophysical experiments are necessary.

The transparency analysis methods presented in this chapter form a very important basis for the transparency investigations of the following chapters.

4 Control in Packet Switched Communication Networks

The Internet is the most attractive medium for data transmission in telepresence systems. The main advantages are the worldwide coverage, easy access, low cost, and flexibility. However, packet switched communication networks, the general class the Internet belongs to, provide a transmission in data packets that are afflicted with unpredictable time-varying delay and loss. Without further measures, a control system with the loop closed over a packet switched network is unstable.

Only few researchers have investigated haptic telepresence over packet switched communication networks or at least the related challenges of time-varying delay and packet loss. Most of the known approaches are based on the passivity paradigm using the wave variable transformation, see Section 2.2.2 for a detailed discussion of the related approaches. Time-varying delay is targeted in [73, 90, 136, 160], only few approaches additionally target the problem of packet loss or communication blackouts [106, 161], not considering though the packet oriented nature of packet switched communication networks. Packet loss generally results in empty sampling instances at the receiver side. The resulting problem of data reconstruction has recently been studied in [15, 52, 125]. However, approaches assuming an upper bound on the time delay [73, 136] or a maximum number of consecutive packets lost [125] are not appropriate for the deployment in current packet switched communication networks. A systematic approach to haptic telepresence in packet switched communication networks does not yet exist. The effects on transparency have not been investigated yet.

The main innovation of this chapter is the systematic consideration of haptic telepresence in packet switched communication networks providing a framework for the design of stabilizing control strategies. The focus is on the reconstruction of lost data and data that arrive too late. Passivity conditions for the data reconstruction are established. The few existing approaches are classified therein, and novel strategies are introduced. With the transparency evaluation tool developed in Chapter 3 a performance analysis is carried out in order to compare different approaches. The results are validated in objective experiments and experimental user studies.

The remainder of this chapter is organized as follows: The main features of packet switched communication networks are studied in Section 4.1, the resulting control relevant model of the haptic telepresence system is introduced in Section 4.2. The time-varying delay problem is targeted in Section 4.2.2. Main focus is on the passive data reconstruction, required for time-varying delay as well as for packet loss. Passivity conditions for the data reconstruction are established in Section 4.3. Further, the analysis of data reconstruction strategies and the introduction of novel approaches is performed therein. Finally, the investigated approaches are analyzed with respect to their transparency in Section 4.4, the results are validated in experiments in Section 4.5.

4.1 Background on Packet Switched Communication Networks

In a packet switched network the communicating end systems exchange information in terms of data packets. Between source and destination, each of these packets traverse communication links, routers and switches. A packet arriving at a router is first stored in the input buffer (also called queue) and then processed as fast as possible to the output buffer that is assigned to the appropriate next communication link on the path. From the output buffer it is transmitted to the next router until the packet reaches its destination.

A main feature of packet switched communication networks is that multiple users run their network applications at the same time sharing the limited resources of the network. The resources are mainly defined by the physical bandwidth of the links being the amount of data that can be transmitted within a certain time interval, and the finite queue sizes in the routers. As the resources are not reserved for an individual application, multiple applications compete for the resources needed and thereby affect the transmission characteristics. Generally, no guarantees for the transmission quality can be given in Internet Protocol (IP) based networks that are considered here.

4.1.1 Network Characteristics and Stochastic Parameter Models

The communication characteristics mainly depend on the network traffic load and the number of nodes. In large scaled packet switched communication networks, as e.g. the Internet, the network traffic is largely unpredictable. Stochastic models are used to model the behavior of the network as seen by an application. The main effects, time-varying delay and packet loss, are studied in the following.

Time Varying Delay

Along the path across the network the packet suffers from several different types of delay. The most important of these delays are the queuing delay, the transmission delay, and the propagation delay; together, these delays accumulate to the total network induced delay.

- The *queuing delay* results from the fact that the packet may have to wait in the input buffers and also in the output buffers of the routers due to other traffic using the same path. The queuing delay may substantially vary over the time depending on the traffic intensity along the path and the routing policies, it is the most significant portion of the overall delay.

- The *transmission delay* is the amount of time required for the routers to push out the packet onto the outgoing links. It is a function of the packet's length and the bandwidth of the traversed links. As the path in a dynamically routed network may vary over time and such the experienced link bandwidth, the transmission delay may vary even in the case of fixed packet length. Generally, the amount of data transferred within one packet in haptic telepresence application is very low, such that this type of delay is a small partition of the overall delay.

- The *propagation delay* depends purely on the characteristics of the physical medium and the distance between the source and the destination. As the path through the network may vary, a slight variation of this delay portion is possible.

In summary, the time-varying delay experienced by the data packets consists of a deterministic component, the minimum time delay determined by the minimum accumulated propagation and transmission delay for a dedicated path. The delay variation, mainly introduced by the queuing delay along a path, is very difficult to model. Stochastic models are generally used to model the network delay variation. Very common are heavy tail distributions, such as Gamma and Poisson like distributions [94]. However, these uncorrelated models may not capture the traffic burstiness, an empirical fitting of a single distribution to model network delay is almost not possible [109]. Therefore, more sophisticated models are based on hidden Markov chains with the states characterized by the network load and associated with a shape of the distribution.

The choice of the delay model will not have any impact on the stability considerations, hence we will assume the well-known Poisson distribution [19] as a simple model for the delay variation.

Remark 4.1 Time-varying delay is in the literature commonly characterized by the parameters latency and jitter. The notion of latency describes the expected value of the time delay. The variability of the delay (not necessarily the delay variance) is commonly termed jitter.

Packet Loss

Since the amount of buffer space in the routers is finite, an arriving packet may find that the buffer is completely filled with other packets waiting for transmission. In this case, packet loss will occur; either the arriving packet or one of the already queued packets will be dropped.

The most simple models assume an uncorrelated probability of packet loss. As before for the time-varying delay, these model cannot describe the observed bursty packet losses as they often occur in packet switched communication networks. Therefore, models with correlated probability are appropriate such as the well-known Gilbert model which is based on a two-state hidden Markov model. Here, the loss probability of a packet is influenced by the state of the previous packet. The system can completely be described by the probability $P_{g,b}$ for a transition from the state 'G' ('good', no packet loss) to the state 'B' ('bad', packet loss) and the probability $1 - P_{b,g}$ to remain in the state 'B', see Fig. 4.1. The probability of being in state 'B', the mean loss probability P_l^0 (called unconditional loss probability) can be computed by $P_l^0 = P_{g,b}/(P_{b,g} + P_{g,b})$.

In our investigations we will consider both, a simple model with an independent, uncorrelated, uniformly distributed packet loss probability and a Gilbert model.

Effect of the Transport Protocol

The network topology, the routing policy and the traffic volume determine the transmission quality. However, the effective delay and loss seen by the processes in the end-systems, i.e. the HSI and the teleoperator, are further influenced by the transport protocol applied. The

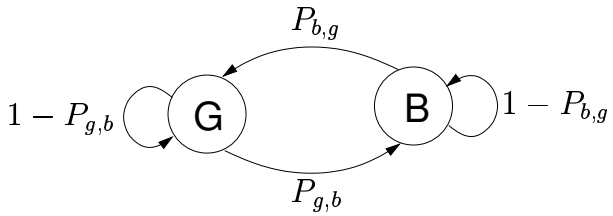

Figure 4.1: Markov chain for packet loss or delay, 'G' denotes the 'good' state - no packet loss or low network load, 'B' the 'bad' state - packet loss or high network load.

transport protocol provides the logical communication between the processes in the end-systems. In IP based networks two protocols are available, namely the TCP (Transmission Control Protocol) and the UDP (User Datagram Protocol).

The TCP provides a reliable service as it detects packet loss and resends the data resulting in a significantly increased delay for the affected packet. Furthermore, the congestion control of TCP, i.e. the sending rate adaption known as window behavior may result in increasing delay. As the protocol overhead is high in relation to the small packet loads common in haptic telepresence systems the additional traffic induced by TCP is high. In summary the TCP trades increased jitter, higher latency to zero packet loss. This trade-off is visualized in Fig. 4.2 where the original network state described as triple of the parameters latency, jitter and packet loss probability is mapped by TCP to the higher latency and jitter, but zero packet loss as seen by the end-systems.

The UDP is an unreliable protocol as it does not recover packet loss. As no implicit congestion control or other services are provided the protocol overhead is comparably low. The UDP does not significantly change the transmission characteristics seen by the processes in the end systems compared to the network induced characteristics, see Fig. 4.2.

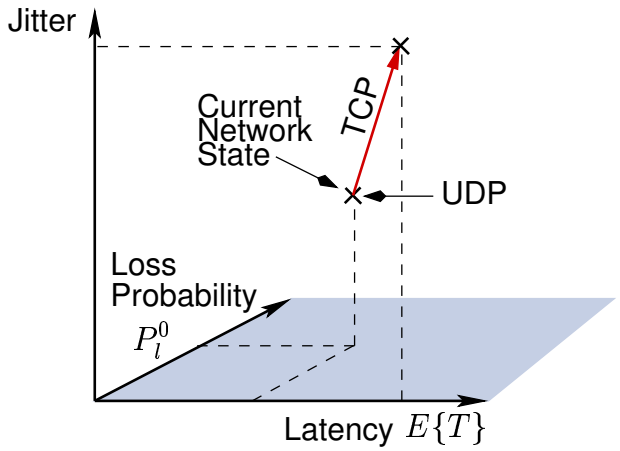

Figure 4.2: Effect of transport protocols TCP and UDP on the communication quality seen by the application in the end systems.

The network traffic of closed loop control systems operated over a network such as haptic telepresence systems and networked control systems is characterized by high packet transfer rates in the range of the sampling rate of the end systems HSI and teleoperator. The packet rate is not flexible in general, hence the rate adapting congestion control of

TCP is not appropriate. The packet loads in such systems are comparably small, as a result the additional traffic induced by the protocol overhead of TCP is high. The resend algorithm of TCP is useless in such time critical applications. For these reasons in networked telepresence systems the UDP is preferred over the TCP with its inferior real-time characteristics, see also [110] for further arguments. The following considerations assume the communication over an IP based network with the UDP as transport layer protocol.

4.2 Control Relevant Model

For the remainder of this chapter the haptic telepresence system is modeled as a sampled-data system. The subsystems HSI/human and teleoperator/environment together with the local control are assumed to be passive continuous time systems, whereas the communication subsystem including the network and the control measures such as the wave variable transformation is considered to be a discrete time system. It is known that the discretization of the power variables may inject energy hence is not passive. An energy consistent hence passive discretization is proposed in [135, 137]. For the following considerations the discretization of the power variables, i.e. the interconnection between the continuous and the discrete time system is assumed to be passive.

The sampling interval is assumed to be equal at the HSI and the teleoperator side. Denoting the independent variable by k, $x(k)$ indicates the value of the discrete variable $x(t)$ corresponding to the interval $t \in [kT_A, (k+1)T_A)$ with T_A being the sampling interval. Discrete time wave variable transformation, see [137], is applied to the sampled power variables using the transformation equations given by (2.8) in discrete time now with the independent variable k. Each sample of the wave variable $u_l(k)$ ($v_r(k)$ for the backward path) is packed into a single data packet as soon as the data is available. No buffering at the sender side is considered. The data packets are put on the outgoing link in equidistant time intervals equal to the sampling interval T_A. Hence the network sampling rate in terms of the packet sending rate is equal to the sampling rate of the power variables.

4.2.1 Control Relevant Network Effects

The effects of time-varying delay and packet loss, relevant for the analysis and synthesis of control strategies, are investigated in the following.

Effect of Time Varying Delay

During transmission over the network each of the data packets experiences a time-varying link delay of $T(k)$; $T_1(k)$ denotes the delay in the forward, $T_2(k)$ in the backward path. As a result of decreasing delay in dynamically routed multi-path networks the packets may arrive at the receiving queue in permuted order. Increasing delay may result in empty sampling instances at the receiver side. The probability of empty sampling instances and out-of-order order arrivals increases with rising jitter and increasing sampling rate.

Example: For illustration the first row of Fig. 4.3 shows the data packets in their sending order, the second row depicts the arriving order at the receiver. The delay increases from $k = 1$ to $k = 2$ resulting in an empty sampling instance at $k = 7$. The delay decreases from $k = 3$ to $k = 4$, such that packet #4 passes packet #3 leading to a out-of-order arrival at $k = 9, 10$.

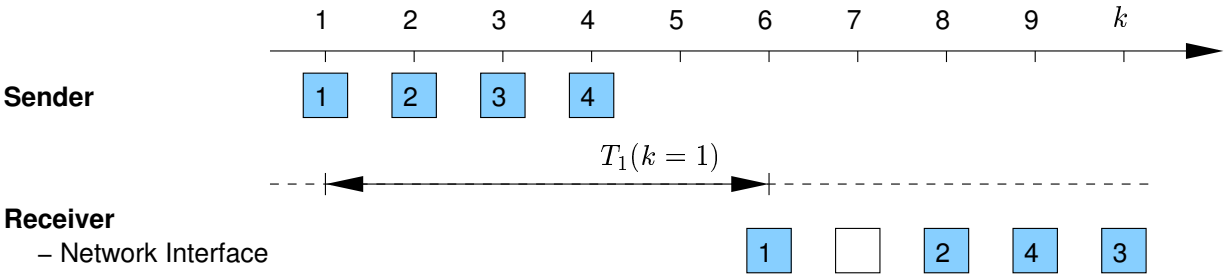

Figure 4.3: Effect of time-varying delay.

Effect of Packet Loss

In a congested network data packets are discarded at congested receive queues of intermittent routers resulting in packet loss. Packet loss leads to empty sampling instances at the receiver.

Example: In the first row of Fig. 4.4 the data packets are shown in their sending order. During transmission the packet #3 is lost. In result an empty sampling instance at the receiver side (second row) at $k = 8$ occurs.

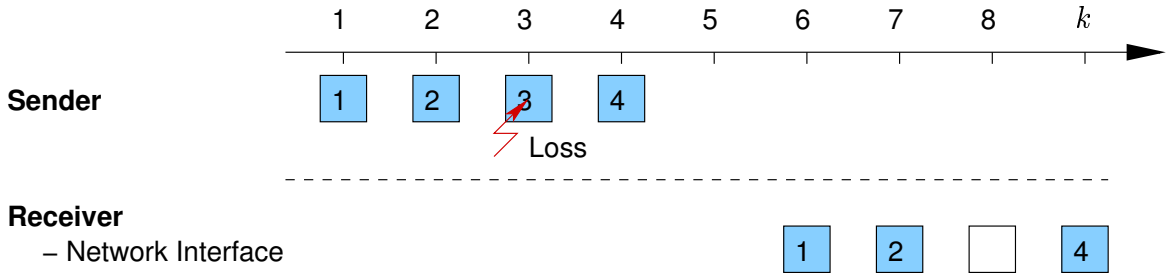

Figure 4.4: Effect of packet loss.

4.2.2 Definition of the Communication Subsystem

In summary time varying delay and packet loss result in delayed data transmission, out-of-order arrivals and empty sampling instances. Control strategies to cope with these effects can be incorporated into a framework for the communication subsystem design that includes the following three stages of control

- Packet processing,
- Data reconstruction, and

- Discrete wave variable transformation,

see Fig. 4.5 for a visualization.

Packet processing is associated with all data buffering strategies, either at the sender or the receiver side. At the sender side buffering will occur if multiple consecutive samples are sent within a single packet, this case though will not be considered in the following as it unnecessarily introduces additional time delay. Packet processing at the receiver side generally implies reordering [73, 136] of the arriving data packets, and discarding of packets that arrive to late [15, 52], hence handles the effects of time-varying delay. Therefore, the transmission of the packet sequence number and/or the time stamp within each data packet is required that is provided by the RTP (Real Time Protocol) as protocol on top of UDP. Packet processing generally introduces additional delay.

Either packet loss or the discarding of packets leads to empty sampling instances. The values of the missing data need to be estimated for the further processing in the local control loops at the HSI and the teleoperator. Therefore, a data reconstruction strategy is necessary [15, 52, 125]. The reconstructed values of the wave variables are then transformed by the discrete wave variable transformation to the desired values of velocity and force for the corresponding end-system, the HSI of the teleoperator.

The three stages of control together with the RTP/ UDP connection over the network constitute the communication subsystem. For the stability of the haptic telepresence system the passivity of the communication subsystem has to be verified. Thus, the control strategies have to be designed, such that the communication subsystem is passive. With the discrete wave variable transformation being a state-of-the-art control method the focus is on the design of the first and second stage of control, the packet processing and the data reconstruction. In our approach the packet processing handles the effects of time-varying delay as explained in the following.

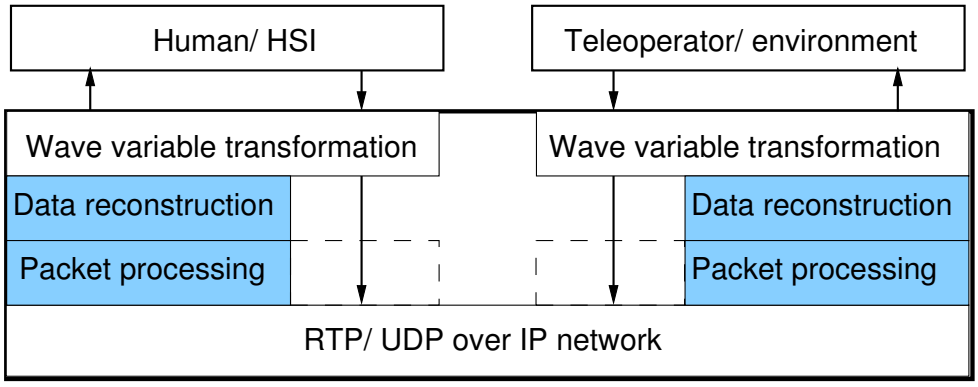

Figure 4.5: Definition of the communication subsystem, packet processing and data reconstruction represent the extension of the control strategy for packet switched communication networks.

Dejittering as Packet Processing Strategy

A packet processing strategy well-known from networked multimedia applications is dejittering. The arriving data packets are buffered and reordered according to their sequence

number/ time stamp. Data packets with lower delay are virtually delayed by $\Delta_{vd,i}(k)$ ($i = 1$ for the forward, and $i = 2$ for the backward path), such that each packet experiences the same predefined delay

$$T_i^* = T_i(k) + \Delta_{vd,i}(k) = \text{constant}.$$

In [73, 136] the delay is assumed to be bounded from above and the receive buffer is designed, such that each packet experiences the maximum communication delay. Full reordering can be performed then. However, no upper delay bound can be given in packet switched communication networks.

Other approaches [15, 52] discard all packets that arrive too late $T_i(k) > T_i^*$, thereby inducing an additional loss of data packets summarized under the notion of pseudo-loss.

Example: In Fig. 4.6 the packet #4 arrives before packet #2. Through dejittering the packets #1 and #4 are virtually delayed and reordered. Packet #3 is discarded as it arrives to late resulting in an empty sampling instance at $k = 9$. All other packets experience the constant time delay T_1^*.

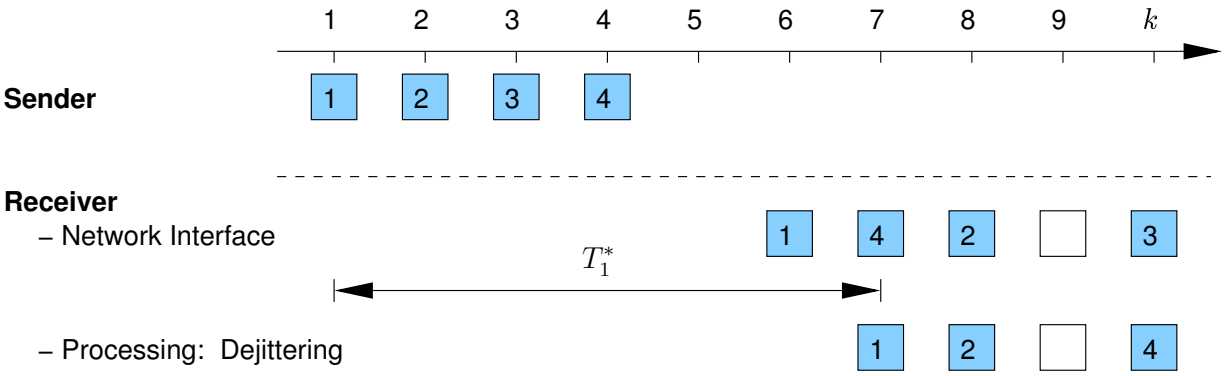

Figure 4.6: Effect of dejittering on transmission characteristics.

With the lower deterministic bound of the network induced time delay $T_{\min}$ and given a delay distribution with the probability density $p(T_i)$, such that

$$\int_{T_{\min}}^{\infty} p(T_i)\,\mathrm{d}T_i = 1, \quad i = 1, 2\,,$$

the probability $P_{l,i}^{\text{pseudo}}$ of pseudo-loss is

$$P_{l,i}^{\text{pseudo}} = \int_{T_i^*}^{\infty} p(T_i)\,\mathrm{d}T_i. \tag{4.1}$$

Clearly, the trade-off between additional virtual delay and pseudo-loss mainly depends on the definition of the chosen end-to-end delay T_i^* in the dedicated path and the networked induced delay distribution as visualized in Fig. 4.7.

Assuming that the delay distribution acts on the packets that are not lost due to network congestion the probability that a packet arrives in time $T_i \leq T_i^*$ is given by $(1 - P_{l,i}^0)(1 - P_{l,i}^{\text{pseudo}})$. Accordingly, the effective overall packet loss is given by

$$P_{l,i} = 1 - (1 - P_{l,i}^0)(1 - P_{l,i}^{\text{pseudo}}) = (1 - P_{l,i}^0)P_{l,i}^{\text{pseudo}} + P_{l,i}^0. \tag{4.2}$$

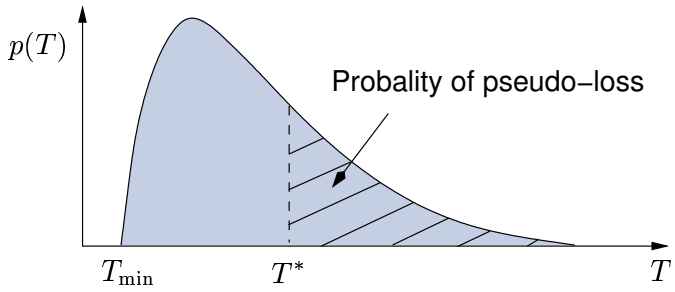

Figure 4.7: Effect of dejitter algorithm on pseudo-loss depending on delay distribution.

Generally, the described dejitter algorithm can be interpreted as a mapping from the network state parameter triple (latency $E\{T\}$, jitter, and packet loss probability P_l^0) to the tupel (constant delay T^*, packet loss probability P_l).

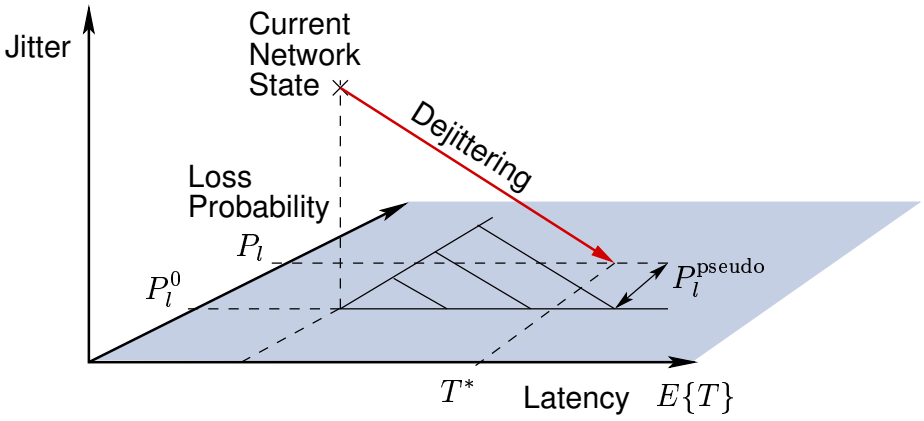

Figure 4.8: Effect of delay distribution on pseudo-loss with dejitter algorithm.

The next stage of control sees only constant delays T_1^*, T_2^* in the forward and the backward path and empty sampling instances with the probability $P_{l,1}^*$ at the teleoperator and $P_{l,2}^*$ at the HSI. The passivity and performance of data reconstruction strategies for the treatment of empty sampling instances are investigated in the next section.

4.3 Data Reconstruction

In order to preserve the passivity of the communication subsystem, the data reconstruction must not generate energy. In the following a passivity condition for the data estimation is established. The underlying control architecture including packet processing and data reconstruction is visualized in Fig. 4.9.

4.3.1 Conditions for Passive Data Reconstruction

Basic Assumptions and Preliminaries

For the following investigations the energy balance $E_{c,in}^{\zeta}$ of the communication subsystem with data reconstruction is considered in discrete time expressing (2.11) as a sum, with

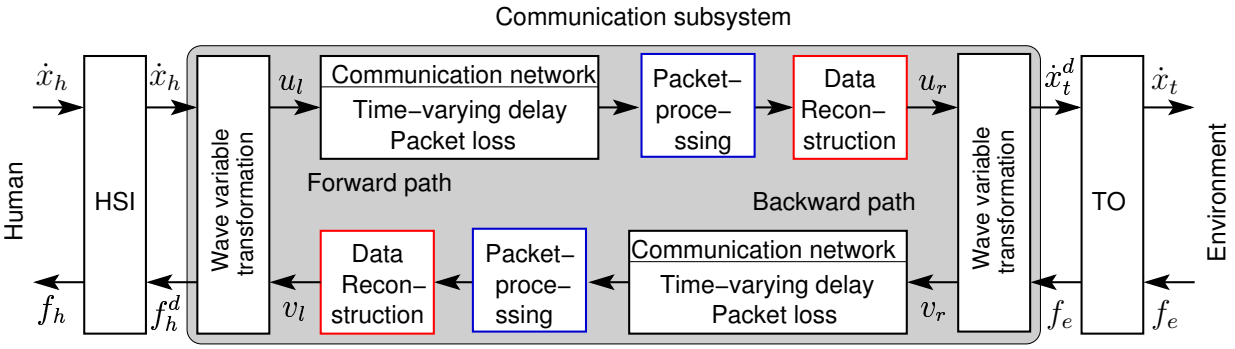

Figure 4.9: Haptic telepresence system in a packet switched communication network: control architecture with packet processing and data reconstruction.

discrete wave variable transformation applied on the discrete power variables yields

$$E_{c,in}^{\zeta}(N) = \sum_{k=0}^{N} u_l^2(k) - u_r^2(k) + v_r^2(k) - v_l^2(k). \tag{4.3}$$

The communication subsystem is passive, if and only if

$$E_{c,in}^{\zeta}(N) \geq 0, \quad \forall N \in \mathbb{Z}_+, \tag{4.4}$$

holds for all admissible inputs. As stated in Section 2.2.1, the structure of the overall storage function (4.3) allows a separate consideration of the energy balance for the forward and the backward path with $E_{cf,in}^{\zeta}$ defined analogously to (2.13) and $E_{cb,in}^{\zeta}$ analogously to (2.14) in discrete time

$$E_{c,in}^{\zeta}(N) = E_{cf,in}^{\zeta}(N) + E_{cb,in}^{\zeta}(N).$$

According to (2.13) and (2.14) for passivity it is sufficient that both of them are non-negative

$$E_{cf,in}^{\zeta}(N) \geq 0 \quad \text{and} \quad E_{cb,in}^{\zeta}(N) \geq 0, \qquad \forall N \in \mathbb{Z}_+. \tag{4.5}$$

The constant delay all packets except the lost ones experience including the additional delay through packet processing is assumed to be an integer multiple of the sampling interval T_A

$$T^* = DT_A, \qquad D \in \mathbb{Z}_+.$$

This assumption is for the ease of notation and is satisfied if the HSI and the teleoperator are synchronized. The delay in the forward path is denoted by D_1, in the backward path D_2. Let us further assume that the sending of packets at the HSI and the teleoperator start at the same time $k = 1$, hence the independent variable k can be further used to denote the packet index. This assumption is not necessary, but for the ease of notation.

Furthermore, a loss indicator is defined indicating the packets lost, either due to congestion or to packet processing

$$l(k) = \begin{cases} 0 & \text{if } k^{th} \text{ packet is lost} \\ 1 & \text{otherwise} \end{cases}. \tag{4.6}$$

A loss in the forward path is indicated by l_1, a loss in the backward path by l_2.

When an empty sampling instance occurs at the teleoperator at the time k due to loss $l_1(k - D_1) = 0$ in the forward path, the missing value of the wave variable $u_r(k)$ has to be estimated. Equivalently at the HSI the value of $v_l(k)$ has to be estimated, if the packet with the index $k - D_2$ has been lost $l_2(k - D_2) = 0$. A general reconstruction operator ζ_u at the teleoperator and ζ_v at the HSI is defined

$$u_r(k) = \begin{cases} \zeta_u(k - D_1) & \text{if } l_1(k - D_1) = 0 \\ u_l(k - D_1) & \text{otherwise} \end{cases}, \tag{4.7}$$

$$v_l(k) = \begin{cases} \zeta_v(k - D_2) & \text{if } l_2(k - D_2) = 0 \\ v_r(k - D_2) & \text{otherwise} \end{cases}. \tag{4.8}$$

The lower cases recover the well-known case for constant delay. This definition implies that the packet loss and thereby the data reconstruction does not effect the passivity of the communication subsystem during the time intervals where no loss occurs. During these time intervals the discrete wave variable transformation renders the communication subsystem passive. A separate consideration of the non-packet loss time intervals with constant delay and the packet loss time intervals is allowed as stated in the following lemma.

Lemma 4.1 The communication subsystem with data reconstruction can be split according to the cases in (4.7) and (4.8) into non-packet loss and packet loss time intervals, i.e. into time interval without and with vacant sampling instances. The sum of the energy balance over the corresponding time intervals yields the overall energy balance $E^{\zeta}_{c,in}(N)$ of the communication subsystem

$$E^{\zeta}_{c,in}(N) = E^{nl}_{c,in}(N) + E^{l}_{c,in}(N), \tag{4.9}$$

with

$$\begin{aligned} E^{nl}_{c,in}(N) =& \sum_{\substack{k=0 \\ l_1(k)=1}}^{N} u_l^2(k) - \sum_{\substack{k=0 \\ l_1(k-D_1)=1}}^{N} u_r^2(k) + \sum_{\substack{k=0 \\ l_2(k)=1}}^{N} v_r^2(k) - \sum_{\substack{k=0 \\ l_1(k-D_2)=1}}^{N} v_l^2(k) \\ =& \sum_{\substack{k=0 \\ l_1(k)=1}}^{N} u_l^2(k) - u_l^2(k - D_1) + \sum_{\substack{k=0 \\ l_2(k)=1}}^{N} v_r^2(k) - v_r^2(k - D_2) \\ =& \sum_{\substack{k=N-D_1 \\ l_1(k)=1}}^{N} u_l^2(k) + \sum_{\substack{k=N-D_2 \\ l_2(k)=1}}^{N} v_r^2(k), \end{aligned} \tag{4.10}$$

constituting the energy balance for the non- packet loss time intervals, and

$$\begin{aligned} E^{l}_{c,in}(N) =& \sum_{\substack{k=0 \\ l_1(k)=0}}^{N} u_l^2(k) - \sum_{\substack{k=0 \\ l_1(k-D_1)=0}}^{N} u_r^2(k) + \sum_{\substack{k=0 \\ l_2(k)=0}}^{N} v_r^2(k) - \sum_{\substack{k=0 \\ l_1(k-D_2)=0}}^{N} v_l^2(k) \\ =& \sum_{\substack{k=0 \\ l_1(k)=0}}^{N} u_l^2(k) - \zeta_u^2(k - D_1) + \sum_{\substack{k=0 \\ l_2(k)=0}}^{N} v_r^2(k) - \zeta_v^2(k - D_2). \end{aligned} \tag{4.11}$$

defining the energy balance for the packet loss time intervals.

The terms $E^{nl}_{c,in}(N)$ and $E^{l}_{c,in}(N)$ are straightforward to reconstruct by calculating the energy balance (4.3) with either the upper or the lower cases from (4.7) and (4.8). The left-hand sum in these equations represents the energy balance of the forward path $E^{nl}_{cf,in}(N)$ and $E^{l}_{cf,in}(N)$, the right-hand sum for the backward path $E^{nl}_{cb,in}(N)$ and $E^{l}_{cb,in}(N)$.

Remark 4.2 This model of the lossy communication subsystem with data reconstruction can be interpreted as a switched system with a common storage function.

With these preliminaries a necessary and sufficient condition for the passivity of the reconstruction algorithm and thereby for the passivity of the communication subsystem can be established.

Passivity Conditions

Theorem 4.1 The communication subsystem with the constant delays D_1 and D_2 in the forward and backward path, respectively, and the discrete wave variable transformation applied is passive iff

$$E^{l}_{c,in}(N) \geq 0, \quad \forall N \geq 0. \tag{4.12}$$

The passivity condition expresses that the energy of the reconstructed data should never exceed the energy of the data lost, otherwise energy is generated rendering the communication subsystem active.

Proof: According to the definition (4.9) the energy balance of the communication subsystem is the sum of the energy balances of the non-packet loss and the packet loss time intervals. During the non-packet loss time intervals the communication subsystem is energetically lossless. If for some N $E^{l}_{c,in}(N) < 0$ corresponding to energy generation during the packet loss time intervals then the overall system generates energy (*necessity*). On the other hand, if $E^{l}_{c,in}(N) \geq 0$ holds then energy is not generated during the packet loss time intervals. The communication subsystem then dissipates energy or is energetically lossless (*sufficiency*). ∎

The passivity condition (4.12) might be difficult to apply, therefore, a sufficient condition for passivity is given in the following.

Theorem 4.2 If the reconstruction algorithm is small gain hence satisfies the condition

$$|\zeta_u(k)| \leq |u_l(k)| \quad \text{and} \quad |\zeta_v(k)| \leq |v_r(k)|, \tag{4.13}$$

then the communication subsystem with the constant delays D_1 and D_2 in the forward and backward path, respectively, and the wave variable transformation is passive.

Proof: With this condition

$$\zeta^2_u(k - D_1) \leq u^2_l(k - D_1) \quad \text{and} \quad \zeta^2_v(k - D_2) \leq v^2_r(k - D_2),$$

holds. Inserting this into (4.11) renders the following inequality true

$$\begin{aligned} E_{c,in}^{l}(N) \geq & \sum_{\substack{k=0 \\ l_1(k)=0}}^{N} u_l^2(k) - u_l^2(k-D_1) + \sum_{\substack{k=0 \\ l_1(k)=0}}^{N} v_r^2(k) - v_r^2(k-D_2) \\ & \geq \sum_{\substack{k=N-D_1 \\ l_1(k)=0}}^{N} u_l^2(k) + \sum_{\substack{k=N-D_2 \\ l_2(k)=0}}^{N} v_r^2(k) \\ & \geq 0 \qquad\qquad \forall N \geq 0, \end{aligned}$$

thereby satisfying the passivity condition (4.12) developed in Theorem 4.1. Thus, if the data reconstruction algorithm satisfies (4.13) then the communication subsystem is passive. ■

Remark 4.3 The condition established with (4.13) is only sufficient. Thus, if (4.13) is not satisfied, the communication subsystem is not necessarily active.

Remark 4.4 The small gain condition on the reconstruction algorithm corresponds with the small gain requirement in the wave variable space resulting from the wave variable transformation and being necessary for stability of the loop in the presence of arbitrary delay, see Appendix B for a detailed discussion.

Remark 4.5 The small gain condition can be extended to general reconstruction operators without any assumption on the packet processing by requiring

$$\sum_{k=0}^{N} |u_r(k)| \leq \sum_{k=0}^{N} |u_l(k)| \quad \text{and} \quad \sum_{k=0}^{N} |v_l(k)| \leq \sum_{k=0}^{N} |v_r(k)|, \quad \forall N,$$

for passivity of the data reconstruction. The proof again uses the energy balance (4.3) of the communication subsystem.

Generally, all data reconstruction algorithms are passive that inject less or as much energy through estimation as the energy carried in the lost data packets.

Accordingly, a passive data reconstruction algorithm

- must not inject energy at all being equivalent for zero output in case of packet loss,
- or needs the knowledge of a lower bound for the energy carried in the lost data packets, such that the energy injected can be bounded (for instance by assumptions on the input signal behavior),
- or needs the exact knowledge of the energy carried in the lost data packets.

These facts are the basis how a passive data reconstruction algorithm can be developed.

However, the commonly known data reconstruction algorithms as widely applied in NCS [6, 88, 109, 142, 150] do not consider the energy balance and possibly inject energy through estimation, hence are active. The non-passivity of this class of algorithms is exemplarily shown for the well-known Hold-Last-Sample algorithm. This result can easily be extended to more sophisticated extrapolation strategies such as ARMA algorithms or higher order Taylor expansions.

4.3.2 Hold-Last-Sample Algorithm

The Hold-Last-Sample algorithm is a simple strategy widely used in NCS. It belongs to the class of algorithms that use the information of previous signal behavior and can be interpreted as a zero order Taylor expansion. In case that there is an empty sampling instance resulting from the loss of the packet indexed $k > k^*$ ($l_{1,2}(k) = 0$), the value of the most recent packet k^* available is held until the next younger packet is available. The reconstruction algorithm with HLS is

$$\zeta_u(k) = u_l(k^*); \qquad \zeta_v(k) = v_r(k^*), \tag{4.14}$$

for the forward path and the backward path, respectively.

Proposition 4.1 The Hold-Last-Sample algorithm is not passive.

In order to verify the non-passivity of the HLS-algorithm, a single configuration has to be found not satisfying the necessary passivity condition (4.12).

Proof: Let us assume that the value of the packets lost is zero

$$u_l(k) = 0, \quad \text{if } l_1(k) = 0 \text{ and } \quad v_r(k) = 0, \quad \text{if } l_2(k) = 0,$$

while all other packets take values unequal to zero

$$u_l(k) \neq 0, \quad \text{if } l_1(k) = 1 \quad \text{and} \quad v_r(k) \neq 0, \quad \text{if } l_2(k) = 1.$$

Consequently, the packets at the sampling instance just before the loss and so the reconstructed values are unequal to zero

$$\zeta_u(k) \neq 0, \quad \text{if } l_1(k) = 0 \quad \text{and} \quad \zeta_v(k) \neq 0, \quad \text{if } l_2(k) = 0.$$

The power carried by the packets lost is smaller than the power of the reconstructed values

$$u_l^2(k) = 0 < \zeta_u^2(k - D_1), \quad \text{if } l_1(k) = 0 \quad ; \quad v_r^2(k) = 0 < \zeta_v^2(k - D_2), \quad \text{if } l_2(k) = 0.$$

The value of the storage function of the packet loss subsystem (4.11) with this configuration is smaller than zero

$$E_{c,in}^l(N) = \sum_{\substack{k=0 \\ l_1(k)=0}}^{N} -\zeta_u^2(k - D_1) + \sum_{\substack{k=0 \\ l_2(k)=0}}^{N} -\zeta_v^2(k - D_2) < 0,$$

energy is generated, the passivity condition (4.12) is not satisfied. ∎

Remark 4.6 The non-passivity of the HLS algorithm is also indicated by the result of the non-passivity of increasing delay given in [90]. The HLS algorithm can be interpreted as increasing delay as with every time step T_A the effective delay increases by one time step T_A corresponding to the rate of change $\dot{T}^* = 1$. The signal is stretched hence with the arguments of [90] implicitly there is the possibility of energy generation due to the HLS algorithm.

Remark 4.7 Note, that the non-passivity of the HLS algorithm does not necessarily lead to unstable behavior of the haptic telepresence system. In fact, there exist configurations of signal behavior during loss, where the HLS acts as a dissipative element. Still, stability cannot be guaranteed.

Simulations

The behavior of the HLS algorithm is illustrated in simulations. The HSI is modeled as a pure velocity source providing a sinusoidal HSI-velocity with a frequency of 2 rad/s. The teleoperator is assumed to have sufficient control bandwidth, such that the teleoperator dynamics has not to be taken into account, when interacting with the damper environment with the damping coefficient $b_e = 0.1\text{kg/s}$ (free space). The sampling interval is $T_A = 1\text{ms}$. The delays in the forward and backward paths are constant $D_1 = D_2 = 100$, a signal outage occurs once for $150T_A$ at time $t = 2.5\text{s}$ in the forward path with HLS applied then.

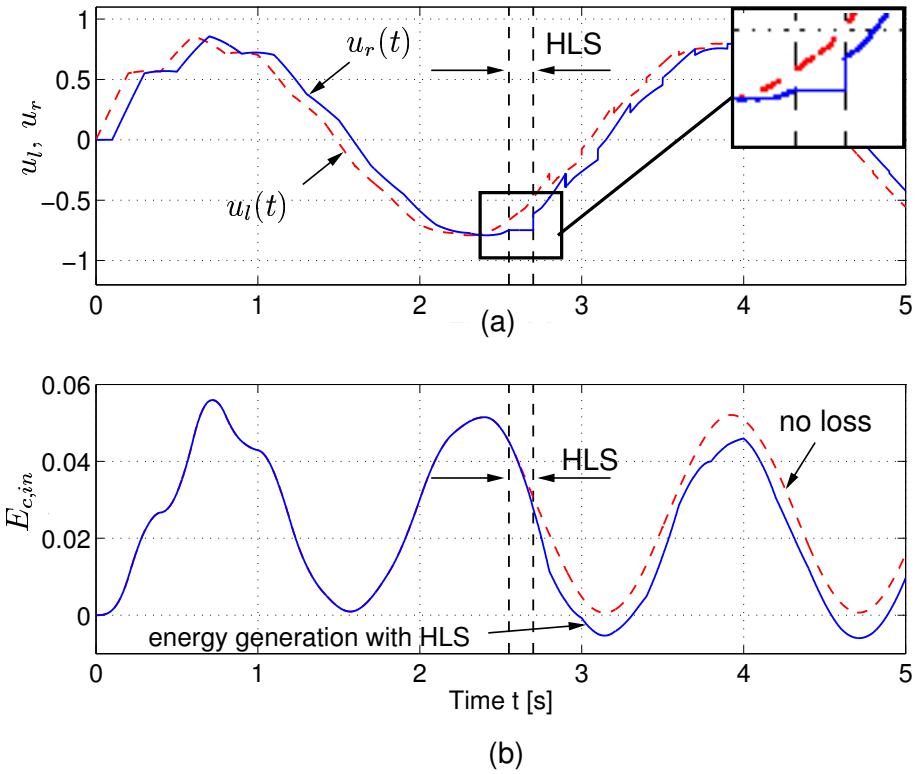

Figure 4.10: Input and output signal with single applied HLS algorithm (a) and energy balance (b) with negative values showing the non-passivity of HLS; in case of no packet loss the communication subsystem is energetically lossless.

The HLS algorithm distorts the wave variable signal as shown in Fig. 4.10(a), where for comparison the input wave variable signal u_l and the output u_r of the HLS algorithm is depicted. The energy balance $E^{\zeta}_{c,in}$ of the communication subsystem with this single HLS can be seen in Fig. 4.10(b), where negative values correspond to energy generation. The passivity condition (4.4) is violated, validating the result from Proposition 4.1.

In fact, the HLS algorithm may lead to instability as shown in Fig. 4.11. With the given packet loss in Fig. 4.11(a) the force at the HSI f^d_h grows unlimited with the bounded HSI velocity $\dot{x}_h$ as input signal, see Fig. 4.11(b), for comparison the case without loss is also depicted. The energy balance $E^{l}_{c,in}$ over the packet loss intervals is negative resulting in a negative overall energy balance $E^{\zeta}_{c,in}$ as shown in Fig. 4.11(c). The necessary condition (4.12) for the passivity of the data reconstruction is violated. The HLS algorithm may drive the system to instability, hence is not appropriate for the data reconstruction in haptic telepresence systems. This holds for all data reconstruction algorithms that

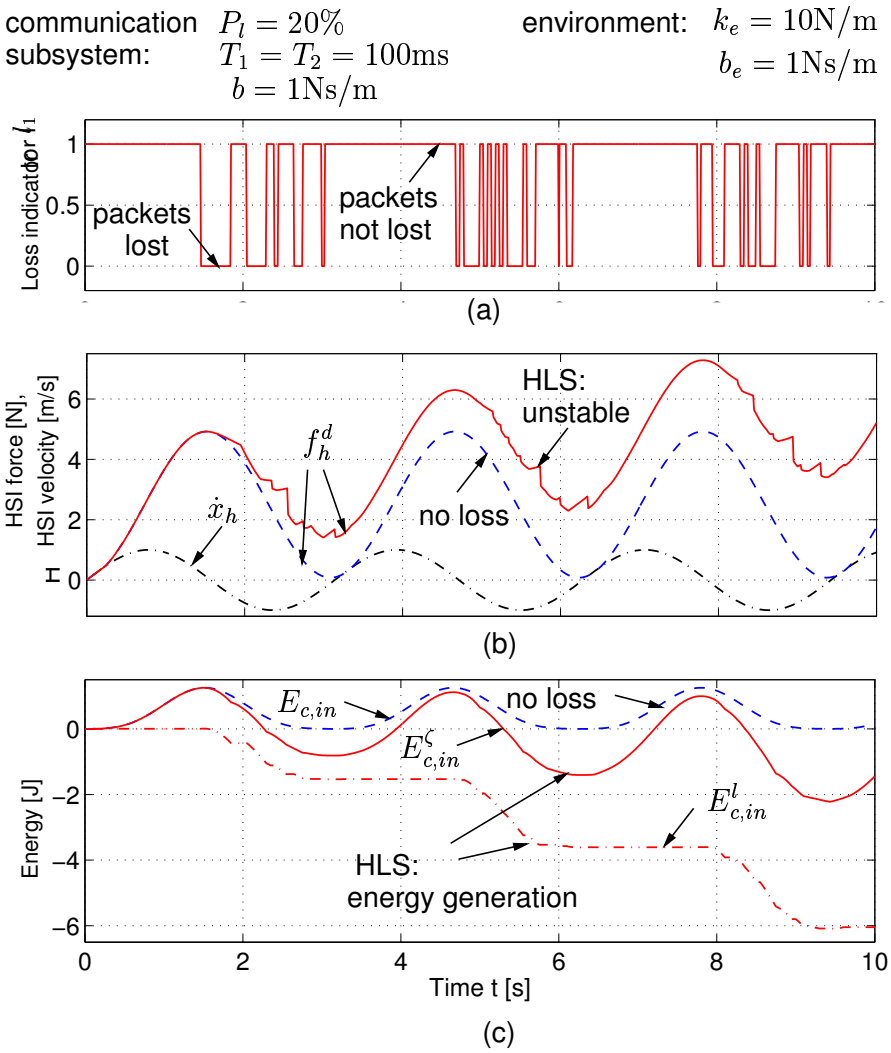

Figure 4.11: Unstable behavior due to HLS during packet loss; (a) loss indicator, (b) HSI force and velocity, (c) overall energy balance of the communication subsystem and over loss intervals: necessary passivity condition (4.12) is violated.

possibly inject more energy through estimation than the energy carried in the lost data packets, hence for all standard extrapolation algorithms without energy considerations. In the following a strictly passive reconstruction strategy is investigated, not injecting energy at all.

4.3.3 Zeroing Strategy

In case that there is an empty sampling instance resulting from the loss of the packet indexed $k > k^*$ ($l_{1,2}(k) = 0$), the value is reconstructed by inserting a zero

$$\zeta_u(k) = 0; \qquad \zeta_v(k) = 0$$

for the forward path and the backward path, respectively.

Proposition 4.2 The zeroing strategy is strictly passive.

Proof: Clearly, the zeroing strategy satisfies the passivity condition established in Theorem 4.2 given by (4.13) as

$$|\zeta_u(k)| = 0 \leq |u_l(k)|; \quad |\zeta_v(k)| = 0 \leq |v_r(k)|,$$

holds $\forall k$. The energy dissipated by this algorithm is equal to the energy carried by the packets lost and can be computed with (4.11). ■

Remark 4.8 The zeroing strategy is also passive for the more general case where no dejittering is assumed.

Simulations

The behavior of the zeroing strategy is illustrated in simulations with simulation conditions equal to the previous one. Again a signal outage occurs once for $150T_A$ at time $t = 2.5$s in the forward path with the zero setting applied then as shown in Fig. 4.12(a).

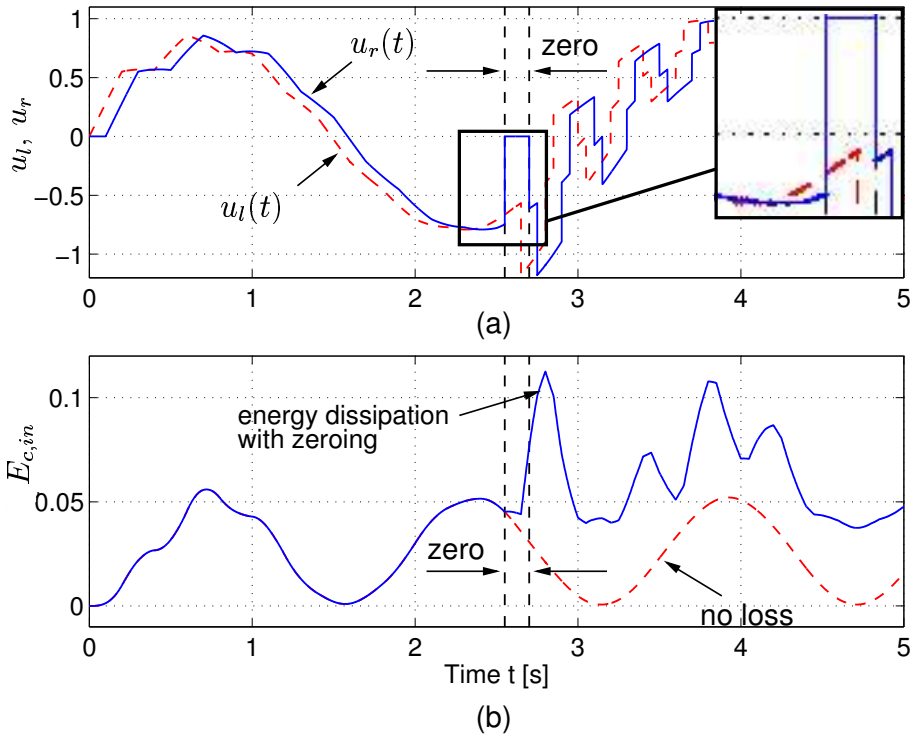

Figure 4.12: Input and output signal with zeroing strategy (a) and energy balance (b); observe that this is strictly passive.

The positive energy balance of the communication subsystem shown in Fig. 4.12(b) indicates the strict passivity of this approach. As a side effect of zeroing high frequencies are introduced resulting in wave reflections, see Fig. 4.12. In a real system these wave reflections disturb the perception of the remote environment, i.e. deteriorate transparency.

In summary the zeroing strategy is strictly passive. The possibly high amount of dissipated energy, hence the conservativeness of the approach induces to low transparency. A novel, less conservative strategy is proposed in the following.

4.3.4 Bounded Rate Strategy

The idea of the bounded rate approach is to use the lower bound of the energy input to the communication subsystem during a loss interval in order to appropriately bound the energy output from above by the reconstruction algorithm. In order to estimate a lower bound of the energy input, in this approach the rate of the input signal is assumed to be bounded

$$|\Delta u_l(k)| \leq \Delta u_{l,\max} \quad \text{and} \quad |\Delta v_r(k)| \leq \Delta v_{r,\max}, \quad \forall k > 0, \tag{4.15}$$

with $\Delta(\cdot)(k) = (\cdot)(k) - (\cdot)(k-1)$. In application this can be guaranteed by a rate limiter block just before the communication two-port. It is easy to show that this rate limiter does not generate energy, hence is passive.

Let us assume one or more consecutive packets with the index $k > k^*$ are lost. The missing values are reconstructed by reducing the absolute value of the last received packet k^* by the maximum rate in each time step. If the reconstructed value would approach zero then it is set to zero

$$\begin{aligned} \zeta_u(k) &= \begin{cases} u_l(k^*) - \operatorname{sign}\{u_l(k^*)\}\Delta u_{l,\max}\Delta k & \text{if} \quad u_l(k^*)\zeta_u(k) > 0 \\ 0 & \text{otherwise} \end{cases}, \\ \zeta_v(k) &= \begin{cases} v_r(k^*) - \operatorname{sign}\{v_r(k^*)\}\Delta v_{r,\max}\Delta k & \text{if} \quad v_r(k^*)\zeta_v(k) > 0 \\ 0 & \text{otherwise} \end{cases}, \end{aligned} \tag{4.16}$$

for the forward path and the backward path, respectively, with $\Delta k = k - k^*$.

Proposition 4.3 The bounded rate data recovery algorithm is passive.

Proof: The passivity of the zeroing strategy has been shown before, passivity has only to be shown for the upper cases in the definition of the algorithm. Therefore, let us look at a single connected complete loss interval $K \geq k > k^*$ with $l_{1,2}(k) = 0$ and further $u_l(k^*)\zeta_u(k) > 0$, $v_r(k^*)\zeta_v(k) > 0$ to ensure the upper case condition in (4.16). The signal dynamics of the lost data is bounded by the maximum rate with (4.15), hence in every time interval with $\Delta k = K - k^*$

$$\begin{aligned} \Delta u_{l,\max}\Delta k &\geq \sum_{k=k^*+1}^{K} |\Delta u_l(k)| \geq \sum_{k=k^*+1}^{K} \Delta u_l(k), \\ \Delta v_{r,\max}\Delta k &\geq \sum_{k=k^*+1}^{K} |\Delta v_r(k)| \geq \sum_{k=k^*+1}^{K} \Delta v_r(k), \end{aligned}$$

holds. As a result the absolute value of the reconstructed value is always smaller than the absolute value of the lost data rewritten as a sum

$$\begin{aligned} |\zeta_u(k)| &= |u_l(k^*)| - \Delta u_{l,\max}\Delta k \leq |u_l(k^*) + \sum_{k=k^*+1}^{k} \Delta u_l(k)| = |u_l(k)|, \\ |\zeta_v(k)| &= |v_r(k^*)| - \Delta v_{r,\max}\Delta k \leq |v_r(k^*) + \sum_{k=k^*+1}^{k} \Delta v_r(k)| = |v_r(k)|. \end{aligned}$$

Thus, the bounded rate data recovery algorithm satisfies the passivity condition given by (4.13) in Theorem 4.2, hence is passive. ∎

Simulations

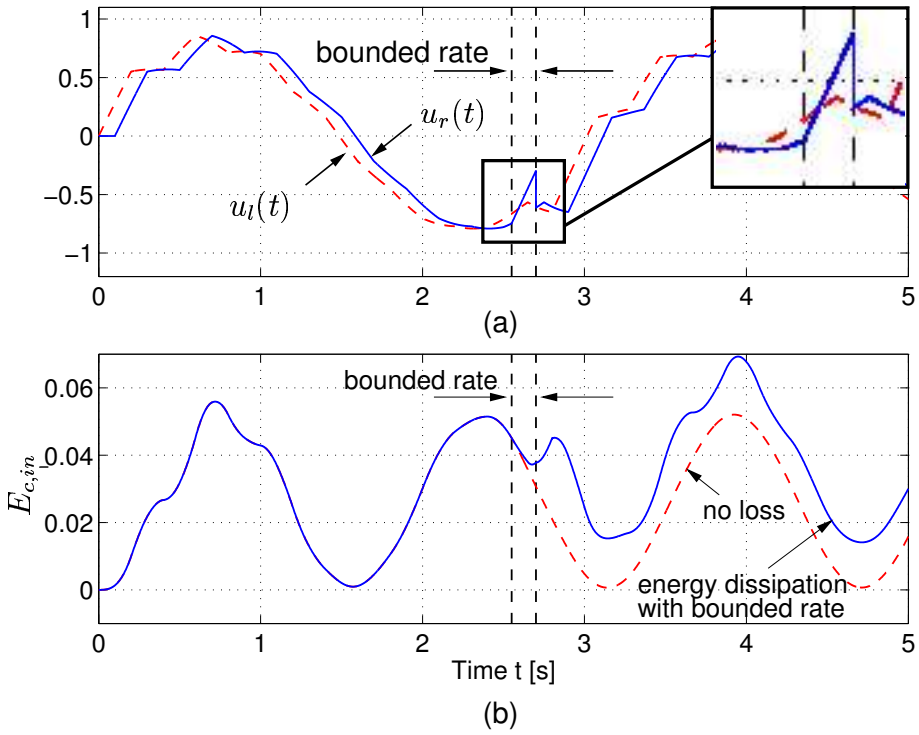

Figure 4.13: Input and output signal with bounded rate strategy (a) and energy balance (b); the bounded rate strategy is passive.

Simulations are performed under the same conditions as above with a rate limiter in the forward path just before the communications ($\Delta u_{l,\max} = 3$) in order to guarantee the bounded rate. Fig. 4.13(a) shows the input signal u_l and the output signal of the reconstruction strategy u_r. According to the energy balance in Fig. 4.13(b) the communication subsystem exhibits strictly passive behavior, but dissipates less energy than the zeroing strategy.

In summary the bounded rate strategy passifies the communication subsystem with packet loss being sufficient for the stability of the haptic telepresence system. Using assumptions on the input signal behavior, this algorithm is less conservative than the zeroing strategy with respect to the amount of dissipated energy. This indicates a better compromise in the trade-off between stability and performance towards the performance, that is evaluated in Section 4.4. However, both passive algorithms satisfy the conservative sufficient passivity condition from Theorem 4.2. In the following a less conservative strategy satisfying the necessary and sufficient condition from Theorem 4.1 is proposed.

4.3.5 Data Reconstruction with Energy Supervision

The basic idea of the following approach, the supervision of the energy balance of the communication subsystem, is related to the concept of time domain passivity [43]. If the input energy to the communication subsystem is known at the receiver then a data reconstruction algorithm can be designed, such that never more energy is extracted from the

communication subsystem than going into it, hence the passivity condition (4.4) is satisfied. A similar idea to communicate the wave variable energy content has been proposed in [106], there the wave integral instead of the wave variables is transmitted resulting in possibly large fluctuations of the wave variable output in case of increasing delay and loss of data. Another similar approach, introduced in [160], does not transmit the input energy but reconstructs it at the receiver side by using time stamps. However, the energy of packets lost can not be considered there, which might lead to conservative behavior in the case of packet loss. Here, a general framework for energy supervised reconstruction strategies in packet switched communication networks is introduced based on the explicite transmission of the wave input energy.

The receiver side is augmented with a virtual energy storage enabling the supervision of passivity by energy balance. The stored energy, dissipated otherwise, is the excess passivity of he communication subsystem, which may compensate the energy generation of a non-passive reconstruction algorithm such as the HLS algorithm.

Energy Supervision in Packet Switched Communication Networks

The energy supervision can independently be applied to each sender-receiver pair. The input wave energy $\sum_k u_l^2(k)$ ($\sum_k v_r^2(k)$ for the backward path) has to be transmitted over the communication network. In order to keep the additional network traffic as low as possible, the value of input energy is transmitted together with the wave variable in the same data packet. As the data packets and such the input energy information may possibly get lost the latest update of the input energy content available at the receiver at the time N is assumed to have the packet index $k^* = N - K$, where $K \geq D_1$ ($K \geq D_2$ for the backward path). The amount of virtual energy $E_{v,f}(N)$ ($E_{v,b}(N)$ for the backward path) is the difference between the wave energy input to the forward path until the time k^* and the wave energy output until the current time N

$$\begin{aligned} E_{v,f}(N) &= \sum_{k=0}^{k^*} u_l^2(k) - \sum_{k=0}^{N} u_r^2(k), \\ E_{v,b}(N) &= \sum_{k=0}^{k^*} v_r^2(k) - \sum_{k=0}^{N} v_l^2(k). \end{aligned} \tag{4.17}$$

Corollary 4.1 The energy supervised communication subsystem is passive, if the virtual energy storages for the forward and the backward path are non-negative $E_v, f(N) \geq 0$ and $E_v, b(N) \geq 0$ $\forall N$.

Proof: Both, the energy balance for the forward path and the backward path rewritten with the virtual energy storage (4.17) is clearly larger than zero

$$\begin{aligned} E_{cf,in}(N) &= E_{v,f}(N) + \sum_{k=k^*}^{N} u_l^2(k) \geq 0, \\ E_{cb,in}(N) &= E_{v,b}(N) + \sum_{k=k^*}^{N} v_r^2(k) \geq 0 \end{aligned} \tag{4.18}$$

as in both equations the terms are not negative with the given assumption. The passivity condition (4.5) is satisfied. ∎

Energy Supervised Data Reconstruction

As long as the energy of the virtual storage element is positive a high-performing but possibly non-passive strategy ζ_{np}, as e.g. the HLS or the compensation algorithm from [160], can be applied for data reconstruction. The energy content is reduced in every time step by u_r^2 (v_l^2). As soon as the storage element reaches its initially stored energy value due to energy generation by the non-passive algorithm, any passive reconstruction strategy ζ_p fulfilling (4.13) has to be employed. The complete energy supervised reconstruction algorithm is defined by

$$\begin{aligned} \zeta_u(k-D_1) &= \begin{cases} \zeta_{np,u}(k-D_1) & \text{if } E_{v,f}(k) \geq 0 \\ \zeta_{p,u}(k-D_1) & \text{otherwise.} \end{cases}, \\ \zeta_v(k-D_2) &= \begin{cases} \zeta_{np,v}(k-D_2) & \text{if } E_{v,b}(k) \geq 0 \\ \zeta_{p,v}(k-D_2) & \text{otherwise.} \end{cases}, \end{aligned} \tag{4.19}$$

for the forward or the backward path. In order to bound the energy output for practical application, the virtual energy storage is saturated $E_v(k) \leq E_{\max}$.

Passivity of Energy Supervised Data Reconstruction

Proposition 4.4 The energy supervised data reconstruction algorithm is passive.

Proof: Clearly, with the ruling of the upper case in the definition (4.19) the virtual energy is always positive definite, thereby fulfilling the passivity condition (4.17), hence (4.5). As the lower case is required to fulfill the small gain requirement (4.13) according to Theorem 4.2 implicitly (4.5) is satisfied. The data reconstruction with energy storage supervision is passive. ■

Remark 4.9 The data reconstruction with energy supervision is also passive for the more general case where no dejittering is assumed.

Remark 4.10 Without sacrificing the passivity of the communication subsystem the virtual energy storage can be initialized with a value different from zero $E_v(0)$. This value then represents the initially stored energy of the communication subsystem. Then for passivity $E_v(k) \geq E_v(0)$ must hold in the upper case of (4.19).

Remark 4.11 In order to avoid non-smooth changes in the signal behavior due to sudden switching between the two reconstruction algorithms in (4.19), either a transition algorithm may be implemented or a simple low pass filter after the reconstruction algorithm. It does not violate the passivity if its H_∞-norm is smaller than one. In fact, as it dissipates energy in the higher frequency range, the transition to the non-passive strategy is possible earlier.

Simulations

Simulations are performed under the same conditions as in Section 4.3.2 except for an additional data loss in the forward path in the time interval [1.2, 1.4] s in order to show the effect of the energy supervision strategy. The HLS algorithm is chosen as non-passive strategy ζ^{np} and the zeroing strategy as passive strategy ζ^p.

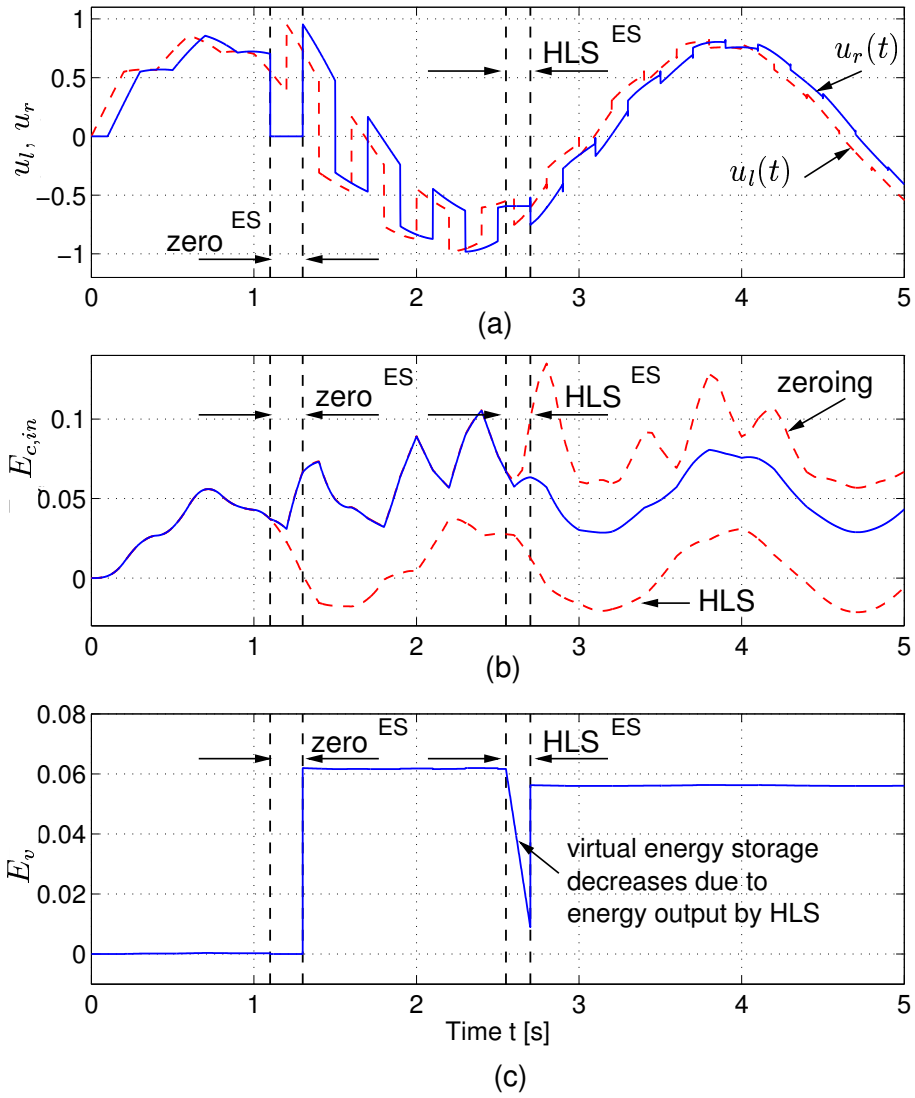

Figure 4.14: Input and output signal with energy supervision strategy based on HLS/zeroing (a) and energy balance for the energy supervision strategy, HLS and zeroing for comparison (b) and virtual energy storage (c); the energy supervision strategy is passive.

Fig. 4.14(a) shows the input signal u_l and the output signal u_r of the energy supervised reconstruction algorithm. In the first loss interval zeroing is applied as the virtual energy storage depicted in Fig. 4.14(c) is zero $E_v = 0$. Due to the dissipative character of the zeroing the virtual energy content suddenly increases $E_v > 0$ at the end of the first loss interval when the energy update is available again. Consequently, in the second loss time interval the HLS algorithm can be applied without sacrificing the passivity of the communication subsystem. Note, that the virtual energy storage is decreased exactly by the amount of energy released by the HLS. The passive behavior is indicated by the positive energy balance shown in Fig. 4.14(b). Until the second loss interval the energy supervision strategy exhibits the same behavior in terms of the energy balance as the zeroing. The energy generated by the HLS in the second interval is compensated by the energy stored in the virtual storage resulting in a less dissipative behavior than the zeroing strategy.

4.3.6 Summary

In summary of this section the class of data reconstruction algorithms without energy considerations turns out to be non-passive as exemplarily shown for the Hold-Last-Sample algorithm. Zeroing is discussed as an example for strategies that are strictly passive. The bounded rate approach as an example for algorithms that use assumptions on the input energy is passive but less conservative in terms of energy dissipation. The energy supervision approach with the HLS as non-passive and zeroing as passive strategy is an example for strategies that use the exact knowledge of the input energy. This strategy is also passive and exhibits the least conservative behavior of all strategies investigated here.

4.4 Towards Optimal Design of Control Strategies

Aiming at transparent haptic telepresence the design of the packet processing and the data reconstruction strategy is essential. The goal of this section is to find the optimal control strategy design with respect to the transparency of the haptic telepresence system. Therefore, first the effect of the investigated passive reconstruction strategies on the transparency of the haptic telepresence system is evaluated. Furthermore, the influence on transparency of the packet processing in terms of the dejitter buffer tuning parameter, the virtual delay for the data buffering, is investigated.

4.4.1 Numerical Performance Comparison for Data Reconstruction

The performance in terms of the transparency is evaluated using the position error in free space motion according to the transparency criteria (2.16) and the impedance parameter criteria in contact with a wall introduced in Chapter 3. Due to the nonlinear nature of the reconstruction algorithms and the stochastic nature of loss a theoretical performance analysis is difficult. Therefore, in the following a numerical analysis using the optimization-based evaluation tool developed in Chapter 3 is performed.

Position Error in Free Space Motion

The deviation of the teleoperator position x_t from the HSI position x_h expressed in continuous time is given by

$$x_h(t) - x_t(t) = \frac{1}{\sqrt{2b}} \int_0^t (u_l - u_r + v_r - v_l)\, \mathrm{d}\tau.$$

Here, sufficient bandwidth of the velocity control loop at the teleoperator is assumed, such that $x_t(t) = x_t^d(t)$. In order to evaluate the influence of the loss only, we assume zero delay. Without loss the wave variable received is equal to the one sent to the network, hence $u_r(t) = u_l(t)$ and $v_l(t) = v_r(t)$. Neglecting the effects of the transition from continuous to discrete time and back the position error is zero.

If the reconstructed wave variable u_r and v_l differs from the value lost u_l and v_r, which is the general case with all considered reconstruction algorithms, then an unrecoverable drift between the HSI and the teleoperator position may occur. The position error mainly depends on the signal behavior at the time when packets are lost and the number of packets lost, hence the loss probability and the time t. If for example the wave variable u_r has high values in the packets lost and is reconstructed by zeroing, then the position error is large. If the signal does only slightly change during the loss interval then a HLS results in a small position error. Monte Carlo simulations are performed for the zeroing, the bounded rate, and the energy supervised HLS/zeroing strategy for uncorrelated and correlated loss, both with the same unconditional loss probability of 20%. The HSI is modeled as a velocity source exciting the system in different frequencies $\dot{x}_h(t) = \sin \omega t$ with $\omega \in [10^{-3}\, 10]$ Hz. The simulation parameters are given in Table 4.1.

Table 4.1: Simulation parameter values

Simulation parameter	Value
environment damping b_e	0.1 Ns/m
environment stiffness k_e	0 N/m
wave impedance b	0.1 Ns/m
sampling interval T_A	1 ms
delay T_1, T_2	1 ms
uncorrelated loss probability P_l	20 %
correlated loss probability $P_{g,b}$	3 %
correlated loss probability $P_{b,g}$	0.5 %
rate limit (bounded rate strategy) $\Delta u_{l,\max}$, $\Delta v_{r,\max}$	0.003 $\sqrt{\mathrm{W}}$
simulation time	30 s
number of trials M per frequency	100

The relative position error $e_x = |(x_h - x_t)/x_{\max}|$ is computed for each frequency. The mean relative position error $\overline{e}_x$ over the M trials per frequency and its variance is presented in Fig. 4.15. As expected at low frequency the energy supervised HLS performs very good as the signal change rate is small ($< 0.1\%$ for $\omega < 0.1$Hz for uncorrelated loss). The zeroing strategy shows the highest position error (up to 12%). Generally, the position

error increases for all strategies at higher frequency, furthermore, the position error is higher for the Gilbert loss model, i.e. if consecutive packets are lost.

To compare the performance of the different strategies the area under the curves hence the integral of the mean relative position error over the frequency $E_x = \int \overline{e}_x \, \mathrm{d}\omega$ is taken as performance measure.

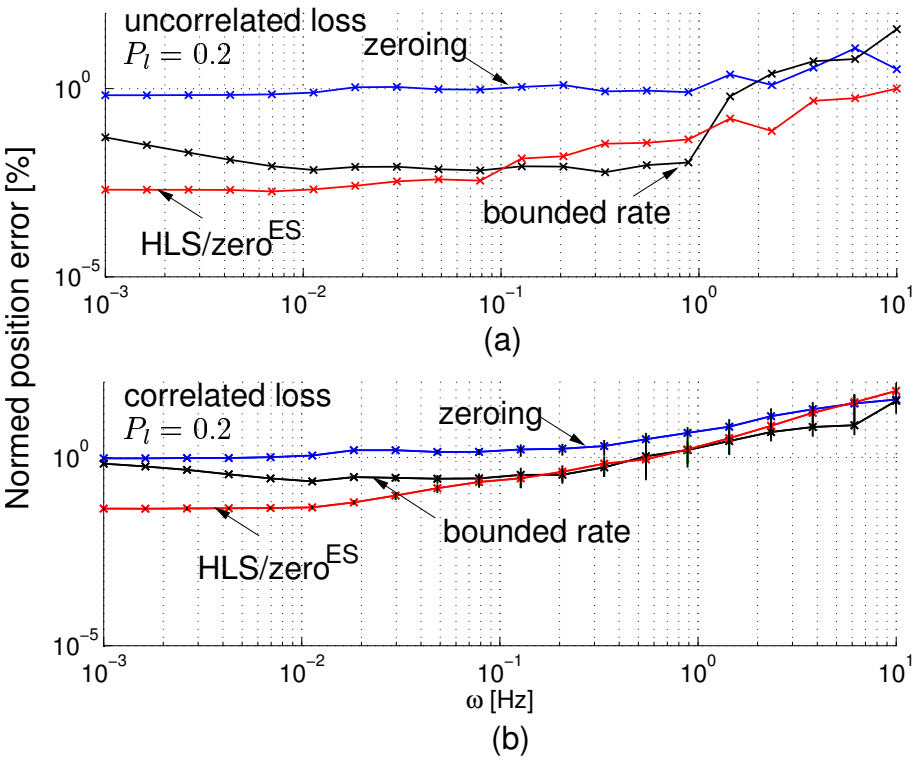

Figure 4.15: Relative position error for uncorrelated (a) and correlated (Gilbert) loss (b).

The results are shown in Table 4.2. The high values of E_x for the zeroing strategy indicate poor tracking performance. This corresponds to the former findings on its very dissipative behavior. In the uncorrelated loss case the energy supervision strategy clearly outperforms all others. With the Gilbert loss model the bounded rate strategy performs slightly better for the given simulation parameters.

Table 4.2: Simulation results for the position error measure E_x

reconstruction strategy	E_x (uncorrelated loss)	E_x (Gilbert model)
zeroing	0.0484	0.1581
bounded rate	0.0466	0.0619
energy supervised HLS/zeroing	0.0029	0.1305

The performance in terms of position tracking can be improved by applying the position feedforward architecture [27], see also Appendix A for an introduction of the extended architecture.

Perceived Stiffness in Contact

The frequency response of the perceived impedance Z_h for different loss probabilities P_l (uncorrelated loss) is estimated in Monte Carlo simulations combined with a cross-correlation analysis as explained in detail in Section 3.1.2. The simulation parameters are listed in Table 4.3.

Table 4.3: Simulation parameter values

Simulation parameter	Value
environment damping b_e	1 Ns/m
environment stiffness k_e	200 N/m
wave impedance b	1 Ns/m
sampling interval T_A	1 ms
delay T_1, T_2	1 ms
rate limit (bounded rate strategy) $\Delta u_{l,\max}$, $\Delta v_{r,\max}$	5 $\sqrt{\text{W}}$

Zeroing: The Bode plot of the identified perceived impedance Z_h for the zeroing strategy is presented in Fig. 4.16. Already for a loss probability of 2% a large difference to the no loss (0%) case is observable in the lower frequency range. The magnitude falling with 20dB/dec together with a phase of -90deg indicates the structural property of stiffness that is lost for a loss probability of 2%. With zeroing the stiffness is not perceivable. An intuitive interpretation of this result is that the Fourier series of the received wave variable no longer contains a constant component or lower frequencies.

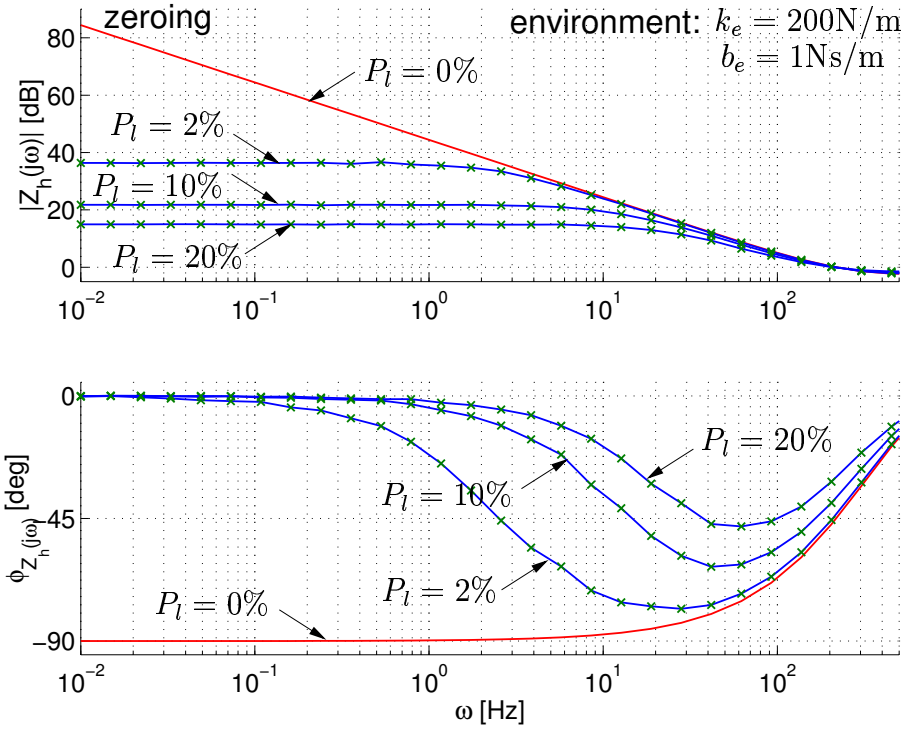

Figure 4.16: Bode plot of the perceived impedance with zeroing strategy.

Bounded rate: Similar to the zeroing strategy, at higher packet loss probability a loss of the stiffness property is observed, see the Bode plot for the estimated perceived impedance. As expected, the transparency degradation is weaker than for the zeroing strategy.

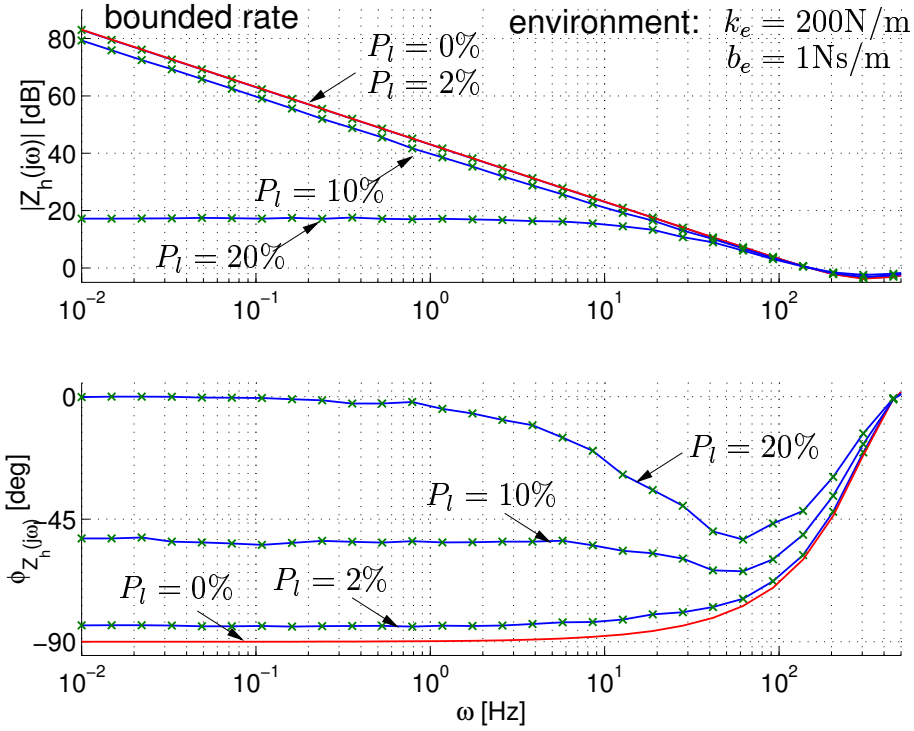

Figure 4.17: Bode plot of the perceived impedance with bounded rate strategy.

Energy supervised HLS/zeroing: For a loss probability of 80%, see the Bode plot of the identified perceived impedance Z_h in Fig. 4.18, still a stiffness is perceived, with a reduced stiffness coefficient though. The estimated stiffness coefficients of the perceived impedance is gained by approximation using the optimization procedure from Section 3.1.2 for different packet loss probabilities. The approximated perceived stiffness depending on the loss probability is presented in Fig. 4.19 showing that even for a high loss probability of 50% the stiffness coefficient is reduced by only 6%. This is according to the human haptic perception limits not perceivable as the JND for stiffness is reported to be 23±3% [64, 66].

In summary, the energy supervised HLS/zeroing strategy performs best from all the investgated data reconstruction strategies. Further improvement can be expected, if a more sophisticated extrapolation strategy such as an ARMA algorithm is used instead of a simple HLS.

Owing to its superior performance the energy supervised HLS/zeroing strategy is considered as the data reconstruction algorithm for the following performance investigations.

4.4.2 Performance Evaluation for Packet Processing

Assuming a time-varying delay with a certain distribution the question arises how the packet processing, namely the dejitter buffer with the virtual delay as tuning parameter, should be designed. Depending on the delay distribution this tuning parameter trades

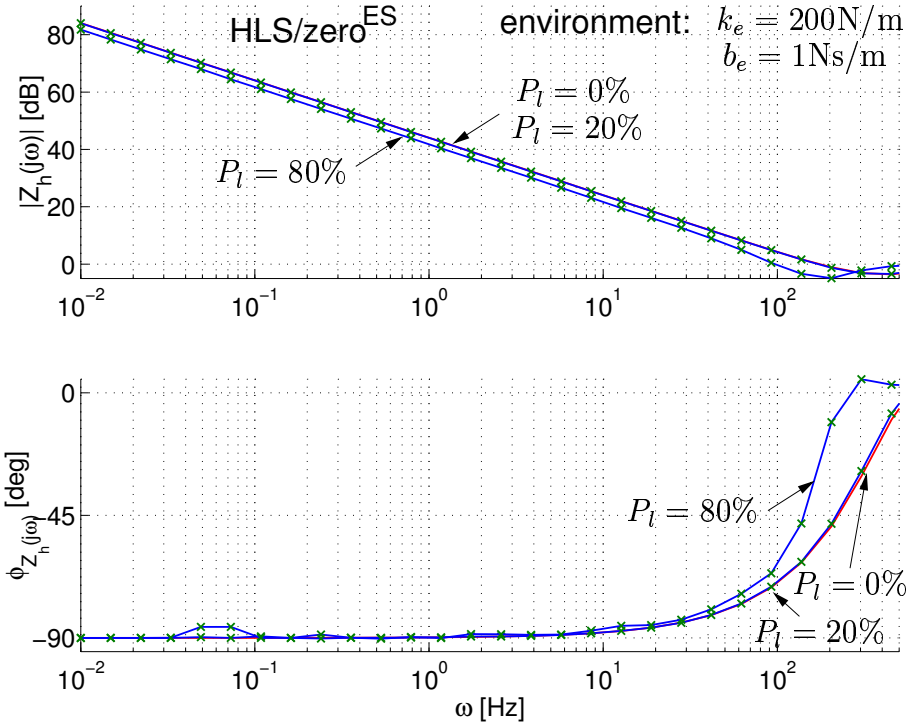

Figure 4.18: Bode plot of the perceived impedance with energy supervised HLS/zeroing strategy.

additional delay versus additional packet loss as discussed in Section 4.2.2. Both, additional delay, see Chapter 3, and packet loss reduce the perceived stiffness in contact.

In order to evaluate the influence of this trade-off on transparency, the optimization-based transparency evaluation method proposed in Section 3.1.2 is applied: the frequency response of the perceived impedance is estimated from Monte Carlo simulations with the subsequent cross-correlation analysis, the perceived impedance is approximated based on optimization, and the stiffness coefficient of the approximated perceived impedance is computed. With the computed characteristic diagram for the coefficient of the perceived stiffness depending on the two parameters delay and loss for a given environment dynamics the optimal value for the virtual delay can be determined for an arbitrary delay distribution.

Exemplarily, this characteristic diagram is computed for the environment used in the previous simulations ($k_e = 200\text{N/m}$, $b_e = 1\text{Ns/m}$). The round-trip delay is varied within the interval $T \in [20,\ 400]\text{ms}$ with $T_1 = T_2 = T/2$, the packet loss, uncorrelated, equal in the forward and the backward path, $P_l \in [0,\ 90]\%$. As expected, high delay as well as high packet loss result in a low perceived stiffness, see Fig. 4.20.

Lets assume a network induced packet loss probability P_l^0 and a time-varying delay with a certain distribution $p(T_1) = p(T_2)$, both equal in the forward and the backward path. The pseudo-packet loss $P_l^* = P_{l,1}^* = P_{l,2}^*$ (4.1) and such the overall packet loss (4.2) can be computed depending on the pre-defined constant delay $T^* = T_1^* + T_2^*$, that results from the introduction of the appropriate virtual delays $\Delta_{vd,1}(k)$, $\Delta_{vd,2}(k)$ for each packet in the dejitter buffer in the corresponding path. With the resulting dejitter buffer function characterizing the trade-off between constant overall delay and the overall packet loss the optimal tuning for the dejitter buffer with respect to the perceived stiffness can be found.

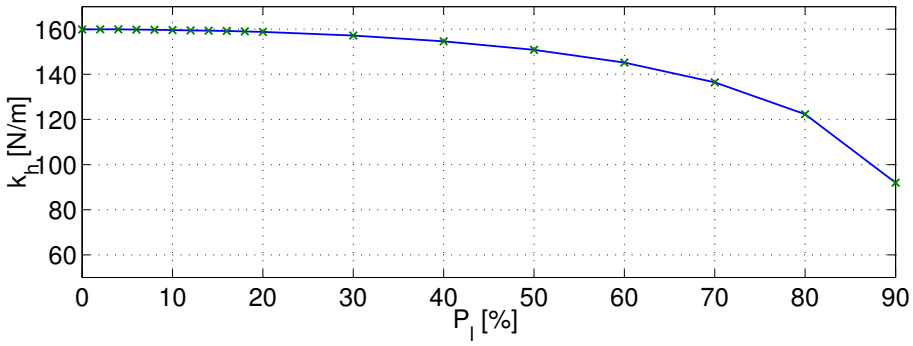

Figure 4.19: Stiffness coefficient of perceived impedance with energy supervised HLS/zeroing strategy.

For the given example with a Poisson delay distribution (parameters $T_{\min} = 70$ms and $\lambda = 3$) and no network induced packet loss $P_l^0 = 0\%$ assumed, the maximum stiffness is perceived for $T^* = 180$ms inducing a pseudo-packet loss of $P_l = P_l^* = 48\%$, see Fig. 4.21. The dejitter buffer in the forward and the backward path should be designed, such that a constant delay of 90ms is experienced by each data packet. Then the maximal stiffness is perceived.

A further very interesting result is gained from the evaluation of the perceived stiffness in different environment conditions as presented in Fig. 4.22, where the normalized perceived stiffness (normalized on the perceived stiffness for zero packet loss) is depicted depending on the packet loss probability. Assuming a constant JND over a broad range of stiffness the transparency degradation is obviously higher for lower environment stiffness. This is a contrary effect to the time delay inluence as investigated in Chapter 3. From these results one would conclude that the perceived stiffness is more sensitive to packet loss with lower environment stiffness, but less sensitive to time delay. This implies that in environments with low stiffness the tuning of the dejitter buffer should rather tend to less packet loss at the cost of more virtual delay.

4.5 Experiments

The experiments show the effect of time-varying delay and packet loss together with the control strategies on the transparency, using the objective measure of perceived stiffness in contact and a psychophysical experiment. The goal is to find the appropriate design of the packet processing strategy in terms of the dejitter buffer length for a given time delay distribution. The energy supervised HLS/zeroing strategy is applied for data reconstruction.

Experimental Setup

For the experiments the experimental haptic telepresence system described in Appendix C is used. The communication subsystem, shown in Fig. C.1 consists of the communication line with time-varying delay and packet loss, the data reconstruction algorithms, and the wave variable transformation with the wave impedance set to $b = 250$Ns/m. The packet rate is equal to the sampling rate of the local velocity and force control loops of $T_A = 1$ms.

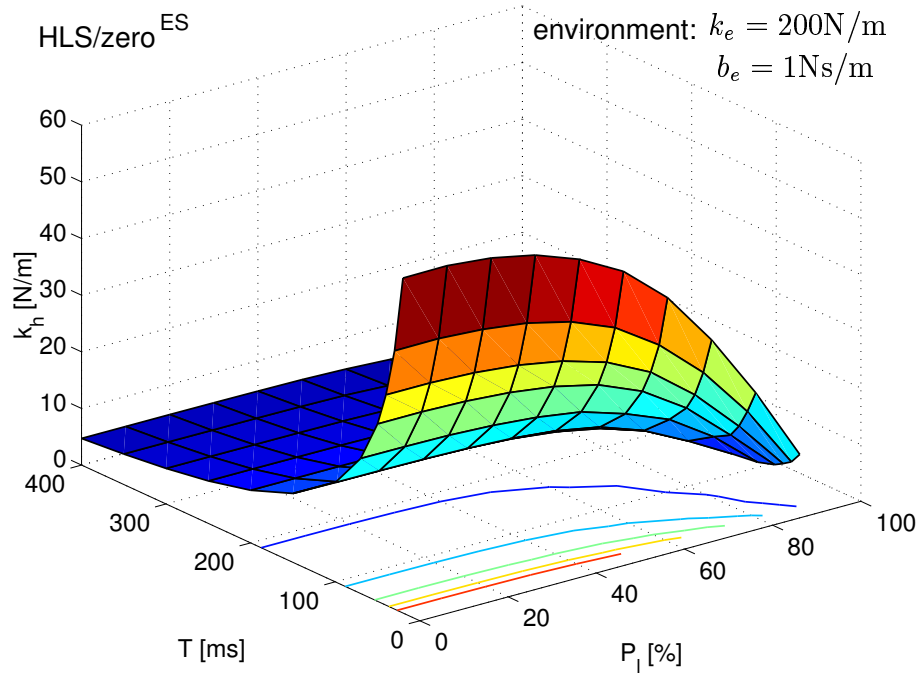

Figure 4.20: Perceived stiffness with energy supervised HLS/zeroing strategy over packet loss probability (uncorrelated) and round-trip delay.

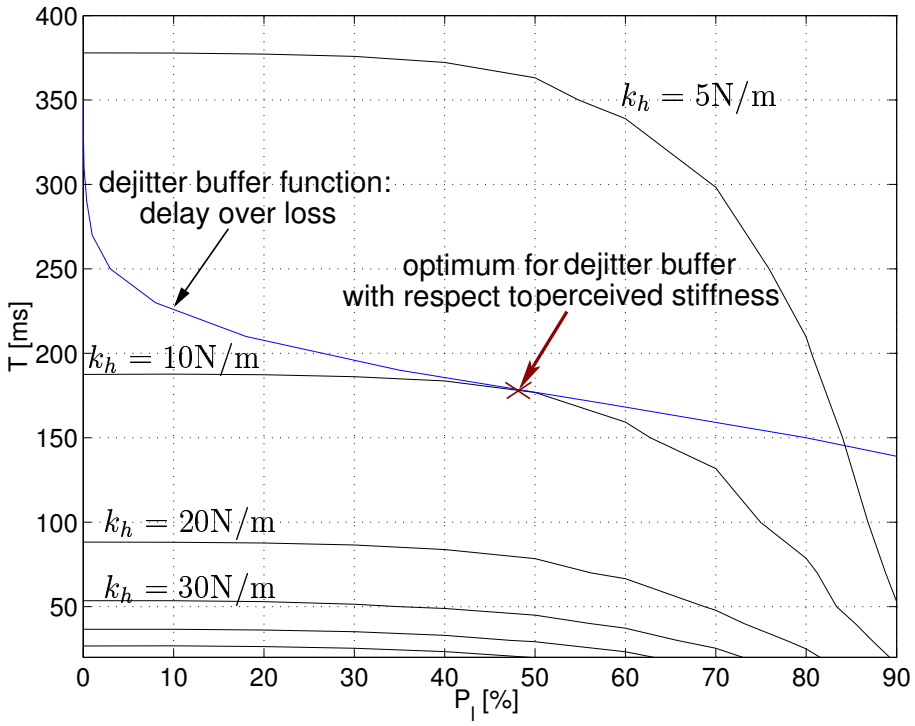

Figure 4.21: Optimal dejitter buffer design with respect to the perceived stiffness for given delay distribution with energy supervised HLS/zeroing strategy.

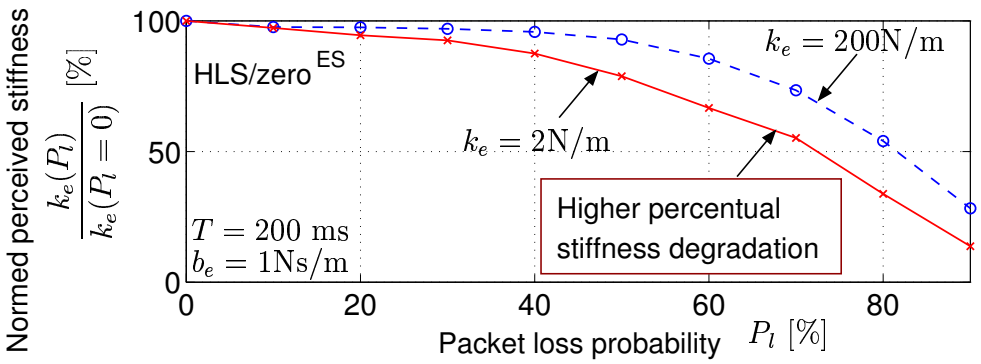

Figure 4.22: Normed stiffness coefficient of perceived impedance with energy supervised HLS/zeroing strategy for different environment stiffness.

A time-varying delay with a Poisson distribution (parameters $T_{\min} = 50$ms and $\lambda = 3$) is assumed in the forward and the backward path, see Fig. 4.23. The dejitter buffer length is varied, trading pseudo packet loss vs. additional delay. The resulting end-to-end characteristics (constant time delay and packet loss) are shown on the x-axis in Fig. 4.24; if for example the dejitter buffer length is choosen, such that the round-trip delay is 120ms, then 80% of the packets in the forward and the backward path are discarded, hence lost.

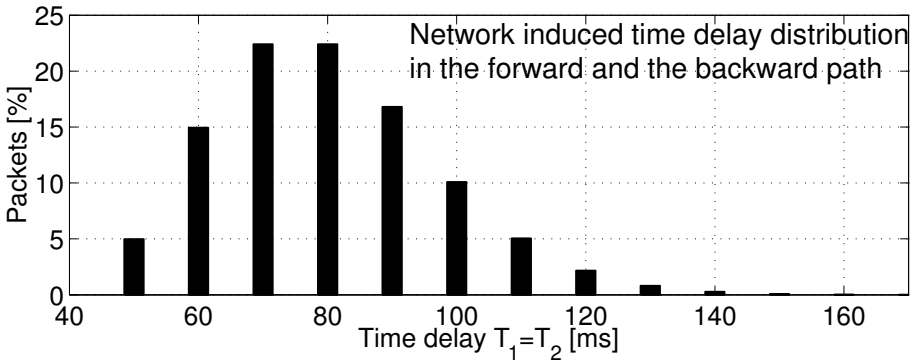

Figure 4.23: Network induced time delay distribution in the forward and the backward path.

4.5.1 Objective Evaluation

During the experiment the round-trip delay and the packet loss is varied according to the values given on the x-axis of Fig. 4.24. The wall environment with a stiffness coefficient of $k_e = 3200\text{N/m}$ is touched. The stiffness coefficient perceived by the operator during contact is computed from the force and the position measured at the HSI using a least squares identification.

The results are shown in Fig. 4.24 (dark bars). High packet loss (95%) as well as high delay result in a substantially reduced perceived stiffness validating the results from Section 4.4.1 and Chapter 3. The maximal perceived stiffness is observed for a round-trip delay of 140ms corresponding to a packet loss of 58%.

4.5.2 Evaluation considering Human Factors

From the foregoing experiment the perceived stiffness in contact is evaluated depending on the packet loss and the time delay. The question is, whether these experiments give an indication on the human perceived transparency. A first result on this kind of mapping is obtained in the experiments performed in Chapter 3 to validate the Hypothesis 3.1. The hypothesis to be validated in the following experiment can be stated as follows:

Hypothesis 4.1 The perceived dynamics feels most realistic in the range of delay and packet loss probability where the observed perceived stiffness coefficient is maximal.

Therefore, the experiments are performed with the same configurations of delay and corresponding packet loss probability as in the foregoing experiments using a so-called stochastic approximation procedure. The goal is to find the configuration out of the given set that feels most realistic. In order to provide the test persons with the feel of the realistic impression, in a familiarization phase the subjects could perform the experiment without delay and packet loss.

Conditions

Altogether 11 subjects (aged 22-30, 3 female, 8 male, 2 with prior contact to the experimental system) were tested. The subjects were told to operate with their preferred hand. They were equipped with earphones to mask the sound the device motors generate. Visual feedback was supplied. The subjects were subsequently presented two different configurations of loss and delay, after 1 min of operation in free space and/or contact for each, they had to tell which one felt more realistic. The prefered one then was combined with a new configuation and presented to the test person. The two configurations were chosen from the set of possible configurations using a successive approximation procedure, starting with the outer configurations (highest delay, highest loss), then halfing the interval.

Results

The result presented in Fig. 4.24 (light bars, right y-axis) show that most subjects (47%) prefered the configuration with 120ms delay and 80% of packet loss. None of them prefered the 100ms delay/95% packet loss and configurations with 200ms delay and more. These results correspond to the objective evaluation: the 4 configurations showing the highest perceived stiffness were prefered. This validates Hypothesis 4.1. ■

Discussion

It should be noted that these experiments have preliminary character and represent a first step towards the combined consideration of packet loss and time delay. In contrast to the objective experiments where only the contact behavior is evaluated, the test persons were allowed to feel contact with the wall as well as they could move in free space motion. Further visual feedback was provided, such that both cues, the haptic as well as the visual were evaluated. As well-known, the visual cue, if not disturbed, is the stronger one with respect to perceived qualities, hence the delayed movement of the teleoperator might have influenced the subjects decision. Still, these results indicate that to some extent the human

oriented evaluation of transparency is possible by objective measures in the case of time delay and packet loss.

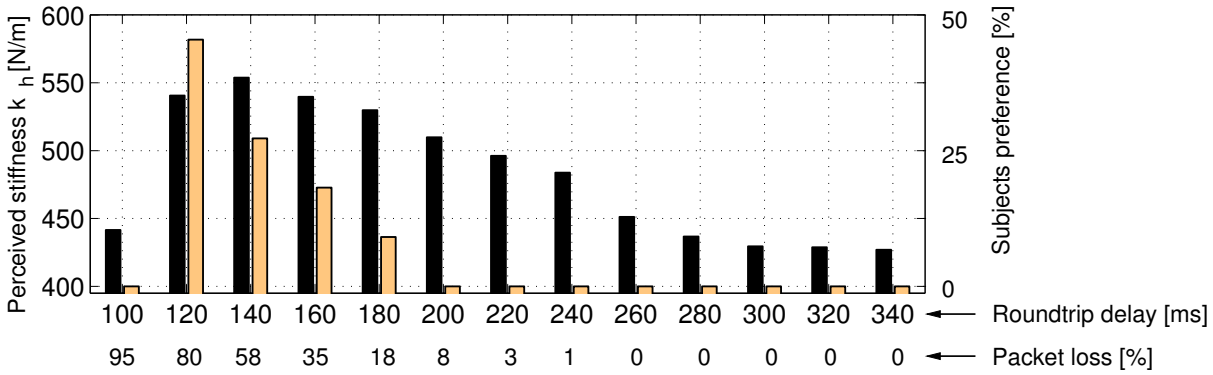

Figure 4.24: Experimental results: Perceived stiffness (dark bars, left y-axis) for different delay/packet loss configurations (x-axis) and subjects preference (light bars, right y-axis).

As a result it is stated that there exists an optimal design of the packet processing strategy with respect to the perceived stiffness validating the results from simulation in Section 4.4.2. The results from the psychophysical experiment indicate that the proposed numerical evaluation is an appropriate measure to find the appropriate design of the packet processing strategy.

4.6 Discussion

Packet switched communication networks, such as the Internet, are the most favored communication medium for telepresence systems. However, the global closed control loop in the haptic telepresence system suffers from potentially destabilizing communication effects such as unpredictable time-varying time delay and packet loss.

In this chapter haptic telepresence systems in packet switched network comprising unpredictable time-varying delay and packet loss are systematically investigated. Main focus is on the reconstruction of lost data. The time-varying time delay problem is reduced to a constant delay problem with packet loss by a buffer-and-discard packet processing strategy. Depending on the buffer design additional packet loss is traded versus additional time delay. Lost data, either communication induced or induced by the packet processing strategy, have to be reconstructed. Standard reconstruction algorithms such as 'hold last sample' are shown to be potentially destabilizing as they do not incorporate energy considerations. In order to provide a framework for passive data reconstruction in haptic telepresence systems, passivity conditions are established in this chapter. Based on this framework novel passive reconstruction strategies are developed, guaranteeing stability for arbitrarily large time-varying delay and packet loss.

For the first time a systematic transparency evaluation of data reconstruction strategies is performed utilizing the transparency analysis method developed in Chapter 3 which allows a human perception oriented interpretation. The data reconstruction algorithms generally reduce the stiffness perceived by the human operator. The data reconstruction

with energy supervision outperforms all other considered strategies. Aside from the data reconstruction, the tuning of the packet processing strategy has an essential influence, in fact, there exist an optimal tuning of the considered buffer-and-discard strategy depending on the communication induced time delay distribution and packet loss probability, and the environment dynamics. An interesting observation is that for transparency in soft environments additional delay is prefered over additional packet loss, in hard environments packet loss is not as crucial as additional time delay. The optimal tuning of the packet processing strategy is determined using the transparency analysis method developed in Chapter 3.

The results of this first combined transparency consideration of time delay and packet loss are validated in objective experiments. In the performed experimental user study the objectively highest displayed stiffness is associated with the most realistic feeling of the remote environment indicating the validity of the chosen transparency analysis approach.

The developed approaches allow stable haptic telepresence over packet switched network with unpredictable, arbitrarily large time-varying delay and packet loss. A method for the transparency optimal control design is developed and verified in experiments advancing the state-of-the-art. Interesting results, not yet stated in the known literature, and with important implications for the transparency oriented design of haptic telepresence systems in packet switched communication networks are gained. However, the time-varying problem is still not comprehensively solved yet with respect to the transparency aspect and will be subject of future research.

5 Communication Bandwidth Oriented Control

In the foregoing chapter the effects of the network characteristics on the stability and transparency of the haptic telepresence system have been investigated. The communication network itself as a medium with *limited communication resources* has not been taken into account. In a packet switched communication network multiple users run their network applications at the same time sharing the limited resources of the physical infrastructure. The aggregate network traffic induced by the applications determines the communication quality for each network application. Higher network traffic load results in a higher probability of congestion and thereby in higher time delay and packet loss, impairing the performance of each network application. From this point of view it is of high interest to minimize the network traffic in network applications in general. In addition, high packet transfer rates, in current haptic telepresence systems typically in the range of the sampling rates of the local control loops, are hard to maintain over long distance packet switched communication networks. For the application of haptic telepresence systems in packet switched communication networks it is of high interest to reduce the packet transfer rate and thereby to decrease the traffic volume.

Network traffic reduction in haptic telepresence systems has not been considered in the known literature yet. Accordingly, sophisticated strategies are currently not available. In the event based approach proposed in [159] there is an implicit reduction of network traffic, however, the transparency compared to other approaches as well as the impact on the network traffic is not discussed. In the closely related field of networked control systems (NCS) the problem of communication constraints has recently been investigated in [63, 116]. Aiming at network traffic reduction in NCS a deadband control approach is proposed [62, 87, 113]. A data packet is send only if the current value has changed more than a given threshold. This kind of sampling is no longer performed in equidistant time steps and can be considered as event based or Lebesgue sampling, see [5]. Another approach for packet rate reduction used in application is the appropriate packetization at the sender side, where multiple samples are packed into a single data packet. The packet rate is reduced, however, disadvantageously additional delay through data buffering at the sender side is introduced. In the favored deadband control approach not all samples are sent, therefore a similar problem of data reconstruction arises as in the foregoing chapter for time-varying delay and packet loss. In NCS the hold last sample algorithm is therefore used. As investigated in the Chapter 4 this reconstruction strategy cannot guarantee the stability of the haptic telepresence system and therefore HLS is not appropriate for haptic telepresence systems.

The innovation of this chapter is in the combined consideration of the haptic telepresence system and the communication network in terms of the network cost associated with the network traffic. The primary goal is to reduce the packet transfer rate without impairing the stability and transparency of the telepresence system leading to an

innovative communication bandwidth oriented control approach for haptic telepresence systems. In order to achieve a reduction of the packet transfer rate the deadband control approach is firstly applied to haptic telepresence systems[1]. The key challenges are the determination of a transparency oriented deadband type, the data reconstruction for data that have not been sent with impairing stability and the performance evaluation in terms of transparency and network cost.

The remainder of this chapter is organized as follows: After the introduction of the deadband control approach in Section 5.1, the stability is discussed in Section 5.2 going along with an extension of the data reconstruction algorithms from Chapter 4. The combined performance in terms of transparency and network cost is then evaluated in simulations in Section 5.3. The substantial benefit of this approach is validated in objective experiments and experimental user studies in Section 5.4.

5.1 Deadband Control Approach

The network traffic generated by current haptic telepresence systems is characterized by constantly high packet transfer rates in the range of the sampling rate of the local subsystems, and low packet load.

In order to reduce the network traffic several approaches exist. They can be basically classified into approaches that reduce the packet load by sophisticated encoding techniques and approaches that reduce the number of packets sent, mixed forms are, of course, also available. An approach belonging to the first class based on the Huffman-coding technique has been proposed for haptic VR applications in [93]. However, looking at the characteristics of network traffic generated by haptic telepresence systems lets the latter approach seem to be more promising with respect to the resulting traffic reduction as the following example shows.

Example: Lets assume a haptic telepresence system with 6 degrees-of-freedom (DoF) operating at a sampling rate of 1000Hz. Corresponding to the number of DoF in each packet at least 6 values of type float (4 Bytes per value) are sent; the packet load is 24 Bytes . Using RTP/UDP/IP as protocol for the transmission the protocol overhead is 40 Bytes (8 Bytes for RTP, 12 Bytes for UDP, 20 Bytes for IPv4). The traffic volume per packet is 64 Bytes (=512 Bits). Sending one packet per sampling instance the minimal required bandwidth is 500 kBit/s. Even though the packet load is low the bandwidth requirement is comparable to compressed streaming video being also a part of the multimodal telepresence induced traffic.

The protocol overhead is the dominant component of the induced network traffic volume, hence reducing the packet rate would significantly reduce the traffic volume itself. Targeting at a packet rate reduction the deadband control approach is investigated here for application in haptic telepresence systems.

[1]The fruitful collaboration with Peter Hinterseer (Lehrstuhl für Kommunikationsnetze, Technische Universität München) providing the preliminaries of this work is highly acknowledged.

5.1.1 Assumptions

As in the previous chapter the haptic telepresence system is modeled as a sampled-data system. The subsystems HSI/human and teleoperator/environment together with the local control are assumed to be passive continuous time systems, whereas the communication subsystem including the network and the applied wave variable transformation (2.8) is considered in discrete time. The interconnection between the continuous and the discrete time system is assumed to be passive using the energy conserving sampling technique proposed in [135, 137]. The sampling time is denoted by T_A. Throughout this chapter the communication channel is assumed to have a constant delay T_1 in the forward and T_2 in the backward path. Assuming the delays to be integer multiples of the sampling time T_A they can also be represented by D_1 and D_2 with $T_i = D_i T_A$. Furthermore, the communication channel is assumed to have no packet loss.

5.1.2 Extended Communication Model

The communication subsystem consisting of the wave variable transformation and the communication channels is extended by the deadband controller inserted between the wave variable transformation and the communication channel, see Fig. 5.1. The deadband control acts on the sampled wave variables u_l in the forward path and v_r in the backward path. Referring to the symmetry the following considerations are done for the forward path only but equivalently apply to the backward path.

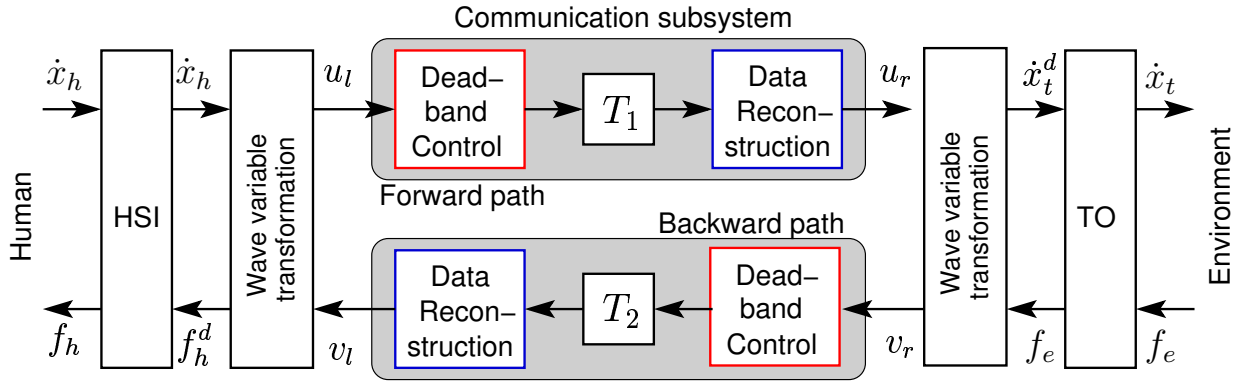

Figure 5.1: Deadband controlled haptic telepresence system with extended communication subsystem.

The deadband controller compares the most recently sent value $u_l(k^*)$ with the current value $u_l(k)$, $k > k^*$. If the absolute value of the difference $|u_l(k^*) - u_l(k)|$ is smaller than the deadband width Δ then no update is sent over the network. Otherwise the value $u_l(k)$ is transmitted and a new deadband is established around this value. For further considerations an event indicator is defined

$$\Omega_u(k) = \begin{cases} 0 \text{ if } |u_l(k) - u_l(k^*)| < \Delta \\ 1 \text{ otherwise} \end{cases}, \tag{5.1}$$

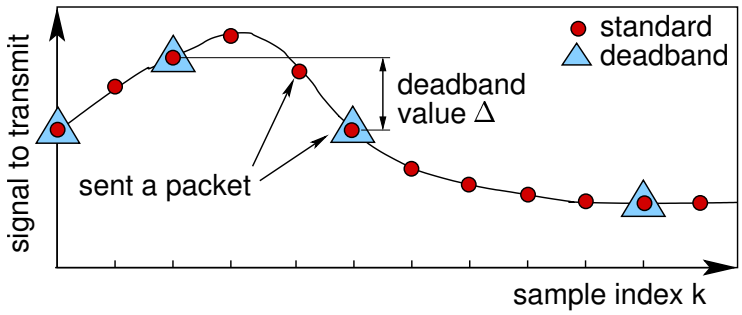

Figure 5.2: Visualization of the deadband control compared to standard approach.

indicating a 'packet sent' over the forward path at time $t = kT_A$ if $\Omega_u(k) = 1$. The event indicator for the backward path, equivalently defined, is denoted by Ω_v.

As not all values are sent empty sampling instances occur at the receiver side. This leads to a similar problem as in the foregoing chapter for the time-varying delay/packet loss problem: data reconstruction for the missing data is necessary as indicated by the corresponding blocks in Fig. 5.1. Analogously to the reconstruction operator (4.7) for the empty sampling instances resulting from packet loss a general reconstruction operator is defined (4.8)

$$u_r(k) = \begin{cases} \zeta_u(k - D_1) & \text{if } \Omega_u(k - D_1) = 0 \\ u_l(k - D_1) & \text{otherwise} \end{cases} \tag{5.2}$$

The corresponding reconstruction algorithm is denoted by $\zeta_u(\cdot)$. The reconstruction operator formalizes the self-evident fact that, if available, the transmitted data are processed, otherwise a data reconstruction algorithm is required.

Different types of deadbands are introduced and discussed with respect to their effect on the network traffic in the subsequent section. It is followed by an extension of the data reconstruction strategies developed in the foregoing chapter together with stability considerations.

5.1.3 Deadband Types

The deadband can be defined to be of constant width or alternatively as a function of the value $u_l(k^*)$. Both types are considered here.

Constant Deadband

The constant deadband control approach has been proposed for NCS in [113]. The deadband has always the same constant width

$$\Delta = \Delta_c = \text{constant} \in \mathbb{R}_+. \tag{5.3}$$

One exception is necessary here for the case that the signal approaches zero. If the most recent transmitted value is close to the origin $|u_l(k^*)| < \Delta$ it may happen that the input to the deadband controller $u_l(k)$ changes the sign. As soon as the input $u_l(k)$ changes the sign it is transmitted as the direction of a variable is considered as the minimum information to

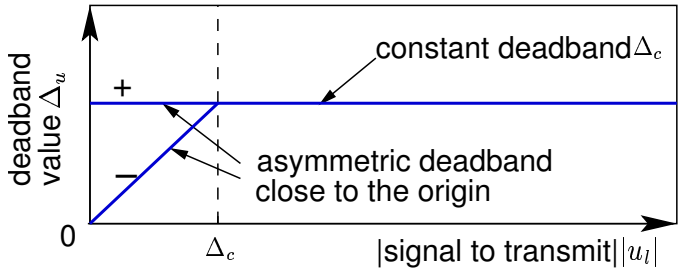

Figure 5.3: Constant deadband definition according to (5.3), and (5.4).

be transmitted. A formal discussion on the necessity of the sign consistency of the signal at the sender and the receiver side for the passivity follows in the next section.

As a result close to the origin the deadband is unequally spaced, while far from the origin the deadband of constant width applies. In order to consider this exception the deadband is implicitely defined by

$$|u_l(k)| \in \begin{cases} [0, |u_l(k^*)| + \Delta_c) & \text{if } |u_l(k^*)| < \Delta_c \\ [|u_l(k^*)| \pm \Delta_c] & \text{otherwise} \end{cases}, \tag{5.4}$$

where the first case corresponds to the exception made close to the origin. With this definition of the deadband the sign consistency

$$u_l(k)u_l(k^*) \geq 0, \tag{5.5}$$

between the transmitted value $u_l(k^*)$ and the consecutive (before the next packet is sent) values at the sender $u_l(k)$ is guaranteed.

Relative Deadband

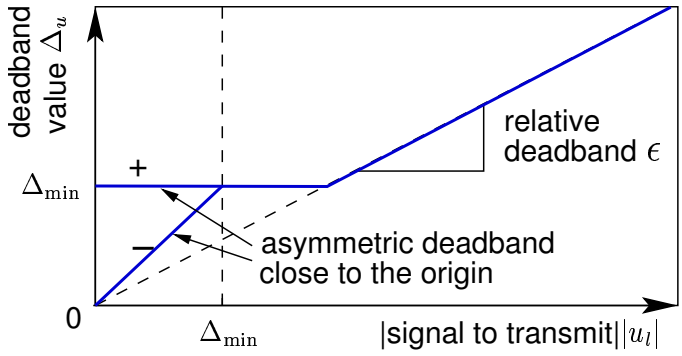

Figure 5.4: Relative deadband definition according to (5.6), (5.7), and (5.8).

The relative deadband grows linearly with the magnitude of the value $u_l(k^*)$. The value of the deadband is given by

$$\Delta = \Delta_{u_l(k^*)} = \Delta(u_l(k^*)) = \varepsilon|u_l(k^*)|, \quad \varepsilon \in \mathbb{R}_+, \tag{5.6}$$

with ε a constant proportional factor. If the signal $u_l(k^*)$ is close to the origin the deadband becomes infinitely small. For practical application the deadband is lower bounded

$$\Delta \geq \Delta_{\min}. \tag{5.7}$$

With the same sign consistency (5.5) argument as for the constant deadband the relative deadband is implicitely defined by

$$|u_l(k)| \in \begin{cases} [0, |u_l(k^*)| + \Delta_{\min}) & \text{if } |u_l(k^*)| < \Delta_{\min} \\ [|u_l(k^*)| \pm \Delta_{u_l(k^*)}] & \text{otherwise} \end{cases}, \tag{5.8}$$

such that (5.5) holds.

Remark 5.1 The application of a relative deadband is inspired by human haptic perception. According to results from psychophysics there exist perception thresholds (just noticeable difference, JND) in human haptic perception for velocity and force signals [22, 64], which are proportional to the magnitude of the percepted quantity. In a first study [56], where no delay in the communication subsystem has been assumed, the relative deadband control approach has successfully been applied to the transmitted velocity and force signals. As the wave variables are linear combinations of velocity and force the potential of a relative deadband approach is also investigated here.

In the following it is assumed that the deadband denoted by Δ fulfills (5.4) for the constant deadband, (5.6) and (5.8) for the relative deadband.

Effect on Packet Rate

With the deadband defined constant (5.3) the packet rate is proportional to rate of change of the transmitted signal. This can be observed in Fig. 5.5(b), where the 'packet sent' indicator Ω_u (5.1) is computed for a given signal u_l, see Fig. 5.5(a). Constant rate of change of the signal results in equidistant time intervals between the transmitted values. Higher deadband width results in lower packet rate.

For the relative deadband (5.6) the packet rate depends not only on the rate of change of the transmitted signal, but also the absolute value of the transmitted signal. The packet rate is very high at small signal values, but decreases with higher signal values, Fig. 5.5(c). The necessity of the lower bound $\Delta_{\min}$ becomes evident, otherwise the packet rate would become infinitely close to the origin.

5.2 Stability with Deadband Control

In order to guarantee the stability of the haptic telepresence system within the considered passivity approach, the passivity of the subsystems has to verified. This is true for the human/HSI and the teleoperator/environment subsystem by assumption, see Section 5.1.1. For stability the passivity of the extended communication subsystem introduced in Section 5.1.2, visualized in Fig. 5.1, has to be guaranteed.

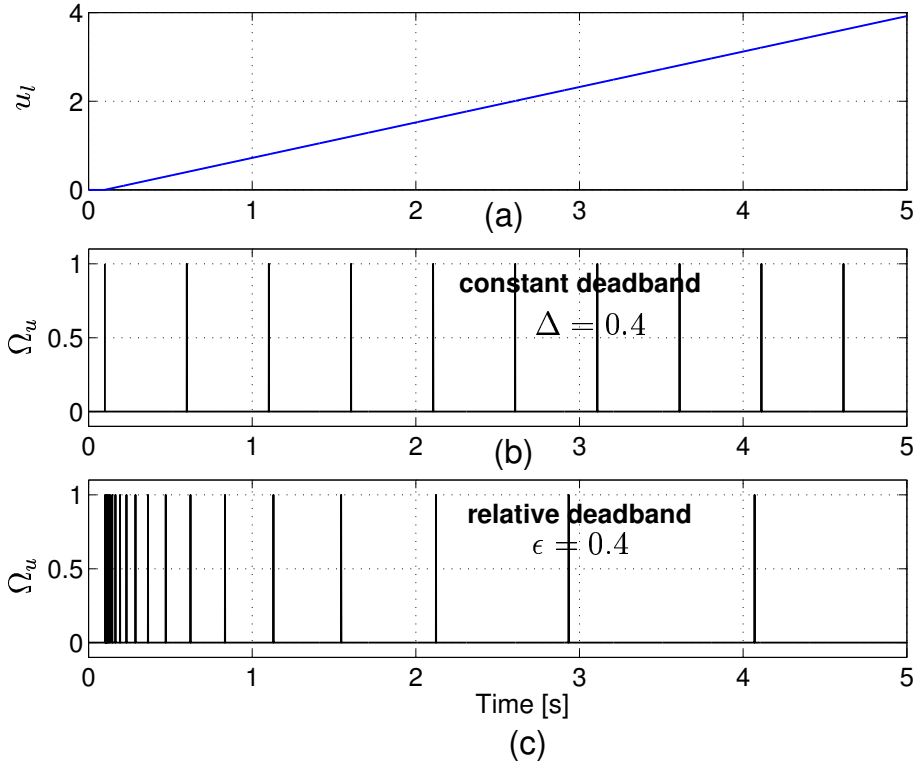

Figure 5.5: 'Packet sent' indicator value for a given signal (a) with constant (b) and relative deadband (c).

5.2.1 Passivity of the Extended Communication Subsystem

Independently of the deadband definition deadband control results in empty sampling instances at the receiver side. The missing values need to be estimated. Formally, the same problem of passive data reconstruction arises as in the foregoing chapter for the time-varying delay/packet loss problem. As only the data reconstruction algorithm but not the deadband controller itself effects the energy balance of the communication subsystem, see Fig. 5.1, for passivity, thus, stability a passive data reconstruction is sufficient.

Proposition 5.1 The communication subsystem with deadband control is passive, if the data reconstruction is passive. Theorem 4.1 and Theorem 4.2 are straightforward to apply.

Sketch of Proof: The passivity analysis follows the argumentation given in the previous chapter for the packet loss problem. Equivalently to the in Lemma 1 proposed splitting into time intervals without and with packet loss, here we separately consider the time instances where packets are sent and time intervals where no packets are sent. Accordingly, the overall storage function of the communication subsystem $E_{c,in}^{\zeta}(N)$ is split (4.9), now with $E_{c,in}^{nl}$ the storage function component corresponding to the first case, and $E_{c,in}^{l}$ corresponding to the latter one. The only difference in the definition of the storage function components (4.10) and (4.11) is, that the loss indicators l_1 and l_2 (4.6) are replaced by the 'packet sent' indicators Ω_u and Ω_v (5.1), respectively. Theorem 4.1 and Theorem 4.2 are based on this energy balance splitting and can therefore directly be applied. ■

Consequently, the results on the passivity of data reconstruction strategies from the previous chapter can be directly carried over. One of these results is that the hold last sample (HLS) algorithm is not passive, thus it cannot guarantee the stability of the deadband controlled haptic telepresence system. The zeroing strategy is proven to be passive but very conservative. The zeroing strategy is a result of the fact that in the packet loss case the value of a lost packet is generally not known. With deadband control though the value of the missing data is known to be within the deadband interval of the most recently received packet. Exploiting this knowledge a novel passive, less conservative reconstruction strategy is proposed: the modified HLS.

5.2.2 The Modified HLS Strategy

The modified HLS reconstructs the missing data at the lower end (closer to the origin) of the current deadband interval, hence differs from the classical hold last sample exactly by the deadband value. This data reconstruction strategy is formally expressed by

$$\zeta_u(k - D_1) = u_r(k^*) - \text{sign}\{u_r(k^*)\} \cdot \Delta_u, \tag{5.9}$$

where Δ_u stands for the corresponding deadband around $u_r(k^*) = u_l(k^* - D_1)$, and k^* for the sampling instance when the most recent value arrived. The deadband can be defined as constant or relative or any other type of deadband, main requirement is that the same deadband is applied at the sender as well as at the receiver side. Here, again only the forward path is considered, all results equally apply to the backward path.

Proposition 5.2 The modified HLS algorithm is passive.

Proof: The passive behavior of the modified HLS algorithm can be verified showing that the sufficient condition for passive data reconstruction (4.13) from Theorem 4.2 is satisfied, hence the reconstruction algorithm is small gain. If an empty sampling instance at time k occurs then no packet has been sent at the corresponding delay time before $\Omega_u(k - D_1) = 0$. Consequently, the missing data value $u_r(k) = u_l(k - D_1)$ must lie within the deadband interval of the most recently received value $u_r(k^*)$. Only if we assume sign consistency between the current values at the sender and the latest sent (5.5) then the complete current deadband interval lies either in the positive or negative area and the following inequality holds

$$|u_l(k^* - D_1)| - \Delta_u \leq |u_l(k - D_1)| \leq |u_l(k^* - D_1)| + \Delta_u. \tag{5.10}$$

Replacing $u_l(k^* - D_1) = u_r(k^*)$ the lefthand term of these equation represents the absolute value of the reconstructed data $|\zeta_u(k - D_1)|$ according to (5.9), hence

$$|\zeta_u(k - D_1)| \leq |u_l(k - D_1)|$$

is true satisfying (4.13) and thereby the sufficient passivity condition from Theorem 4.2. The modified HLS algorithm is passive. ■

Simulation

The effect of the deadband control together with the modified HLS as data reconstruction strategy is visualized in simulations. Therefore, the forward path of the communication subsystem is simulated with a predefined input signal $u_l(t) = \sin t + t$ a delay $D_1 = 100$, a network sampling time $T_A = 1$ms. The effect of the modified HLS algorithm on the signal development of u_r is depicted in Fig. 5.6. At the time instances where packets arrive the value of the original signal are taken, otherwise the missing data are reconstructed by the modified HLS.

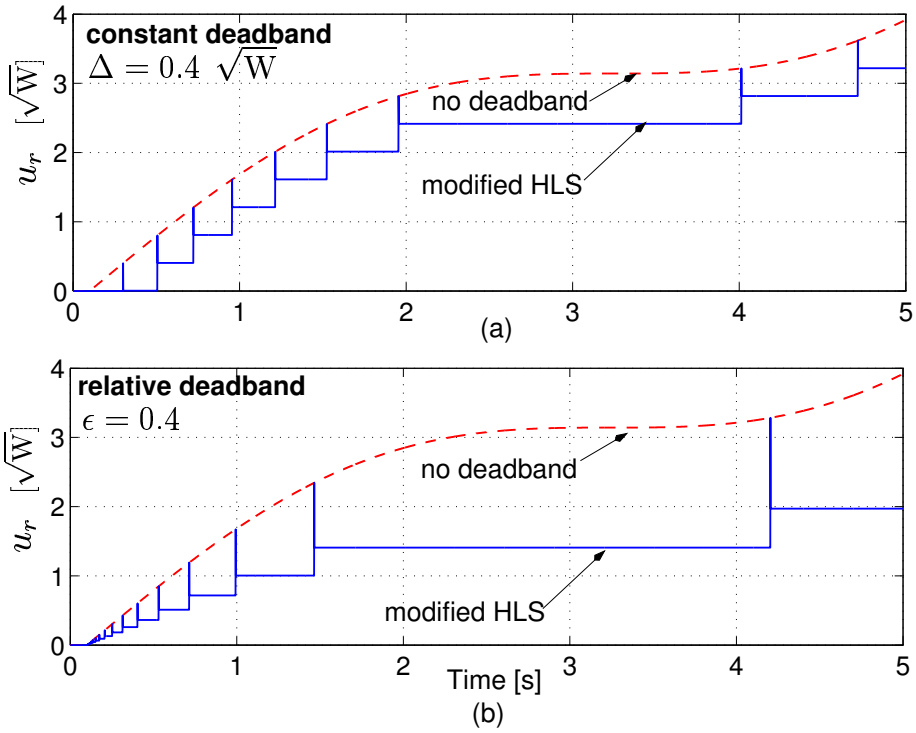

Figure 5.6: Modified HLS as reconstruction algorithm for constant (a) and relative deadband (b)

The modified HLS algorithm can be interpreted as a worst case estimation of the untransmitted data corresponding to a minimal wave input energy assumption. With this data reconstruction algorithm the communication subsystem generally dissipates energy, but less than with the zeroing strategy. Using the modified HLS instead of the zeroing, see Section 4.3.3, the transparency of the proposed reconstruction strategy with energy supervision, see Section 4.3.5, is improved.

5.2.3 Energy Supervised HLS/modified HLS Algorithm

The energy supervised data reconstruction, introduced in Section 4.3.5, uses the observation of the energy balance in the forward and the backward path to choose the appropriate reconstruction algorithm to achieve transparency while at the same time maintaining the passivity of the communication subsystem, see Fig. 5.7. Therefore, the virtual energy storage element has been introduced in Section 4.3.5 described by the energy content E_v.

As long as the virtual energy E_v is positive a transparent, but possibly energy generating algorithm such as the HLS (4.14) is applied. When the energy balance reaches its initial value then a strictly passive algorithm is used. Instead of the strictly passive zeroing algorithm, which is employed in Section 4.3.5, here now the less conservative modified HLS is applied as strictly passive algorithm. Accordingly, the energy supervised HLS/modified HLS algorithm is defined by (4.19) with ζ_{np} denoting the non-passive HLS and ζ_p the strictly passive modified HLS algorithm. For a detailed discussion and the passivity proof refer to Section 4.3.5.

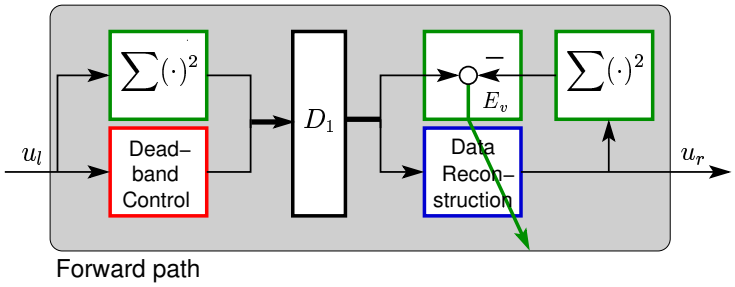

Figure 5.7: Principle of energy supervised data reconstruction for deadband controlled telepresence system.

Simulation

The output signal distortion of the energy supervised HLS/modified HLS (4.19) using the same simulation condition as in Section 5.2.2 is depicted in Fig. 5.8 for the constant and the relative deadband. For the energy supervised reconstruction the switching from the HLS to the modified HLS can be observed as in the starting phase the energy level of the virtual storage element is not high enough to allow a simple HLS until the next packet arrives.

The passivity of the communication subsystem for all considered deadband/reconstruction approaches is indicated by the positive values of the energy balance of the forward path in Fig. 5.9. Generally, higher deviation from the original signal results in a more conservative behavior corresponding to higher positive values in the energy balance of the communication subsystem. Clearly, the modified HLS is more conservative than the HLS/modified HLS with energy supervision.

The interesting question is, whether the constant or the relative deadband control approach performs better.

5.3 Effect on Performance

The primary goal of this section is to compare the different deadband types (constant and relative deadband) and the considered data reconstruction algorithms (modified HLS and HLS/modified HLS) with respect to the performance.

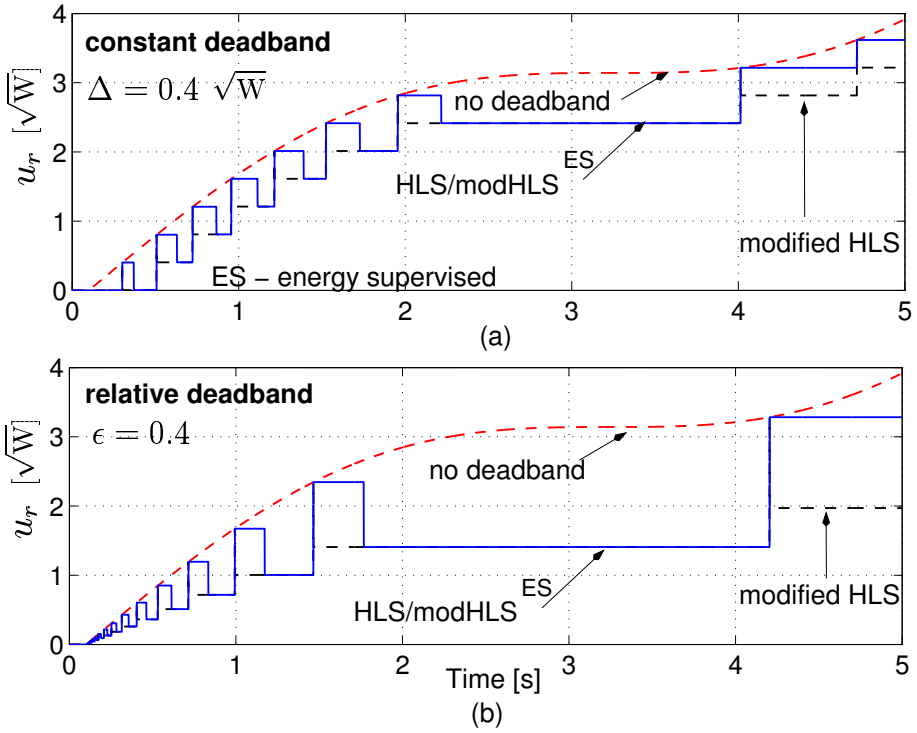

Figure 5.8: Energy supervised HLS/modified HLS as reconstruction algorithm for constant (a) and relative deadband (b)

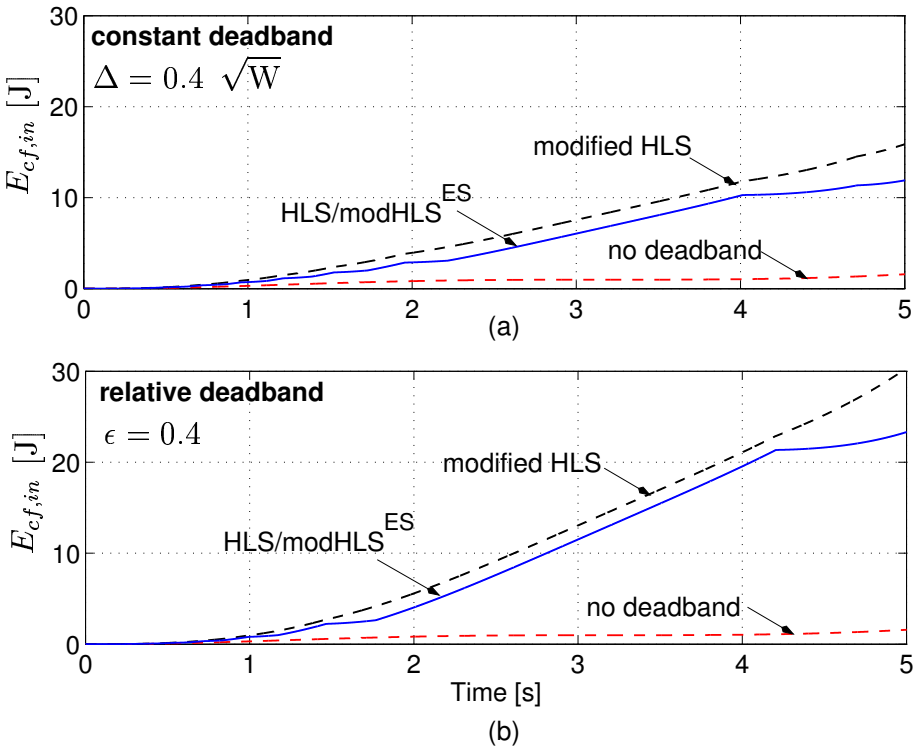

Figure 5.9: Energy balance of the communication subsystem for constant (a) and relative deadband (b) with modified HLS and energy supervised HLS/modified HLS as reconstruction algorithm

5.3.1 Extended Performance Metrics

In order to evaluate the efficiency of the deadband control approach in addition to the traditional haptic telepresence systems transparency the induced network traffic as communication performance measure has to be taken into account. Therefore a new performance metrics is necessary covering network perfomance in terms of packet rate together with the transparency of the haptic telepresence system.

The performance of haptic telepresence systems is evaluated using the transparency measure introduced in Section 3.1. This measure compares the perceived impedance at the operator side with the real environment impedance in terms of their mechanical parameters stiffness, damping and mass. The resulting normed errors of these parameters allow the application of psychophysical results in terms of JND considerations, see Section 2.3.2 for more details.

The performance with respect to the communication subsystem is determined by the network traffic. A low number of transmitted packets corresponds to high performance. The network performance measure is defined by the ratio of transmitted packets with deadband control over the transmitted packets without deadband control. Best performance has the approach that has the smallest values in either of the considered performance measures.

An analytical performance evaluation as performed in Section 3.1.1 is difficult as an analytical representation of the perceived impedance depending on the deadband value is not available. Therefore the performance is numerically evaluated using the developed analysis tool from Section 3.1.2 and in experiments. It should be noted, that due to the non-linear dynamics the deadband control approach introduces into this complex system the numerical approximation is valid around the operating point chosen.

5.3.2 Numerical Performance Evaluation

The effect of the deadband control approach on the perceived impedance is exemplarily studied for the relative deadband type, with the teleoperator in contact with an environment with a spring-damper characteristics ($k_e = 200\text{N/m}$, $b_e = 1\text{Ns/m}$). The sampling time is $T_A = 1\text{ms}$. The delay in the forward and the backward path is $D_1 = D_2 = 1$, the wave variable parameter is set to $b = 1\text{Ns/m}$. The deadband control applies with the same deadband parameter and reconstruction algorithm in the forward and the backward path.

The frequency response is obtained from the cross-correlation analysis as described in Section 3.1.2. The resulting Bode plot, presented in Fig. 5.10, shows that a spring characteristics is still perceived with the applied deadband control as indicated by a phase of approximately 90° in the lower frequency range. In the magnitude response in this range though does not decrease with -20dB as for a linear impedance, the non-linear characteristic becomes obvious, the approximated stiffness coefficient is a function of the exciting frequency. With increasing deadband the environment feels softer. However, further generalizing statements are not possible due to the snapshot character of this result.

In the following the influence of the relative deadband control approach on the network traffic is qualitatively studied.

Therefore, the HSI is modeled as a velocity source providing a constant velocity of $\dot{x}_h(t) = 1\text{m/s}$. In difference to the previous simulations the environment has a spring characteristics ($k_e = 1\text{N/m}$), and the communication delay is $D_1 = D_2 = 100$. The perceived

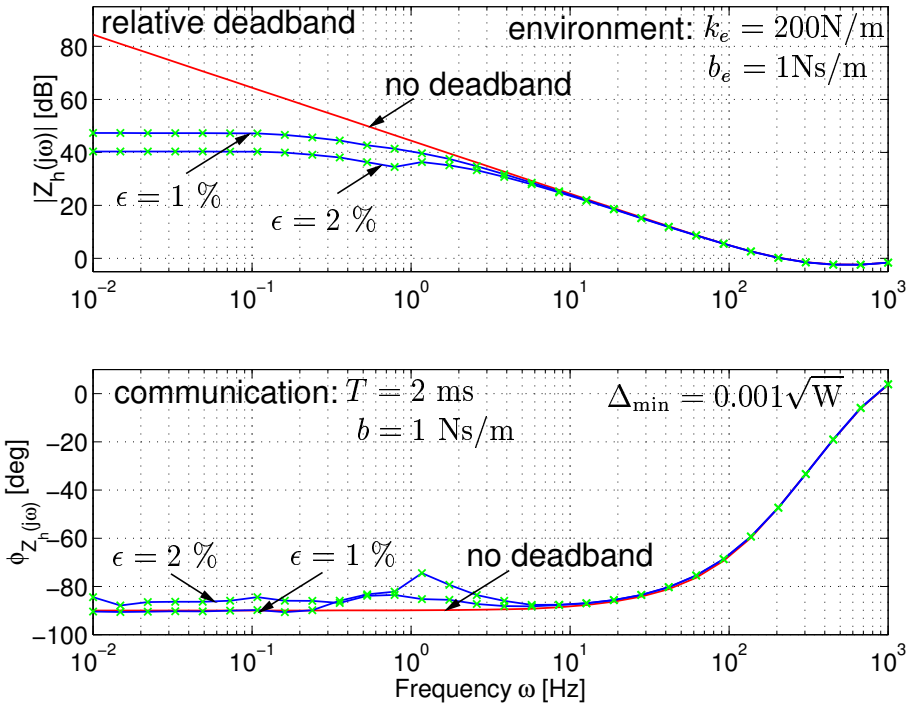

Figure 5.10: Bode plot of the perceived impedance with the relative deadband control approach

stiffness coefficient as well as the percentage of transmitted packets is then computed for a simulation time of 10s.

The results are presented in Fig. 5.11. With increasing deadband the environment feels softer, as shown in Fig. 5.11(a), where the coefficient of the approximated perceived stiffness for the dedicated HSI velocity signal is depicted depending on the value of the deadband. Note, that due to the delay the perceived stiffness without deadband ($\varepsilon = 0$) is smaller than the real environment stiffness, see Chapter 3 for a detailed investigation. Generally, with increasing deadband the transparency is degraded. On the other hand with increasing deadband less packets are transmitted, see Fig. 5.11(b) validating the effectiveness of the approach with respect to the network cost.

Remark 5.2 Further investigations reveal that in free space motion an inertia is perceived, that increases with the deadband value.

As expected, the energy controlled HLS outperforms the modified HLS as reconstruction strategy, this approach shows the highest performance in terms of network and telepresence system performance. A general rating on the choice of deadband type though is not obvious from the performed simulations. Experiments are conducted in order to evaluate these approaches from a practical point of view.

5.4 Experiments

The first goal of the experiments is to rate the deadband/reconstruction strategies in an objective performance evaluation using the extended performance metrics. The second

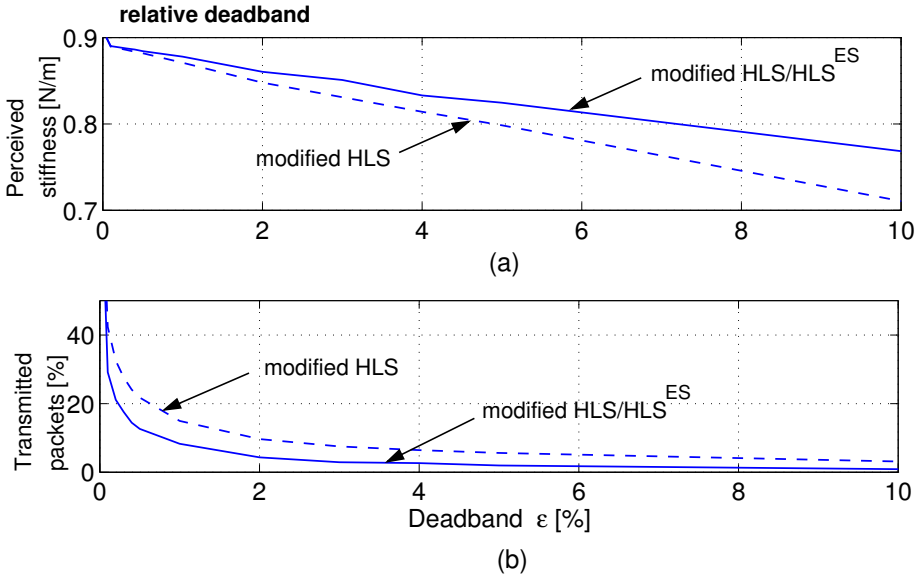

Figure 5.11: Perceived stiffness and percentage of transmitted packets depending on the relative deadband width.

goal is to find the best performing deadband type and the appropriate deadband value in psychophysical experiments.

Experimental Setup

For the experiments the experimental haptic telepresence system described in Appendix C is used. The communication subsystem, shown in Fig. C.1 consists of the communication line with constant delay, the deadband control, the data reconstruction algorithms and the wave variable transformation with the wave impedance set to $b = 250\text{Ns/m}$. The control loops operate at a sampling rate of 1000Hz representing the standard packet rate without deadband control, $T_A = 1\text{ms}$.

The deadband control and the data reconstruction strategy are equally applied with the same deadband value in the forward and the backward path. The lower bound for the relative deadband is heuristically set to a small value of $\Delta_{\min} = 0.002\sqrt{\text{W}}$. The round-trip delay is constant $D = D_1 + D_2 = 200$ sample intervals T_A in the first and $D = 100$ in the second experiment. In order to have an appropriately delayed visual feedback the delay in the backward path is set to $D_2 = 1$.

5.4.1 Objective Performance Evaluation

The combinations of constant and relative deadband control approaches with the modified HLS and the energy supervised data reconstruction are compared with respect to the extended performance metrics.

Procedure

During the experiment the deadband value is varied with $\Delta \in \{0.002, 0.02, 0.1, 0.2, 0.4\}\sqrt{\text{W}}$ and $\varepsilon \in \{0.1, 1, 5, 10, 20\}\%$. The stiffness parameter k_h perceived by the operator during

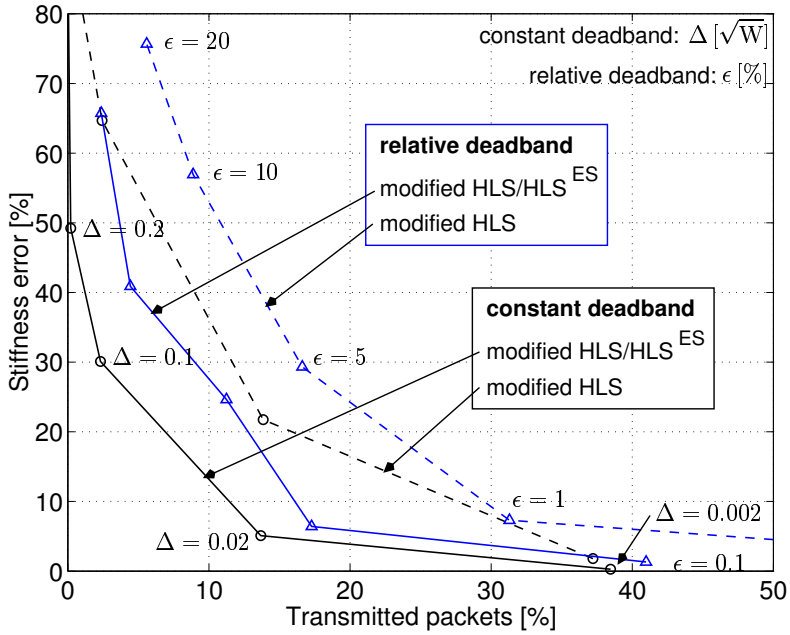

Figure 5.12: Normed error of perceived stiffness depending on the percentage of transmitted packets

touching the wall is computed by means of a least square identification on the position and force signals measured at the HSI. Note that due to dependency of the perceived stiffness on the exciting signal frequency, the perceived stiffness can be interpreted only as an approximated mean perceived stiffness. For comparison the perceived stiffness without deadband control is used which is $k_{h,0} = 540\text{N/m}$. The normalized stiffness error $\frac{k_{h,0}-k_h}{k_{h,0}}$, see also (3.16), depending on the percentage of transmitted packets is depicted in Fig. 5.12.

Result

Highest performance in this experiment shows the constant deadband control approach with energy supervised data reconstruction validating the simulation results. In order to display the same stiffness fewer packets need to be transmitted than in all other approaches.

5.4.2 Evaluation considering Human Factors

Psychophysical experiments are conducted in order to determine the detection threshold for the deadband value Δ for the constant and ε for the relative deadband control approach. Furthermore, the effect of the deadband control on the packet rate is quantitatively evaluated. The energy supervised HLS/modified HLS strategy is applied for data reconstruction.

Conditions

Altogether, 11 subjects were tested, see Table 5.1 for a more detailed description. The subjects were told to operate with their preferred hand. They were equipped with earphones to mask the sound the device motors generate. The subjects were provided with visual

Table 5.1: Subjects description.

Subjects	Age	Sex	Prior contact	Detection situation
11	22-30	f: 3 m: 8	yes: 2 no: 9	free space motion:5 contact: 4 both: 2

feedback. During a familiarization phase subjects were told to feel operation in free space and in contact with a stiff wall without deadband control. As soon as they felt familiar with the system the measurement phase began.

In the experiment detection thresholds for the deadband parameters Δ (ε) were determined using a three interval forced choice (3IFC) paradigm, see Section 3.3.2 for a detailed description of the procedure. In two of the three presented consecutive 20s intervals the system worked without the deadband algorithm just as in the familiarization phase. In one of the three intervals which was randomly determined the deadband algorithm with a certain value Δ (ε) was applied. The experiment started with an initial deadband parameter $\Delta = 0.045\sqrt{\mathrm{W}}$ ($\varepsilon = 2\%$). The average over the 3 passes was taken as the subjects' specific detection threshold.

Results

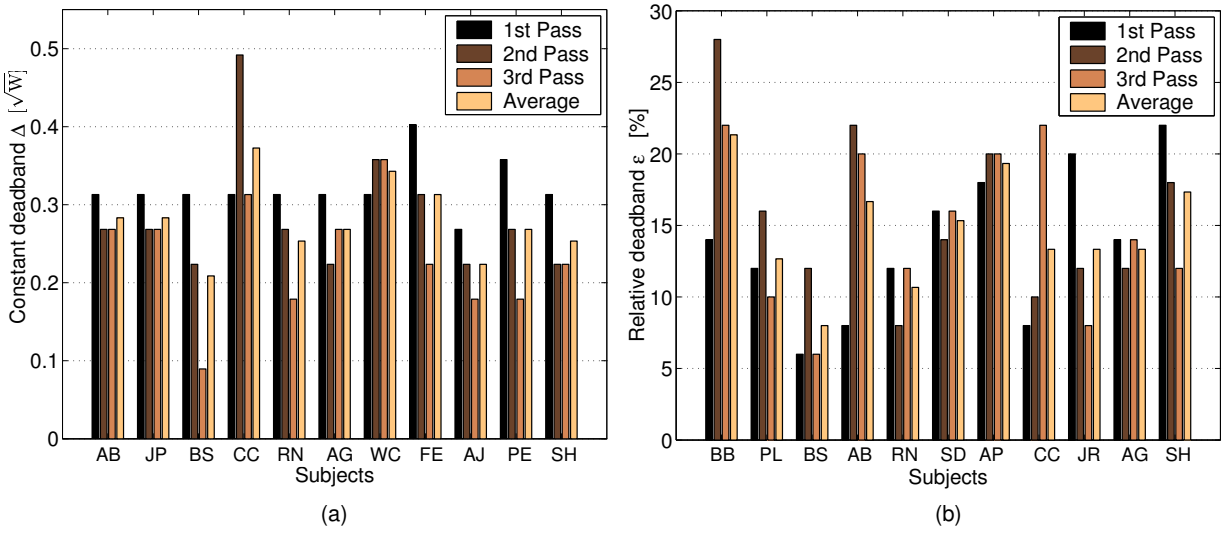

Figure 5.13: Subjects' results for constant (a) and relative deadband (b).

The specific situation, free space motion or contact, in which the subjects detected the transparency degradation is listed in Table 5.1. According to that no specific situation accounts for the detection.

The detection thresholds for every subject in the three passes together with average over the three passes, which is taken as the specific detection threshold for this subject, are presented in Fig. 5.13. Only one person (a dental technician with highly trained sensorimotor capababilities) managed to feel the transparency degradation introduced by

a deadband value of $\Delta = 0.21\sqrt{\mathrm{W}}$ for the constant and $\varepsilon = 8\%$ for the relative deadband control approach. All other tested subjects have higher detection thresholds. These lower bounds are taken as detection threshold for further evaluation.

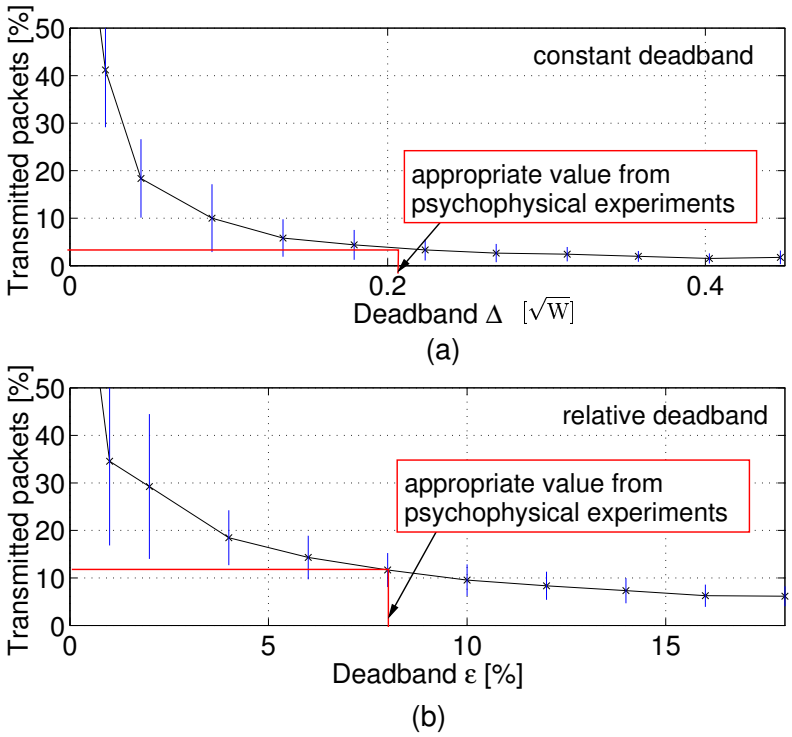

Figure 5.14: Experimental results: Influence of the deadband width on packet rates for constant (a) and relative deadband (b).

The potential of the deadband control approach to reduce network traffic can be seen in Fig. 5.14, where the average packet rates measured during the psychophysical experiments are depicted as a function of the deadband width. As expected, increasing deadband width leads to a traffic reduction. According to the determined detection thresholds a substantial traffic reduction of 95% for the constant and 87% for the relative deadband control approach is achieved. Only 5% (13%) of the packets containing haptic information need to be transmitted without impairing transparency. This corresponds to the results found for the relative deadband control approach for velocity and force signals without communication delay [48, 56].

Discussion

The constant deadband control approach performed generally better. The relative deadband control approach though provides better scalability; further, the lower threshold bound $\Delta_{\min}$ not varied in these experiments has a large influence on the packet rate and such the performance. In order to give a final rating on the best choice of deadband type in future experiments the appropriate lower threshold bound $\Delta_{\min}$ should be determined, further, more complex tasks with multi-DoF telepresence systems should be considered and the influence of the time delay on the obtained results should be investigated. The asymmetry in the human haptic action/perception bandwidth, see Section 2.3, should be

taken into consideration: different deadband values and maybe even different deadband types for the forward and the backward path could be considered. Further improvement is expected, if position feedforward [27] is used that is straightforward to apply, see also Appendix A for details.

5.5 Discussion

State-of-the-art haptic telepresence systems require high packet rates for the transmission of the haptic information, that are hard to maintain on long distances in current packet switched communication networks. The thereby induced network traffic volume is comparable to streaming video. Strategies to reduce the network traffic in haptic telepresence sytems have not been considered in the known literature yet.

In this chapter an innovative communication bandwidth oriented control approach substantially reducing the network traffic in haptic telepresence systems with time delay is proposed. A significant reduction of up to 95% of the number of transmitted packets, i.e. the network traffic volume, is achieved without impairing the transparency.

The underlying approach is based on deadband control, where data is sent only if the difference to the previously sent value exceeds a certain threshold, the deadband. One of the key challenges is the data reconstruction: the data of the packets not sent, have to be reconstructed without generating energy in order to guarantee the stability of the telepresence system. A novel data reconstruction algorithm, developed in this chapter based on the framework for passive data reconstruction proposed in Chapter 4, ensures the passivity of the communication subsystem and such the stability of the telepresence system. Two different types of deadbands, namely a constant and a relative deadband, are investigated with respect to the transparency using the transparency measure proposed in Chapter 3. Generally, large deadband values reduce the network traffic but also the perceivable stiffness. In a combined performance consideration this trade-off between network traffic and transparency is investigated. Objective experiments validate the obtained result. In order to determine the largest deadband value at which a transparency degradation is not perceivable by the human, experimental user studies are performed. As a result only 5% for the constant and 13% for the relative deadband of the packets containing haptic information need to be transmitted without impairing the human perceived transparency.

For the first time the combined performance of the haptic telepresence system and the communication network in terms of transparency and network traffic is considered in this chapter. Exploiting the human haptic perception limits a significant network traffic reduction is achieved. Future research includes the extension of this approach to communication networks with time-varying time delay and packet loss as well as the experimental evaluation in multi-degree-of-freedom haptic telepresence systems.

6 Towards Quality-of-Service Telepresence Control

The transparency of a telepresence system is strongly related to the quality of communication as shown in Chapters 3 and 4. In order to ensure the operability of multimodal tele-applications, a guaranteed minimum level of transparency is required. Consequently, a certain communication quality has to be guaranteed in order to promote high level tele-applications. Aside from telepresence systems there is a rising number of other advanced network applications associated with real-time requirements, such as video-on-demand and Internet-telephony, that also need guarantees about the communication quality. In contrast to telepresence systems no stability problems with the resulting hazard to the human or the environment may occur. With their communication requirements these applications contrast the large number of network applications without any real-time requirements (elastic applications). The current Internet with its best effort and 'common service for all' paradigm can neither give any guarantees nor may it account for the different communication quality requirements. The research focus within the networking community is on the service differentiation for different network traffic going along with communication quality guarantees, the *Quality-of-Service* (QoS) concept.

The interesting question is how QoS concepts can be beneficially included into the control of networked haptic telepresence systems. The very few approaches available in the literature are dedicated to multimedia applications. In order to formulate the application specific QoS requirements, recently the influence of the communication quality on the application performance has been investigated for standard multimedia applications and networked control systems [40, 123]. For telepresence systems such a QoS mapping is not available yet. Under this aspect the results from Chapter 3 and Chapter 4 are highlighted as a first step towards a QoS mapping for haptic telepresence systems. In [151] the frame rate of the video feedback in a telepresence system is adjusted based on a Fuzzy approach. QoS in the context of haptic telepresence is preliminarily studied in [152], where the control parameters are adjusted according the current communication quality exploiting the QoS concept in terms of the guaranteed communication quality. However, the developed QoS architectures allow to some extent the *control* of the communication quality. Preliminary results in the field of QoS control for networked control systems [26] are very promising.

The innovation in this chapter lies in the first consideration of the combined control of the haptic telepresence system and the communication network, the QoS control. Currently available QoS communication architectures are studied with respect to their control relevant implications. As a result, two novel QoS control architectures are proposed and compared with respect to their benefits and challenges in terms of the transparency and QoS architecture requirements. Visionary ideas are discussed combining the results of the previous chapters. The open problems highlighted in this chapter are expected to direct

future research in this direction, in the control as well as in the communication community.

The remainder of this chapter is organized as follows: the two main different QoS architectures are studied in terms of their control relevant implications in Section 6.1. Novel control concepts for telepresence over QoS networks are introduced and compared with respect to transparency and network cost in Section 6.2, showing the benefits of these approaches. A discussion of open problems in Section 6.3 concludes this chapter.

6.1 Quality-of-Service Communication

The default service offering associated with the Internet is characterized as a best-effort. Within this service profile the network makes no attempt to actively differentiate its service response between the traffic streams generated by concurrent users of the network. As the load generated by the active traffic flows within the network varies, the network's best effort service response will also vary. Bounds on delay, delay jitter and packet loss cannot be given.

Generally, QoS refers to the capability of a network to provide better service to selected network traffic. The primary goal of QoS is to provide priority including dedicated bandwidth, controlled jitter and latency, and improved loss characteristics. These network performance describing parameter are in this context called QoS parameters.

A number of QoS architectures with different underlying principles have been developed in the networking community. The most important ones, the Integrated Service (IntServ) and the Differentiated Service (DiffServ) approach are briefly introduced and the resulting characteristics of the QoS guarantees discussed.

6.1.1 Communication Architectures

Integrated Services

The Integrated Services (IntServ) architectural principle [17, 25, 156] is, that the service differentiation is accomplished with per-flow end-to-end resource reservations. Here, the applications have to know the characteristics of their traffic before hand and signal the intermediate network elements to reserve certain resources to meet its traffic properties. According to the availability of resources, the network either reserves the resources and sends back a positive acknowledgment, or answers in the negative (admission control).

The service models that have been discussed or standardized in the IntServ architecture include a deterministic maximum end-to-end delay [127], a sufficiently low loss rate [158], and a minimum end-to-end rate [12].

With its by the resource reservation implicitly guaranteed end-to-end behavior the IntServ architecture is appropriate for applications that have hard network perfomance requirements, and cannot tolerate or adapt to a performance level that is lower than what they ask for.

One of the main factors leading to the currently weak deployment in practice is that the IntServ architecture is not scalable [91] with the number of flows. As any flow receives its indivdual treatment the complexity and such the computational cost increases as the number of flows increases. To solve the problem of scalability and manageability, the Differentiated Service architecture (DiffServ) was proposed.

Differentiated Services

The major premise of the Differentiated Services (DiffServ) architecture [16, 101] is that individual flows, or microflows, with similar QoS requirements can be aggregated in larger traffic sets, called macroflows. All packets in a macroflow receive the same 'forwarding behavior' in routers. So, a macroflow is the minimum level of granularity in a DiffServ network in terms of service differentiation. As only a few service classes exist, the aggregation addresses the scalability of the DiffServ. Furthermore, the network management as well as the pricing/accounting becomes simpler. Even though resource provisioning for the expected traffic load in a dedicated class is considered in some service models [29, 30, 102, 121], guaranteed end-to-end QoS is not available. DiffServ only guarantees that higher traffic classes have a better network performance than the lower ones. This is the fundamental drawback of the DiffServ architecture with respect to the QoS achievements.

6.1.2 Control Relevant Implications

The different QoS architectures have different control relevant implications that are studied in the following with the focus on haptic telepresence systems. Generally, we will refer to the IntServ architecture as with strong and for the DiffServ architecture with weak QoS guarantees.

IntServ vs. DiffServ

There exist a number of conditionally stable telepresence system architectures that assume bounds on the delay and do not consider packet loss, see Section 2.2 for a detailed review. These architectures need strong QoS guarantees, hence the IntServ architecture, otherwise stability cannot be guaranteed. The telepresence system architecture proposed in this thesis is stable independent of the time delay and the packet loss, for stability the weak QoS guarantees provided by the DiffServ architecture are sufficient.

Considering the transparency we may classify tele-applications or tasks within a tele-application according to the required level of transparency. In some applications/tasks statistical bounds on the transparency level might be sufficient, here the DiffServ architecture is appropriate. In safety relevant applications/tasks, as e.g. tele-surgery, for the operability a minimum transparency must be guaranteed leading to the IntServ architecture with guaranteed service. An overview on the appropriate QoS architecture is given in Fig. 6.1.

Generally, the IntServ architecture is preferred and considered in the following. For the development of IntServ architecture based QoS concepts in telepresence systems the availability of the requested resources and the response time of the network to such a request has to be taken into account. In the following the main benefits of novel QoS based telepresence control for the transparency improvement is investigated.

6.2 Transparency Improvement through QoS

The impact of the communication quality on the transparency of the haptic telepresence system has extensively been studied in Chapter 3 and Chapter 4.

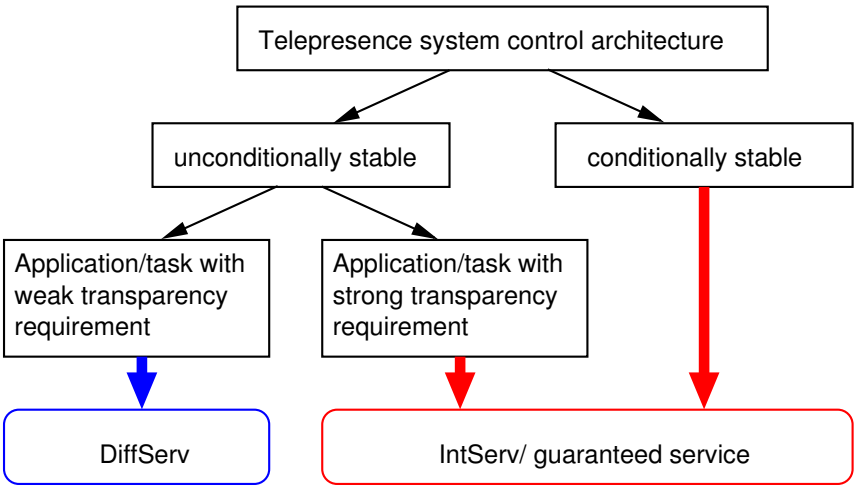

Figure 6.1: Appropriate QoS architecture

As a result an analytical mapping for the QoS-Parameter delay on the transparency in terms of the perceived impedance has been derived. Furthermore, the influence of the packet loss has been investigated. The results are roughly summarized as follows:

1. High delay results in low transparency: in contact high stiffness error between the environment stiffness and the preceived stiffness, in free space motion large inertia is perceived,

2. Delay induced upper perceivable stiffness bound,

3. At high delay different environment stiffnesses difficult to distinguish,

4. High packet loss results in low transparency with similar effects as in delay case.

Hence, the communication quality does not only influence transparency but also determines the maximum achievable level of transparency. Using now the inverse of the investigated QoS-mappings the maximum allowed QoS-parameters can be determined in order to achieve a required level of transparency.

Example: Lets assume a task where it is necessary that the human perceives at least a stiffness of $k_h = 1000$ N/m in contact with a hard wall with a stiffness coefficient of $k_e = 50000$ N/m. Furthermore, lets assume the wave impedance is tuned to $b = 10$ Ns/m. The perceived stiffness depending on the delay can be calculated according to (3.13). Using the inverse function

$$T = 2b(\frac{1}{k_h} - \frac{1}{k_e}),$$

the end-to-end round-trip delay for the given values should not exceed $T = 19.6$ ms in order to meet the transparency requirement.

Clearly, if QoS communication is available with guaranteed bounds on the QoS-parameters a desired level of transparency can be guaranteed.

In the following the advantages of possible QoS control concepts for haptic telepresence systems are investigated. These concepts are classified by the responsiveness of the network to a changing QoS request. The first scheme considers an offline agreement about QoS parameters which then are static for the session. In the second scheme we assume that the QoS parameter may change on request within a session which requires a higher reponsiveness of QoS control.

6.2.1 Increased Transparency through Offline QoS Request

Idea

In this scheme it is assumed that the QoS level is negotiated offline in the initialization phase and it does not change during a session.

From the communication point of view this requires only the reservation of ressources and the assignment of the traffic to these ressources. There are weak real-time requirements for the allocation of the ressources as the application starts after the initialization phase. As a result of the offline QoS negotiation the QoS parameters have a fixed value for the session. This is in contrast to the network characteristics without QoS, where the network parameters are of stochastic nature without any bounds.

Control Architecture

The control architecture for haptic telepresence systems in packet switched communication networks proposed in Chapter 4, see Fig. 4.9 for a visualization, is straightforward to carry over for the offline QoS approach. Knowing the bounds or even exact values for instance for the delay the relevant control system parameters, as e.g. the dejitter buffer length (see Chapter 4), can be designed accordingly. This allows a less conservative design than in networks without QoS leading to increased transparency.

Towards Optimal Network Resource Utilization

On the other hand the costs increase with lower QoS parameters corresponding to higher transparency. Most of the proposed cost models are based on the traffic volume or equivalently the data rate. With the standard approach of constant data rate in networked haptic telepresence systems significant costs will arise for good transparency. A cost reduction can be achieved by applying the proposed deadband control approach, see Chapter 5, that significantly reduces the data rate without impairing transparency.

A further cost reduction can be achieved if a new QoS level can be negotiated within a session for tasks that require only a low level of transparency; therefore a further novel QoS control approach is proposed in the following.

6.2.2 Task Dependent Transparency Control

Idea

In most tele-applications, there are task components that require a high level of transparency, others can satisfactorily be completed with less transparency. Generally, for the contact with a task relevant object a high level of transparency is required. In free space

motion, though, with a large distance to task relevant objects the human haptic perception is of less importance, a lower level of transparency does possibly not disturb the task completion.

The idea is to adapt the transparency level according to the task requirements by means of the QoS parameter adaption: a task dependent transparency level control.

Control Architecture

The underlying control architecture of the haptic telepresence system can directly be derived from the control architecture proposed in Chapter 4. The principal architecture for this approach is depicted in Fig. 6.2. The first stage of control, the dejitter buffer maps time-varying time delay either on additional loss or additional constant delay. The end-to-end delay is constant with a value depending on the dejitter buffer length. Here, now the goal is to vary the QoS parameters and so the delay according to the needs. Therefore, the dejitter buffer must be shifted forward or backward in time without impairing the passivity. If the time delay decreases the dejitter buffer must reduce its length and shift backwards in time. As result a number of samples in the dejitter buffer are discarded, passivity is preserved as shown in Chapter 4. If the delay suddenly increases the dejitter buffer must be shifted forward in time. A number of empty sampling instances occur, the missing data have to be estimated and may induce additional energy possibly leading to non-passivity. As stated in Chapter 4 the superior reconstruction algorithm with energy supervision does preserve passivity also for systems with varying end-to-end delay and packet loss. In order to compensate for the position drift resulting from the varying delay and packet loss, the proposed architecture is extended by position feedforward [27] as described in Appendix A. This control architecture is proposed for the task dependent transparency level control.

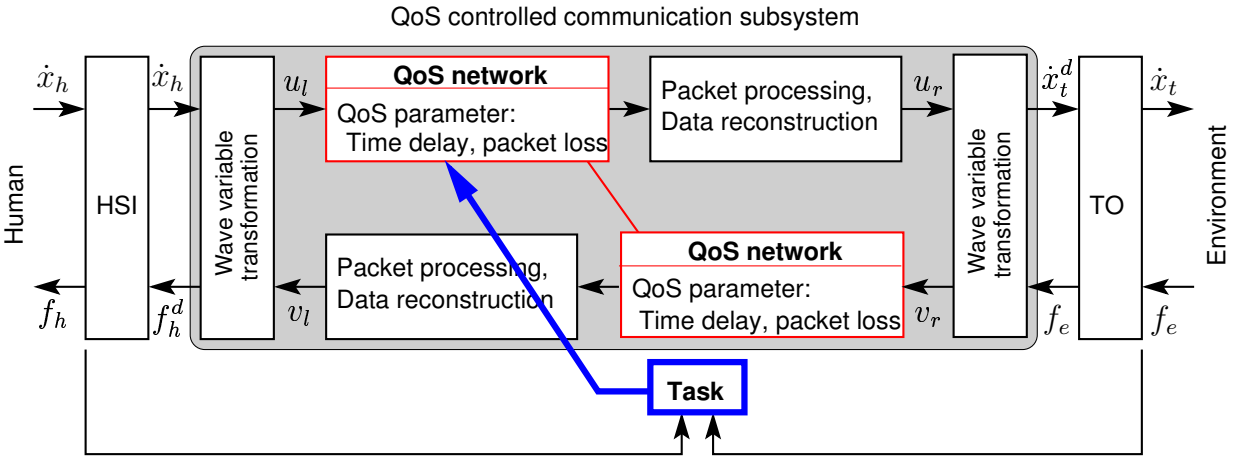

Figure 6.2: Principal architecture of haptic telepresence system with QoS control: task dependent transparency control.

Benefits and Challenges

The benefits of this concept lie in the reduced costs in terms of ressources compared to the offline QoS approach. High communication quality is only required in the time intervals when high transparency is required.

The great challenge from the communication point of view lies in the real-time requirement for the response to a new QoS request. Even though no evaluations about the necessary responsiveness are available at this time a rough estimate can be given. It has been observed that the human interacts with a telepresence system up to the bandwidth defined by the reciprocal of the end-to-end round-trip delay. From an application point of view the request for better QoS parameters is especially important in order to guarantee some certain level of transparency for safe operation in sensitive tasks. Hence, a change in the QoS level to better parameters should be performed within the current communication round-trip delay. The request for worse parameters is only interesting with respect to the cost reduction. As a rough overall estimate on the required responsiveness of the QoS control loop the maximum round-trip delay can be taken.

6.2.3 Numerical Performance Comparison

In order to visualize the benefits of QoS communication and to compare both QoS approaches, simulations are performed. Therefore, a one degree-of-freedom haptic telepresence system is considered. The task is, to haptically explore an object placed in free space (variable structure environment). Proximity and contact with the object are considered as sensitive task with a high transparency requirement. In distance from the object less transparency is required.

Three cases are considered in simulations:

1. Communication without QoS guarantees (no QoS)
2. Offline QoS (QoS/OL) approach
3. Task dependent transparency control (QoS/TC).

Simulation Conditions

Without QoS we assume a high delay and packet loss according to the parameters in the set denoted by QoS_d in Table 6.1, where also all other simulation data are listed.

With the QoS/OL approach the QoS parameters are chosen to satisfy the high transparency requirement during the proximity and contact phase, the parameter set is indicated by QoS_{pc}. For both, the QoS/OL and the no-QoS the QoS parameters are kept constant over the simulation time.

For the QoS/TC method two sets of QoS parameters are defined corresponding to two different QoS levels, QoS_d for distance and QoS_{pc} for proximity/contact. The first one is equal to the set used for the no-QoS approach, the latter one is equal to QoS/OL parameter set. The switching between these sets occurs at a certain distance to the object.

The data packets are sent over the communication network with constant sampling rate. The communication subsystem is passified by the wave transformation and the energy supervised HLS/zeroing. The teleoperator is modeled after an existing experimental system, the force feedback paddle, as a mass-damper system (m_t, b_t) comprising a velocity control with the proportional gain P and position feedforward compensation with the gain f_p. The object has a spring-damper (k_e, b_e) characteristics. The human together with the HSI is modeled as a spring-damper system ($k_{hu,h}$, $b_{hu,h}$), in reaction to an environment force the intended velocity trajectory is modified; the loop is closed over the human.

Table 6.1: Simulation parameter values

Simulation parameter	Value
environment (no contact)	$k_e = 0$ N/m, $b_e = 0.0001$ Ns/m
environment (contact)	$k_e = 10$ N/m, $b_e = 0.01$ Ns/m
environment contact at position	$x_t = 1$ m
QoS parameters (distance) QoS_d	$T_1 = T_2 = 100$ ms, $P_l = 90\%$
QoS parameters (proximity/contact) QoS_{pc}	$T_1 = T_2 = 50$ ms, $P_l = 1\%$
switching $\text{QoS}_d \leftrightarrow \text{QoS}_{pc}$	$x_t = 0.7$ m
wave impedance	$b = 1$ Ns/m
network sampling interval	$T_A = 1$ ms
teleoperator with control	$m_t = 0.23$ kg, $b_t = 0.04$ N/m $P = 100$ Ns/m, $f_p = 20$ N/m
human with HSI	$k_{hu,h} = 1$ N/m, $b_{hu,h} = 1$ Ns/m
intended velocity	square pulse, period 5 s

Communication without QoS vs. Offline QoS Approach

From the position and force trajectories depicted in Fig. 6.3(a) the higher perceived stiffness for the QoS/OL approach compared to the case without QoS becomes obvious as at lower HSI position higher force is displayed. This result validates the findings from Chapter 3 and Chapter 4. The squared position error between the teleoperator and the delayed HSI position

$$e_x^2(t) = (x_t(t) - x_h(t - T_1))^2, \tag{6.1}$$

shown in Fig. 6.3(b) additionally validates the outperforming transparency of the QoS approach.

Generally, it can be stated, that QoS communication is beneficial for the transparency.

Offline QoS vs. Task Dependent Transparency Control

The QoS parameter values of the QoS/OL approach remain constant, while they switch for the QoS/TC method depending on the teleoperator position as depicted in Fig. 6.4(a). The difference in the positions and forces between the two approaches are below the graphical resolution in the proximity/contact phase, see Fig. 6.4(b). In the squared position error (6.1) in Fig. 6.4(c) the difference becomes visible. In distance, where the corresponding QoS parameters have an substantially higher value than for the QoS/OL, the error is higher for the QoS/TC. The error is approximatly similar for proximity/contact, the remaining difference results from transient error behavior, it will converge to zero for zero velocity input. Note, that for the same reasons the squared error for the QoS/TC approach is also in the distance phase substantially smaller than for the case without QoS.

In order to compare both approaches also with respect to the network cost, an abstract cost function accounting for the increased network costs with decreasing QoS parameters

$$J = \int_0^t (TP_l)^{-1} \, \mathrm{d}\tau \quad \text{with} \quad T = T_1 + T_2,$$

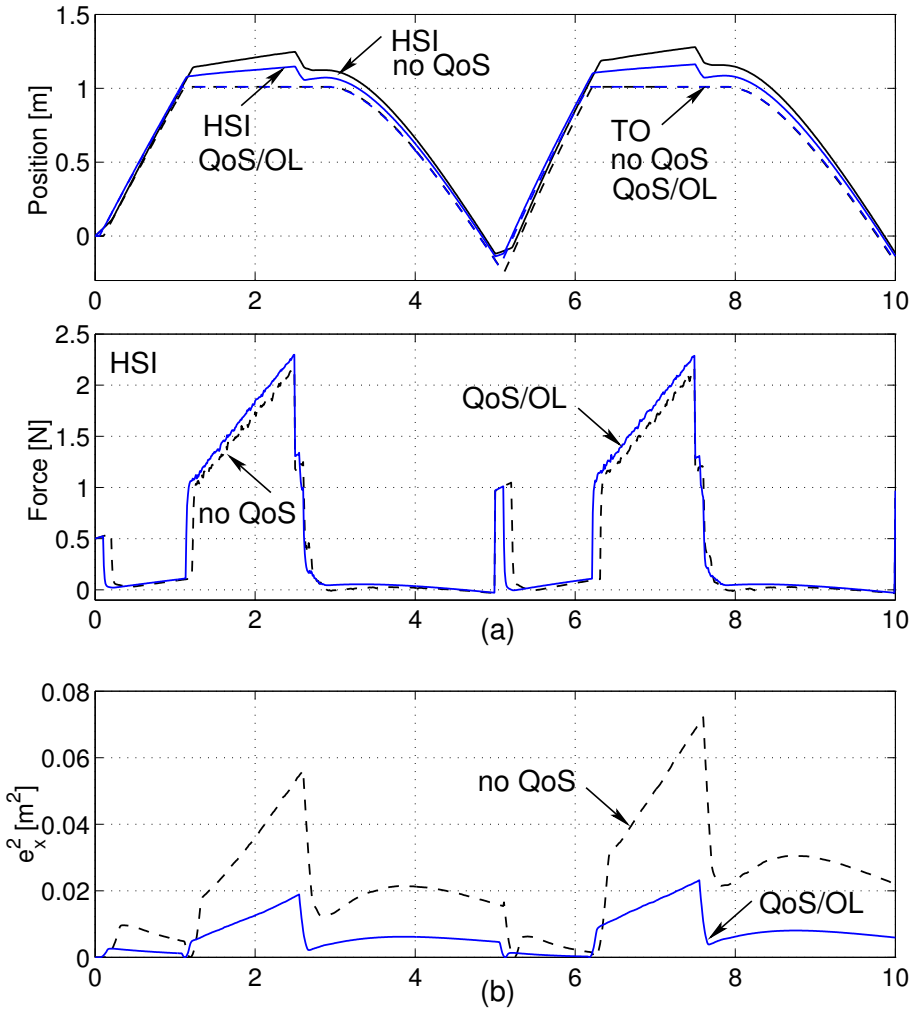

Figure 6.3: Offline QoS (QoS/OL) vs. no QoS control, HSI/TO positions and HSI force (a) and squared position error (b).

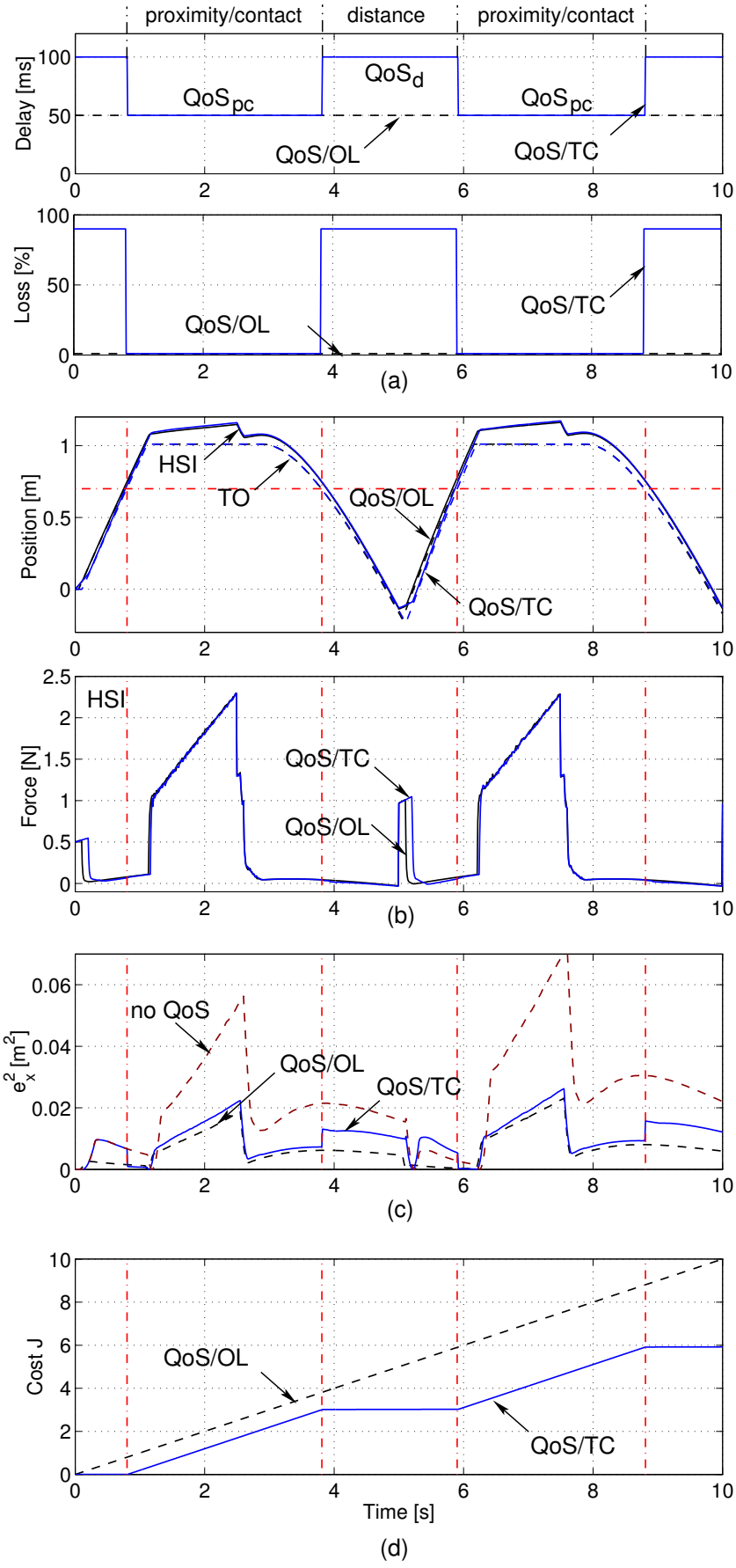

Figure 6.4: Task dependent transparency control (QoS/TC) vs. offline QoS (QoS/OL) with the QoS parameter delay and loss (a), HSI/TO positions and HSI force (b), squared position error (c) and cost function (d).

is introduced. The network cost and such the cost for the user are much higher for the QoS/OL approach as shown in Fig. 6.4(d).

As a result the transparency with the QoS/TC approach is comparable to QoS/OL during the important phases, but the cost is substantially lower.

Remark 6.1 The conceptual extension of QoS control to the closely related networked control systems is straightforward. However, different stability analysis methods and decision strategies are required. Preliminary results stated in [26] are very promising.

6.3 Open Problems

Aside from the implementation specific issues of the QoS network architecture and the resulting characteristics of the QoS parameters a number of problems with respect to QoS control architectures for haptic telepresence systems are still open. The main challenges in terms of control systems, human-machine-interaction/psychophysics and communication architectures are:

1. The network cost with the considered task dependent transparency control approach are clearly lower than with the offline QoS approach. The question is, whether the by the first approach induced change of transparency is acceptable for the human. First results from experimental user studies confirm that [124].

2. For the definition of the appropriate communication quality, i.e. QoS level, a transparency requirement catalog for tele-applications/ tasks is inevitable. In order to map the required transparency to a required QoS level in Chapter 3, an analytical QoS mapping for constant delay with existing inverse could be derived. For packet loss and time-varying delay numerical and experimental observations exist, see Chapter 4. For a generalizable QoS mapping further investigations are necessary.

3. The availability of a requested QoS level, is generally not guaranteed, especially for the IntServ architecture comprising an admission control mechanism. Strategies considering the non-availability of the requested QoS level have to be developed.

4. The response time of the network to a QoS request is critical in the task dependent transparency control approach. As the QoS level in the offline QoS approach is negotiated during the initialization phase the network response is less time critical. For both approaches the required time constant of the QoS control loop has to be defined.

5. Based on the availability and network response time considerations a requirement catalog for the further development of QoS architectures has to be established, feasibility studies from the networking point of view are necessary.

6. Assuming traffic volume based network cost under the QoS architecture the integration of data reduction algorithms, such as the deadband control approach proposed in Chapter 5, into the QoS control approach are of high interest.

7. The combined consideration within the QoS control approach of all modalities addressed by the multi-modal telepresence system (including visual and auditive feedback) is very important.

8. A general control theoretic formulation of the QoS control system in terms of stability, reachability and detectability will build the fundament for future research in QoS control.

6.4 Discussion

The Quality-of-Service (QoS) concept applied in packet switched communication networks may guarantee control of the communication quality. This paves the way for the development of novel telepresence system control architectures incorporating QoS concepts. However, such architectures combining the control of the telepresence system and the communication network have not been considered in the known literature yet.

In this chapter the innovative future research direction of Quality-of-Service control for telepresence systems is studied. The benefits of incorporating Quality-of-Service (QoS) communication architectures into the haptic telepresence system control are twofold. First, the QoS guarantees on the communication quality results in guarantees on the transparency level, as both are strongly related. This is indispensable for sensitive tele-applications. Secondly, the control of the communication quality can be beneficial under the aspect of economically efficient network usage.

In order to form a basis for the development of QoS control strategies, the QoS architectures, currently under research in the networking community, are reviewed with respect to their control relevant implications. The Integrated Service architecture conforms with the hard real-time constraints posed by haptic telepresence systems and is taken as the basis for further investigations. Based on the results from the previous chapters two novel QoS control strategies, the offline QoS approach and the task dependent transparency control approach, are proposed and compared with respect to their benefits in terms of transparency and induced network cost. The results clearly show the benefits of QoS control for telepresence systems. The challenges and open questions, as mentioned in this chapter, are expected to direct the future research in the area of QoS control and QoS network architectures.

In this chapter a very innovative idea for the combined control of haptic telepresence system and communication network based on the QoS concept is proposed with very promising results. The foundation of a unified framework for QoS control for general networked systems along with the control theoretic investigation of the basic characteristics in terms of stability, controllability, and observability of such a control approach remains subject of future research.

7 Conclusions and Future Directions

7.1 Concluding Remarks

The work presented focuses on the human oriented control design for haptic telepresence systems in packet switched communication networks. Conceptually innovative is the emphasized combined consideration of the research fields of control system design, communication systems, and human-machine interaction. From this integrated approach novel ideas and concepts are developed in this thesis. The analysis of the developed control approaches and strategies addresses the multiple aspects of stability, communication network characteristics, and human perception revealing the strong relation between these different research areas in the context of haptic telepresence in packet switched communication networks. The human perception aspect is mainly addressed in the evaluation methods and tools: the definition of the transparency measure and the experimental validation through user studies. The integration of the communication network into the control and the performance considerations, stronger from chapter to chapter, accounts for the communication aspect. The stability analysis and the objective performance evaluation constitute the general basis of all developed approaches from the control point of view. The main approaches along with the major results are highlighted in the following.

How naturally the human can act by means of a telepresence system in a remote environment and perceive its characteristics (transparency), is a key issue for the deployment of tele-applications and such for the control design. However, communication unreliabilities as they occur in packet switched communication networks deteriorate the transparency. The knowledge to which extent this happens and how the human subjectively perceives the transparency degradation, is indispensable in order to determine the limits of tele-applications. In Chapter 3 a transparency measure is introduced based on the physical parameters of the perceived mechanical impedance, such as inertia, stiffness and damping. Readily available psychophysical results on the human haptic perception of these properties motivate this measure allowing a *human oriented evaluation of transparency*. The results of the performed experimental user studies are conform with the predictions through this transparency measure indicating that the developed transparency measure gives a good estimation of the human perceived transparency.

However, the analytical description of the dependency of the perceived impedance parameters on the communication parameters is often difficult to obtain. This is mainly due to the stochastic nature of packet switched communication networks, further due to the transcendent nature of time delay systems. In order to compute the impact of communication parameters on the perceived impedance parameters, i.e. the transparency level according to this measure, two novel transparency analysis tools are developed, an analytical and an optimization-based numerical approach. The first mainly targets the transparency evaluation for *constant delay* in the communication system. The latter, a generic numerical approach valid for *time-varying delay and packet loss*, uses Monte Carlo simu-

lations to account for the stochastic nature of the communication parameters, a standard identification method (cross-correlation) for the computation of the perceived impedance frequency response, and an optimization to identify the mechanical parameters of the computed perceived impedance. In fact, the developed optimization-based tool is not only well suited for the transparency analysis, but also for the optimal design of transparent, so-called impedance matched, control architectures. The developed tools together with the transparency measure constitute a transparency analysis method appropriate for a generic human oriented transparency evaluation of general haptic telepresence systems.

In order to design the control of telepresence systems in packet switched communication networks, a deep understanding of the control relevant effects is required. Communication over packet switched communication networks introduces destabilizing effects into the closed control loop, such as *time-varying time delay* and *loss of data*. The appropriate reconstruction of lost data and data that due to time-varying time delay arrive too late is identified as the main issue for the stability of haptic telepresence systems in packet switched communication networks. With the formulated stability conditions a general framework for the analysis and design of data reconstruction strategies is provided in Chapter 4 of this thesis. Standard reconstruction strategies widely used in networked control systems are shown to be potentially unstable. The approaches developed in this thesis guarantee stability for arbitrarily large constant/time-varying time delay and packet loss. They form the basis for further integration of the communication network into the control.

As a first step, the combined performance of the telepresence system and the communication network, the transparency and the network cost, is considered. This consideration accounts for the fact, that a packet switched communication network has limited communication resources. Thus, it is of high interest to reduce the network traffic and such the network cost. Driven by well-known human perception limits an innovative deadband control approach is introduced in Chapter 5 targeting this challenge. As a result of experimental user studies a substantial *network traffic reduction of up to 95%* is achieved *without impairing transparency*. In order to guarantee stability and transparency, the reconstruction strategies from Chapter 4 are further developed. With the influence of this control concept on the packet rates, i.e. the states of the packet switched communication network, the integration of the communication into control becomes obvious.

Novel impulses for further integration of the communication into haptic telepresence system control are induced by the lately emerging Quality-of-Service (QoS) communication architectures that allow the control of the communication network to some extent. The very innovative idea of simultaneous control of the haptic telepresence system and the communication network, the *QoS control*, is proposed for the first time. Based on the investigation of the control relevant implications of QoS network architectures, currently under research, two novel concepts for a QoS control architecture are studied in Chapter 6. The QoS control is shown to be beneficial with respect to transparency and network cost.

In summary, the ideas, concepts and approaches developed in this thesis significantly advance the state-of-the-art in telepresence system control analysis and design in packet switched communication networks, with emphasis on the integration of human perception and communication aspects. The results are expected to have a high impact on the development of future tele-applications in packet switched communication networks.

7.2 Outlook

Telepresence technology satisfies the demand for global acting in the human society. Accordingly, there is a vast potential of multifaceted industrial and societal applications for telepresence systems. Further research on telepresence systems will close the still existing technological gap between the scientific state-of-the-art and readily available commercial telepresence systems and applications. With the combined consideration of control, communication and human related aspects for telepresence systems the research presented in this thesis constitutes the basis for future developments in this area. There is a number of exciting research directions directly emerging from this thesis, some are:

- *Human adapted telepresence system design* - By further exploitation of human perception characteristics for the control design the development of telepresence system architectures with improved transparency is expected. The main methodical issue is the bridging of the gap between traditional engineering and psychological approaches.

- *Communication oriented telepresence system design* - The most promising innovative research direction in this context is the here proposed QoS control for telepresence systems. In order to successfully target the numerous challenges, a unified approach combining control theory and communication approaches is indispensable requiring a deep understanding of both aspects.

- *Generalization to networked control systems* - Significant advances are expected by the generalization of the telepresence system control methods to networked control systems. This holds for the passivity based approaches to achieve robust stability in packet switched communication networks, and also for QoS control.

The future research on human adapted control will force a deeper understanding of the fundamentals of the human perception and action. In turn, this understanding will enable the development of powerful human-machine interaction paradigms. Incorporating this knowledge into human-machine-interface technology will significantly increase their intuitive operability, efficiency and safety.

The economical benefits of using common purpose communication networks for control can hardly be overestimated. Research on the control oriented design of communication networks and vice versa on the communication oriented design of control systems will highly advance the state-of-the-art with a large impact on future technology and applications.

A Generalizations Towards Transparency

Targeting at improved transparency of the standard wave variable based control architecture as introduced in Chapter 2, a number of extensions and modifications are discussed in the following. Aiming at good position tracking between the HSI and the teleoperator, a position feedforward extension is studied in Section A.1. The feedback of the environment force to increase transparency is discussed in Section A.2. Impedance matching as a prerequisite for tranparency as well as impedance matched control architectures are studied in Section A.3.

A.1 Passive Position Feedforward for Time-Varying Delay and Packet Loss

With the wave variable approach as introduced in Chapter 2 position tracking between the HSI and the teleoperator is only implicitly achieved by the transmission of the velocity encoded in the wave variable. However, varying time-delay and packet loss with hthe subsequent data reconstruction, see Chapter 4, distort the wave signal and hence the therein encoded velocity signal. As a result an unrecoverable position drift between HSI and teleoperator may occur [27, 103, 106, 160], see also Section 4.4.1. An initial position offset cannot be eliminated. As a result, the standard wave variable based architecture cannot guarantee position tracking. Clearly, a position error does not only deteriorate the transparency according to (2.16) [162], but may also drive the HSI/teleoperator to their physical workspace limits resulting in inoperability of the telepresence system or at least in a decreased workspace.

In order to cope with the position tracking problem, in [103] an outer position feedback loop is closed adding a drift correction term to the wave variable signal. However, this correction is possible only at times where no energy is injected by that in order to preserve the passivity property. The adjusted wave signal must have a lower magnitude than the uncorrected wave signal. As a result the operator must move or apply a force in order to allow a correction. In [106] position tracking is achieved by the transmission of the integrated wave variable that contains position and momentum information, an energy conserving reconstruction filter ensures the passivity of the communication subsystem. In [160, 161] the wave integral is not transmitted but reconstructed from the restored undistorted wave signal by the use of time stamps. Passivity of the communication subsystem is preserved by energy monitoring. However, both the approaches based on the wave integral may not recover an initial position drift.

A.1.1 Position Feedforward for Time-Varying Delay

Targeting the position tracking problem primarily in the time-varying delay case in continuous time, an alternative approach is proposed in [27] and discussed in the following.

The extension to the packet loss problem is straight forward. Additionally to the wave variables the HSI position is forwarded to the teleoperator where a local position control loop is closed as shown in Fig. A.1, compare to Fig. 2.2 where the unmodified wave variable based control architecture is visualized.

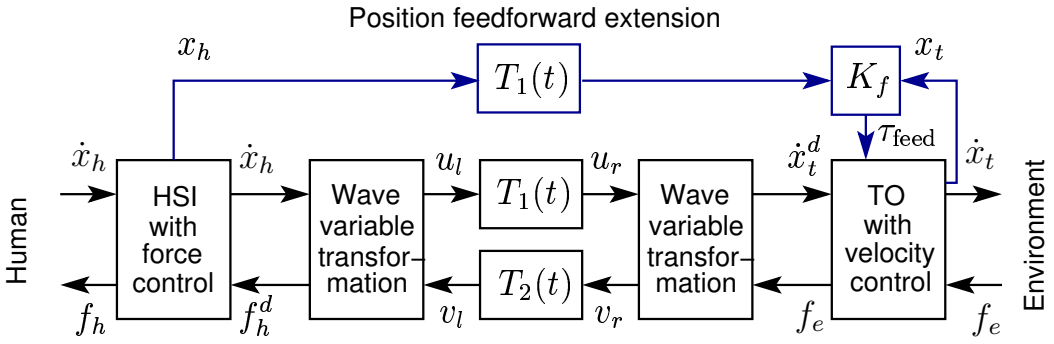

Figure A.1: Wave variable based telepresence system control architecture with position feedforward extension for improved position tracking.

This additional control input may result in a non-passive teleoperator behavior. In contrast to the previously discussed approaches the stability analysis is performed using the overall Lyapunov function for the system exploiting the passivity property of the environment, the human and the communication subsystem. The appropriately tuned position controller

$$\tau_{\text{feed}} = K_f \text{sat}_p(e_x) \quad \text{with} \quad 0 < K_f < \sqrt{2b_t},$$

ensures the stability of the overall system. Here K_f represents the controller gain, b_t the teleoperator damping, $e_x = x_h(t - T_1(t)) - x_t(t)$ the position error based on the delayed HSI position, and sat_p the saturation function defined by

$$\text{sat}_p(e_x) = \begin{cases} e_x & \text{if } |e_x| \leq p \\ p\frac{e_x}{|e_x|} & \text{othewise} \end{cases}.$$

The tuning of the parameter $p > 0$ in the saturation function determines the set of the for stability allowed initial states of the system represented by the vector $[\dot{x}_h(0)\ \dot{x}_t(0)\ (x_t^d(0) - x_t(0))]$, see [27] for more details. The choice of the feedforward gain K_f can be interpreted in terms that excess passivity of the teleoperator is used to compensate for possibly non-passive behavior introduced by the additional control input. If the natural damping b_t of the teleoperator is low the consequently low feedforward gain results in a slow convergence of the teleoperator to the HSI position. In order to allow a higher feedforward gain, the damping can be increased by a teleoperator velocity feedback resulting in a teleoperator control law

$$\tau_t = \tau_{\text{feed}} + K_{P,t}(\dot{x}_t^d - \dot{x}_t) - K_t \dot{x}_t,$$

where K_p represents the proportional gain, and K_t the additional teleoperator damping provided through control. In consequence, the feedforward gain K_f has to fulfill the following inequality $0 < K_f < \sqrt{2(b_t + K_t)}$ for stability. With the modified architecture the position error converges to zero in steady state.

A.1.2 Position Feedforward in Packet Switched Networks

In packet switched networks additionally packet loss has to be considered, the time varying delay problem with the control architecture proposed in Chapter 4 reduces to a similar problem as packet loss. Packets that arrive too late are discarded resulting in pseudo-packet loss, all other packets experience a constant delay by the appropriate buffering and reordering strategy. In order to keep the protocol overhead as low as possible, we assume the HSI position sample sent together with the wave variable sample in a single data packet.

Accordingly, in case of packet loss in the forward path $l_1(k - D_1) = 0$ (4.6) also the HSI position information $x_h(k - D_1)$ is lost, where D_1 represents the constant time delay comprising the network delay and the buffering delay expressed as number of sample intervals, see Chapter 4. No reliable HSI position information is obtainable then. The desired teleoperator positon could be estimated from previous HSI position measurements. However, the passivity of the approach has to be investigated. Here, a velocity PI control is proposed during time intervals of packet loss, using the position information in the passively estimated value of the lost wave variable, see Chapter 4. During loss time intervals the integral gain $K_{I,t}$ of the teleoperator velocity control loop is set to a value larger than zero starting from an integrator initial state of zero, while the feedforward gain K_f is set to zero then. The teleoperator tracks the desired velocity value resulting from the reconstructed wave variable, see Chapter 4 for details. As soon as a new HSI position update is available the feedforward gain K_f is set to its original value and $K_{I,t} = 0$. The resulting control law, here for simplicity in continuous time, is

$$\tau_t = \begin{cases} K_{I,t} \int_{t^*}^{t} (\dot{x}_t^d - \dot{x}_t) \mathrm{d}\tau + K_{P,t}(\dot{x}_t^d - \dot{x}_t) - K_t \dot{x}_t & \text{if} \quad l_1(t - T_1) = 0 \\ \tau_{\text{feed}} + K_{P,t}(\dot{x}_t^d - \dot{x}_t) - K_t \dot{x}_t & \text{otherwise} \end{cases},$$

with t^* representing the time instance where the most recent packet arrived. For both cases passivity is preserved, for the upper case due to the appropriate definition of the feedforward gain K_f, for the lower case the standard PI-velocity control is applied which does not inject extra energy due to its initialization to zero whenever it is activated. In steady state, given that the at least one of the packets arrives during the steady state phase, then the position error converges to zero.

The position feedforward architecture is capable to eliminate initial position offset between HSI and teleoperator in contrast to [106, 160, 161] and in contrast to [103] continuously adjusts the teleoperator position to the HSI position as long as a HSI position update is available. This approach outperforms all other mentioned approaches with respect to the achievable tracking performance. An extension to this approach feeding back the teleoperator position to the HSI thereby guaranteeing the boundness of the position error is developed in [28]. However, this approach is limited yet to constant delay.

A.2 Environment Force Feedback

In the original approaches [1, 103, 107] the coordinated torque, i.e. the controller output at the teleoperator τ_t, is fed back as a measure for the environment interaction force f_e. As a result the operation in free space motion feels 'sluggish'. This can easily be observed

in the transfer function of the terminating impedance $Z_{t/e}$ which consists of the velocity controlled teleoperator, for simplicity here with one DoF, and the environment impedance Z_e

$$Z_{t/e} = Z_\tau = \frac{\tau_t}{v_t^d} = \frac{Z_e G_{c,t} G_{p,t} + G_{c,t}}{1 + G_{p,t}(Z_e + G_{c,t})},$$

with $G_{c,t}$ the controller, and $G_{p,t}$ the teleoperator device transfer function as depicted in Fig. A.2; the Laplace variable s is omitted. Transparent feedback in free space motion $Z_e = 0$ would require zero coordinated torque feedback, however, the coordinated torque is unequal to zero depending on the plant and the control dynamics

$$Z_\tau\Big|_{Z_e=0} = \frac{\tau_t}{v_t^d} = \frac{G_{c,t}}{1 + G_{p,t} G_{c,t}} \neq 0.$$

High gain control and negligible teleoperator dynamics would theoretically bring the torque close to zero. However, in real application the control gain is limited by the unmodelled dynamics and the noisy measurements. Further, in large teleoperator devices such as the antropomorphic 7 DoF robotic arm used in experiments [58, 133], or the 10 DoF haptic device ViSHaRD10 [146, 147], the dynamics is not at all negligible.

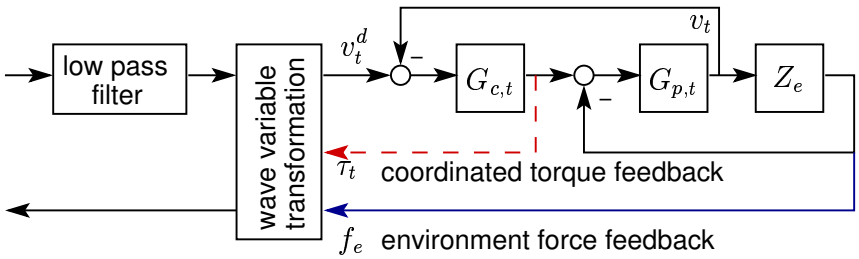

Figure A.2: Teleoperator/environment impedance with low pass filter in the wave domain.

Therefore, here the feedback of the directly measured environment interaction is proposed as an alternative to the traditional coordinated torque feedback. The terminating impedance is described by

$$Z_{t/e} = Z_{fe} = \frac{f_e}{v_t^d} = \frac{Z_e G_{c,t} G_{p,t}}{1 + G_{p,t}(Z_e + G_{c,t})},$$

resulting in a transparent feedback of zero force in free space motion

$$Z_{fe}\Big|_{Z_e=0} = 0.$$

Further motivation for direct environment force feedback is given by a very recent work [144], where the high frequency component of the environment force is used to modulate the returning wave v_r. This improves the perception of the contact instance with a rigid wall for example. As the coordinated torque is encoded in the wave variables the transparency of free space motion is not increased, however.

Main argument for the coordinated torque feedback is the guaranteed passivity of the terminating impedance, and thereby guaranteed stability of the telepresence system. With the environment force feedback there may exist environment conditions where passivity is no longer guaranteed. This is especially true for very stiff, poorly damped environments. The non-passive behavior can be observed in the violation of the small gain condition of the reflection factor(B.4), see Appendix B for a more detailed discussion on the relation between passivity and the small gain theorem.

In the following case study it is shown that the small gain condition for environment force feedback can be recovered by appropriate wave low pass filtering. Therefore, the following teleoperator, controller and environment dynamics are assumed

$$G_{p,t}(s) = \frac{m_t}{s}; \quad G_{c,t}(s) = K_{P,t} + \frac{K_{I,t}}{s}; \quad Z_e = b_e + \frac{k_e}{s}, \tag{A.1}$$

with m_t the teleoperator inertia, $K_{P,t}$ the proportional, $K_{I,t}$ the integral gain of the velocity controller; b_e and k_e represent the environment damping and stiffness, respectively.

The violation of the small gain condition can be observed in Fig. A.3 where the magnitude response of the reflection factor is depicted for different environment stiffness coefficients. The simulation parameters are listed in Table A.1.

Table A.1: Simulation parameter values

Subsystem	Simulation parameter value
teleoperator	$m_t = 0.2$ kg
velocity control	$K_{P,t} = 100$ Ns/m, $K_{I,t} = 10$ N/m
environment	$b_e = 0.1$ Ns/m, k_e [N/m] varies
wave impedance	$b = 1$ Ns/m

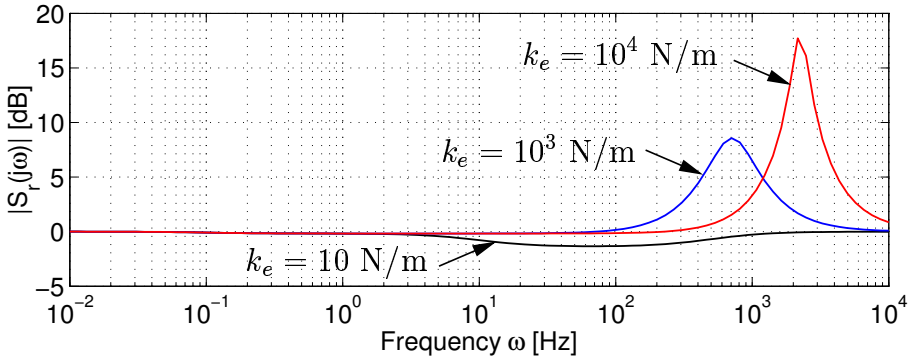

Figure A.3: Magnitude response of the reflection factor with environment force feedback: small gain condition is violated.

Applying a unity gain low pass filter in the wave domain as visualized in Fig. A.2 the magnitude peaks of the reflection factor can be attenuated. Wave domain low pass filter, also referred as wave compensators in [103, 107, 143], are typically applied for the reduction of wave reflections as in [144] and the attenuation of measurement noise in real application. The effect on the magnitude response of the reflection factor can be observed in Fig. A.4:

the small gain condition is satisfied, i.e. stability is guaranteed. Here a second order low pass filter with a damping of $D = 0.707$ and a natural frequency of $\omega_0 = 100$Hz is used. In fact, for the given case it is verified that the reflection factor together with the applied

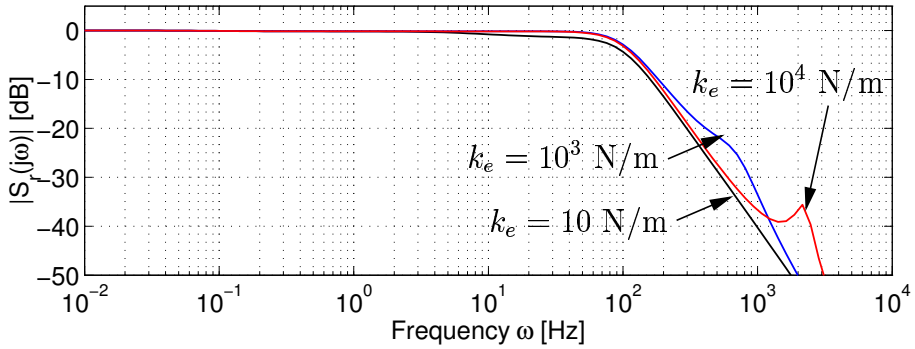

Figure A.4: Magnitude response of the reflection factor with environment force feedback and low pass filter in the wave domain: small gain condition is satisfied.

low pass filter is small gain for all values of environment stiffness coefficients $k_e \in \mathbb{R}_+$. The stability of the haptic telepresence system is guaranteed. The frequency band relevant for human haptic perception is not touched by this low pass filter as its cut-off frequency is higher than the human haptic perception bandwidth. Aiming at stability the placement of the low pass filter within the wave domain is arbitrary. In order to account for the asymmetric haptic action/perception bandwidth, it should be placed in the forward path as stated in [144], see Fig. A.2. The effectiveness of the environment feedback approach has been validated in many experiments [48, 55, 56, 58, 78, 79, 133]. A rigorous passivity proof for all environment and teleoperator configurations going along with a design methodology for the low pass filter is subject of future work.

A.3 Impedance Matched Control Architecture Design

The underlying control concept in this thesis, the wave variable approach, has its origin in network theory. The effects well-known from there can be interpreted in terms of mechanical systems in analogy to the electrical system. According to network theory transparency is achieved only, if the impedances of the network elements match. If the teleoperator/environment impedance $Z_{t/e}$ differs from the wave impedance of the communication line, then the energy received from the transmission line is not completely absorbed by the teleoperator system, wave reflections occur, that deteriorate transparency as discussed in Section 2.2.1 and Section 3.1.2. In fact, repeated reflections lead to oscillatory behavior, which may be compared to natural standing wave phenomena. In general wave reflections should be avoided as stated in [105].

The impedance matching technique introduced in [105] adjusts the impedance of the teleoperator to the wave impedance by appropriately chosen controller parameters of the local velocity/force control loops. This restricts the controller parameters to certain values, a trade-off between control loop performance and impedance matching is usually necessary. Impedance matching is generally achieved for certain frequencies only.

The impedance matching technique suggested in [9, 11, 50] aims at matching over a broader range of frequencies. The approach uses appropriately designed dynamic impedance matching filters. In [11] these filters are designed for a special case of teleoperator control and environment dynamics under restricting assumptions such as low teleoperator inertia. The proposed design rule cannot be generalized, a general design methodology does not exist.

In the following a novel, generalizable design method based on the impedance matching filter architecture from [9] is proposed. This optimization based procedure is similar to the transparency evaluation method proposed in Chapter 3. The basic idea, the design approach and the effect on transparency is discussed in the following.

A.3.1 Impedance Matching Filter Architecture

Impedance matching filters N_x, N_0 are introduced [9] into the standard architecture modifying the communication subsystem incorporating the constant time delay and the wave variable transformation as depicted in Fig. A.5. For simplicity here a 1 DoF telepresence system is assumed. The two DoF case is considered and experimentally validated in [78].

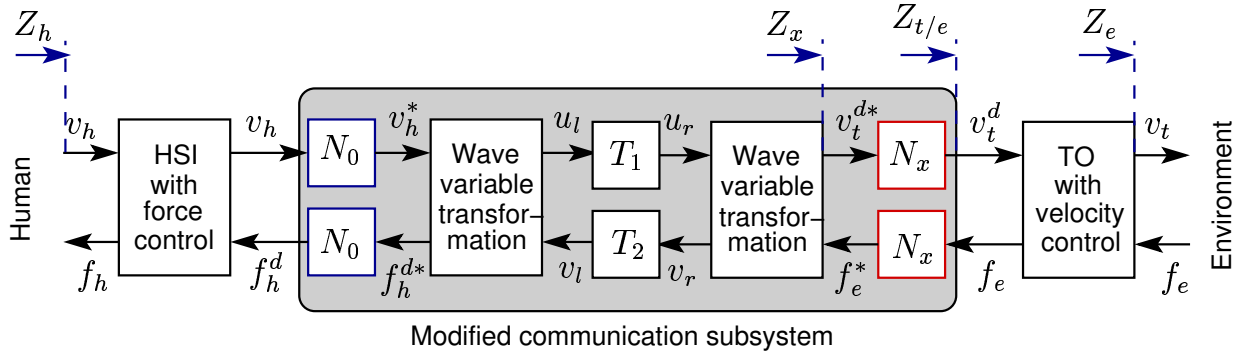

Figure A.5: Wave variable based telepresence system control architecture with position feedforward extension for improved position tracking.

With the design rule

$$N_x(s) = \sqrt{\frac{b}{Z_{t/e}(s)}}, \tag{A.2}$$

the filters N_x match the terminating impedance Z_x consisting of the teleoperator/environment impedance $Z_{t/e}$ and the filters to the wave impedance b

$$Z_x(s) = \frac{f_e^*(s)}{v_t^{d*}(s)} = N_x^2(s)\, Z_{t/e}(s) = b, \tag{A.3}$$

where v denotes the velocity in the frequency domain. The transmitted variables at the teleoperator side are transformed by these filters indicated by *. The back-transformation is performed by the filters N_0 at the operator side with the inverse transfer function of the N_x-filter

$$N_0(s) = N_x^{-1}(s). \tag{A.4}$$

Inserting the terminating impedance (A.3) into (2.15) in place of the there considered terminating impedance using (A.4) the reflection factor is now defined by

$$R = \frac{Z_{t/e} - bN_0^2}{Z_{t/e} + bN_0^2}.$$

With the design rule (A.2) the reflection factor becomes zero, and such the reflected wave has avalue of zero, showing the connection between impedance matching and wave reflections. Neglecting the HSI dynamics the perceived impedance (3.1) with (A.4) and (A.2) may be rewritten as

$$Z_h(s) = bN_0^2(s)\frac{1 + R\,e^{-sT}}{1 - R\,e^{-sT}} = bN_0^2(s) = Z_{t/e}(s).$$

Thus, the operator perceives the teleoperator/environment impedance. The transparency condition (2.17) is met. The passivity of the modified communication subsystem is preserved, see [9] for a detailed discussion.

The design rule for the filters suggested by the filter definition(A.2) requires the computation of the square root of the teleoperator/environment impedance, that is not possible in general. A novel approach to obtain the square root approximation for an arbitrary stable and passive teleoperator/environment transfer function by optimization is proposed.

A.3.2 Optimization Based Design Procedure

The goal is to find the filter design N_x according to (A.2), thus the transfer function that well approximates the inverse of the square root of the teleoperator/environment impedance $Z_{t/e}$, that is assumed to be a passive, observable minimal phase LTI system. Reformulating this requirement, the goal of optimization is to design the filter N_x such that the terminating impedance Z_x approximates the desired terminating impedance $Z_x^d = b$ according to (A.3).

For stability and feasibility of the system the following is required for the filter transfer function N_x:

1. The filter transfer function is stable, hence has all poles in the closed left hand half of the complex plane

2. The filter transfer function is minimal phase, hence all zeros are in the left right hand half of the complex plane. This requirement is necessary for the stability of N_0, the inverse of N_x.

3. For feasibility the transfer function is required to be proper, hence has not less poles than zeros. For feasibility of both the filters, N_x and its inverse N_0, the transfer function must be biproper, hence have an equal number of poles and zeros, i.e. a relative degree of zero.

Thus, the filter N_x is required to be a biproper, stable minimum phase system.

The filter N_x considered as a lead-lag filter of order $(2N + 1)$ with the transfer function

$$N_x(s) = k\frac{s + a_1}{s + b_1}\prod_{i,j=1}^{N}\frac{s^2 + a_{2i}s + a_{2i+1}}{s^2 + b_{2j}s + b_{2j+1}},$$

with the gain k and the coefficients a_i and b_j, $i, j = 1, 2, ..., (2N + 1)$ representing the optimization parameter vector $\boldsymbol{q} = [k,\, a_i,\, b_j]$.

In order to satisfy the requirements #1 and #2 from the previous section, the coefficients according to Hurwitz the must be positive real $a_i, b_j \in \mathbb{R}_+$. Consequently, we constrain the parameter space of optimization to positive real values $\boldsymbol{q} \in \mathbb{R}_+^{(4N+3)}$. By its parametrization the transfer function is always biproper (requirement #3).

Remark A.1 The order of the transfer function can be chosen arbitrary. As this represents a polynomial approximation of an arbitrary function, higher order will result in better approximation in general, but also results in more parameters to optimize, hence higher computational cost.

The objective function J to be minimized in order to find the optimal filter parameter incorporates an impedance matching quality measure J_t and a passivity penalty term J_p

$$J(\boldsymbol{q}) = J_t(\boldsymbol{q}) + J_p(\boldsymbol{q}) \rightarrow \min_{\boldsymbol{q}}.$$

The impedance matching objective can be similarly formulated as the perceived impedance approximation objective in the optimization-based transparency analysis method proposed in Section 3.1. Therefore, a cost function analogously to (3.6) as the integral over a squared impedance error norm is computed in the frequency domain

$$J_t(\boldsymbol{q}) = \int_{\omega_{\min}}^{\omega_{\max}} \left[G_h(j\omega)\Delta Z(j\omega, \boldsymbol{q})\right]^2 \, \mathrm{d}\omega\,,$$

with the impedance error norm ΔZ, a weighting filter G_h emphasizing frequency bands of interest, and $[\omega_{\min},\, \omega_{\max}]$ the frequency window for optimization. The impedance error norm ΔZ is defined similarly to the given by (3.5), now as difference between the desired and the current terminating impedance

$$\Delta Z(j\omega, \boldsymbol{q}) = Z_x^d - Z_x(j\omega, \boldsymbol{q}) = b - Z_x(j\omega, \boldsymbol{q}).$$

The impedance error (3.5) is based on the error in the magnitudes. Alternatively here, both, the magnitude and the phase error is incorporated, see Fig. A.6 for a visualization in the Nyquist plot. The closer in terms of the error norm a solution is to $Z_x^d = b$, the less it is penalized. If a solution $Z_x(\boldsymbol{q})$ is equal to $Z_x^d = b\ \forall\omega \in [\omega_{\min},\, \omega_{\max}]$, the impedance matching objective J_t computes to zero.

In order to enforce candidate solutions, that yield a passive terminating impedance, an additional passivity penalty term J_p is considered in the objective function. Passivity in the frequency domain can be analyzed based on the phase behavior of a systems transfer function. Basically, a stable SISO system is passive ,if its transfer function Z is positive real $|\mathrm{Re}\,[Z(j\omega)]\,| \geq 0$, i.e. its Nyquist plot lies in the right half of the complex plane. This means that its absolute value of the phase does not exceed 90°, for more details refer to [68]. In order to enforce a passive terminating impedance, any candidate solution $Z_x(j\omega, \boldsymbol{q})$, for which the Nyquist plot leaves the sector $[-\Phi, +\Phi]$, $\Phi \leq 90°$, is penalized. Choosing $\Phi < 90°$ implies a passivity reserve of the solution which is desirable for robustness considerations. The squared phase difference integrated over the frequency window $[\omega_{\min},\, \omega_{\max}]$ is used as a measure of non-passivity. The passivity penalty term is defined by

$$J_p(\boldsymbol{q}) = \begin{cases} 0 \quad \text{for } |\angle Z_x(j\omega, \boldsymbol{q})| < \Phi \\ \beta \int_{\omega_{\min}}^{\omega_{\max}} \left[\Phi - |\angle Z_x(j\omega, \boldsymbol{q})|\right]^2 \, \mathrm{d}\omega \quad \text{otherwise,} \end{cases} \tag{A.5}$$

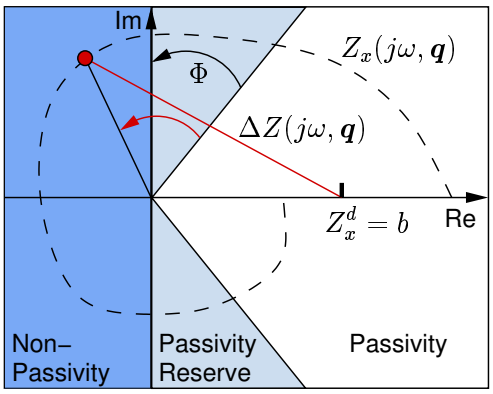

Figure A.6: Filter optimization by loopshaping of the terminating impedance $Z_x(j\omega, \boldsymbol{q})$ in the Nyquist plot.

with β a scalar weighting factor. Solutions with the Nyquist plot remaining within the sector $[-\Phi, +\Phi]$, represented by the white area in Fig. A.6, are not penalized corresponding to the first case in J_p, high phase difference $[\Phi - |\angle Z_x(j\omega, \boldsymbol{q})|]$ results in high penalty.

Remark A.2 The proposed design procedure has a general character and can also be applied for the design of other impedance matching architectures such as the one in [105]. This is especially beneficial if the dynamics of the terminating impedance $Z_{t/e}$ is very complex and analytical approaches are difficult to apply.

Remark A.3 The impedance matching filter architecture is originally applied to a position based wave variable architecture where the position instead of the velocity is encoded into the wave variable [9, 11, 50] in order to achieve superior position tracking. As the mapping from position to force is not passive in general, these filters additionally have to guarantee the passivity of the terminating impedance. The validity of the approach for the velocity/force architecture as well as for multi-DoF telepresence systems is shown in [78].

In order to show its efficiency, the optimization based impedance matching method is applied to a numerical example in the following section, more detailed transparency investigations are conducted in [50].

A.3.3 Effect on Transparency

For the following exemplary numerical transparency evaluation a PI velocity controlled teleoperator and a spring-damper environment is assumed as given by (A.1). The corresponding parameter values are listed in Table A.1, the environment stiffness coefficient is assumed to be $k_e = 1000\,\mathrm{N/m}$. A second order lead-lag structure is chosen for the impedance matching filter

$$N_x(s) = q_1 \frac{s^2 + q_2 s + q_3}{s^2 + q_4 s + q_5}.$$

The optimization is performed using the cost function (A.3.2) with in the frequency window $[\omega_{\min}, \omega_{\max}] = [10^{-2}, 10^{3}]$ Hz and the weighting filter $G_h(j\omega) = 1$. The passivity reserve for the passivity penalty term is set to $\Phi = 70°$ The parameter vector resulting from the optimization by means of the `fminsearch`-algorithm of MATLAB

$$\boldsymbol{q}^* = \begin{bmatrix} q_1 & q_2 & q_3 & q_4 & q_5 \end{bmatrix}^T = [0.52 \;\; 20.38 \;\; 0.07 \;\; 112.65 \;\; 3.70]^T,$$

optimally matches the terminating impedance Z_x to the wave impedance $b = 1\text{Ns/m}$ with respect to the given cost function (A.3.2).

In order to show the effect of the impedance matching architecture on the transparency, the time responses of the teleoperator velocity and the desired HSI force are compared for the impedance matched, the original non-impedance matched architecture $N_x = N_0 = 1$, and for zero time delay. Therefore the HSI is modeled as a pure velocity source, that provides a sinusoidal chirp signal starting at a frequency of 0.1 Hz at $t = 0\,\text{s}$, finishing with a frequency of 1 Hz at $t = 10\,\text{s}$; the amplitude is 1 m/s. For the architectures without filters a second order low pass filter is applied in the wave domain in order to guarantee stability with environment force feedback, see Section A.2 for the details and the design parameters. The time delay is equal in the forward and the backward path $T_1 = T_2 = 100\,\text{ms}$. The

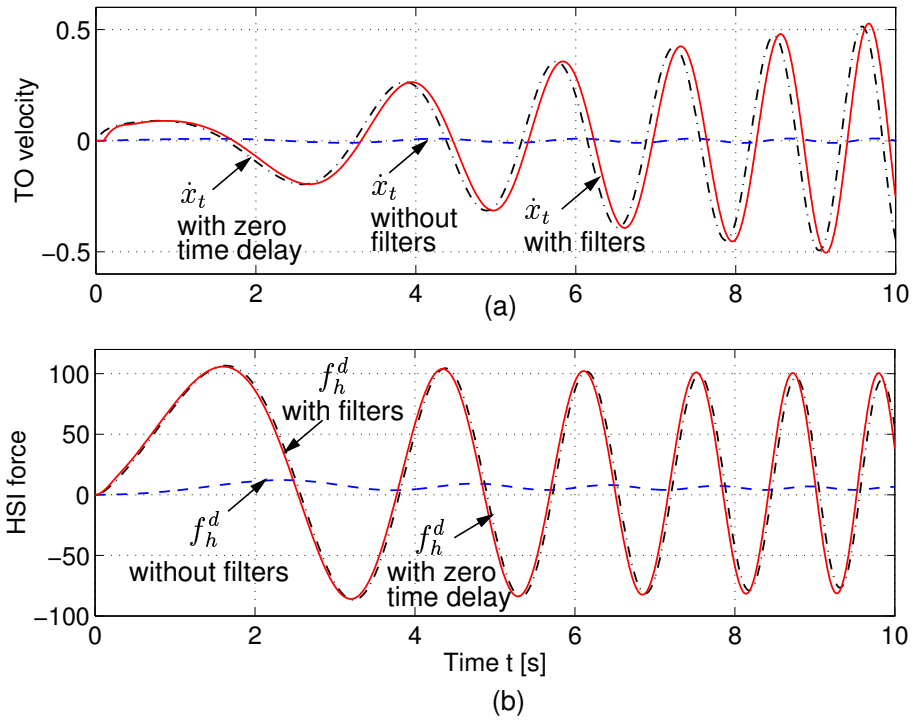

Figure A.7: Simulation results: comparison of impedance matched with non-impedance matched architecture; teleoperator velocity (a) and desired HSI force (b), for comparison with zero time delay.

simulation results are presented in Fig. A.7. For transparency reference the telepresence system architecture without time delay is taken, the HSI velocity directly acts as desired teleoperator velocity, the desired HSI force is equal to the environment force. The communication system then has no impact on the transparency, hence the transparency should

be superior neglecting the impact of the teleoperator control. The large deviation between the signals for zero delay and for the original (without filters) architecture indicates very poor transparency. The tracking behavior with the impedance matching filter architecture is superior; the velocity as well as the force signals show only a very small deviation which is induced by the communication time delay. The transparency of the impedance matched architecture is very good and even comparable to the zero delay case.

Remark A.4 In order to design the impedance matching filter, knowledge about the environment dynamics is required in advance. The system performance is optimal only for the nominal environment. With small changes in the environmental parameters the achievable transparency is still good [50]. However, the approach in this form is not appropriate for large changes in the environment dynamics as they occur from free space motion to contact or vice versa.

B Wave Variables and the Small Gain Theorem

The entire concept of wave variables is based within the framework of passivity and was particular motivated by scattering operators [34]. Scattering operators link passivity to the small gain theorem. Without developing the rigoros definitions needed to properly discuss operators the results from [34] are stated in the following and interpreted for haptic telepresence systems. Assume the operator $\boldsymbol{H}$ maps the input vector $\boldsymbol{x}$ to the output vector $\boldsymbol{y}$, which are assumed to be of identical dimension

$$\boldsymbol{y} = \boldsymbol{H}\boldsymbol{x}.$$

The scattering operator of $\boldsymbol{H}$ is then defined as

$$\boldsymbol{S} = (\boldsymbol{H} - \boldsymbol{I})(\boldsymbol{H} + \boldsymbol{I})^{-1}, \tag{B.1}$$

where the inverse of $(\boldsymbol{H} + \boldsymbol{I})$ is assumed be well defined, $\boldsymbol{I}$ is the unity matrix. The scattering operator maps the sum to the difference of the former input $\boldsymbol{x}$ and output $\boldsymbol{y}$

$$(\boldsymbol{y} - \boldsymbol{x}) = \boldsymbol{S}(\boldsymbol{y} + \boldsymbol{x}).$$

Building on these definitions a system is passive, if and only if its scattering operator satisfies the small gain theorem, hence has a norm less or equal to unity

$$||\boldsymbol{S}||^2 = \max_{\boldsymbol{x}\neq 0} \frac{||\boldsymbol{S}\boldsymbol{x}||_t^2}{||\boldsymbol{x}||_t^2} \leq 1 \quad \forall t, \tag{B.2}$$

with the norm $||\cdot||_t^2$ defined by

$$||\cdot||_t^2 = \int_0^t (\cdot)^T(\cdot)\mathrm{d}\tau.$$

Considering LTI systems, the scattering operator can be expressed in the Laplace domain now relating the transfer function $H(s)$

$$\boldsymbol{S}(s) = (\boldsymbol{H}(s) - 1)(\boldsymbol{H}(s) + 1)^{-1},$$

assuming $(\boldsymbol{H}(s) + 1)^{-1}$ to be well-defined. Expressed in the frequency domain, the system is passive, if and only if

$$||\boldsymbol{S}||^2 = \sup_{\omega} ||\boldsymbol{S}(j\omega)||^2 = \sup_{\omega} \gamma_{max}(\boldsymbol{S}^*(j\omega)\boldsymbol{S}(j\omega)) \leq 1, \tag{B.3}$$

with $\gamma_{max}(\cdot)$ the largest eigenvalue equivalent to the largest singular value of $\boldsymbol{S}$. For SISO LTI systems this implies that the magnitude of $\boldsymbol{S}$ is less or equal to unity for all frequencies and its graph is within the unit circle in the complex plain. The scattering operator maps the entire right half plain corresponding to passive systems into the unit circle.

B.1 Interpretation in Haptic Telepresence Systems

With the wave variable transformation according to (2.8) the scattering operator finds its analogon in the reflection factor (2.15) relating the wave variables. Now the power variables velocity and force are considered as input and output of the passive systems represented by the human/HSI and the teleoperator/environment. In contrast to the scattering operator a weighting b of the velocity and a power normation is introduced not corrupting the foregoing results. We assume LTI systems for the human/HSI impedance $Z_{hu/h}$ and the teleoperator/environment impedance $Z_{t/e}$ (2.5). Then, for the right end side of the telepresence system the transfer function between the wave variables, being equal to the reflection factor (2.15), is given by

$$S_r = \frac{v_r}{u_r} = \frac{\frac{1}{b}Z_{t/e} - 1}{\frac{1}{b}Z_{t/e} + 1}, \tag{B.4}$$

with the independent variable s being omitted. For the operator side accordingly

$$S_l = \frac{u_l}{v_l} = -\frac{\frac{1}{b}Z_{hu/h} - 1}{\frac{1}{b}Z_{hu/h} + 1}, \tag{B.5}$$

with the impedance $Z_{hu/h}$ describing the relation between the HSI velocity $\dot{x}_h$ and the desired HSI force f_h^d

$$Z_{hu/h} = \frac{f_h^d}{\dot{x}_h}.$$

Note, that the direction of the force transmitted to the operator side has to be reverted in order to display the reaction force of the environment at the HSI. As a result the transfer function S_l has a negative sign.

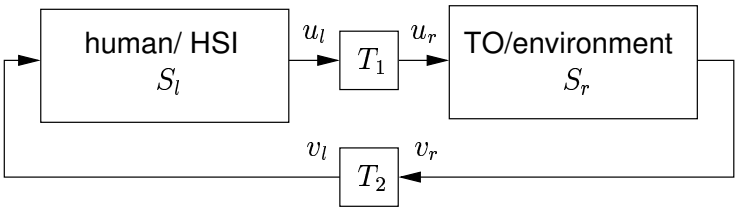

Figure B.1: Control loop in wave variables.

If the human/HSI impedance $Z_{hu/h}$ and the teleoperator/environment impedance $Z_{t/e}$ are passive, then the impedances $\frac{Z_{t/e}}{b}$ and $\frac{Z_{hu/h}}{b}$ are also passive as the wave impedance b by definition is a positive constant. The analogy between the scattering operator (B.1) the wave transfer functions (B.5) and (B.4) is obvious. The small gain condition (B.2) is applicable. According to that the wave transfer functions S_l and S_r have a gain less or equal to unity

$$||S_l||^2 \leq 1 \quad \text{and} \quad ||S_r||^2 \leq 1. \tag{B.6}$$

With the given wave transfer functions the global control loop of the haptic telepresence system is now considered in the wave variable space. As shown in Fig. B.1 the control loop consists of the wave transfer functions S_l, S_r, and the delays in the forward and backward path. As the delay elements have a unity gain and with the result from (B.6) the overall loop is small gain. As a result the closed loop system with passive subsystems and the wave variable transformation is stable for arbitrary large constant delays.

Remark B.1 Note, that the force applied by the human consists of two components, the reaction force to a velocity input described by the human impedance and an external force that is intentionally applied for the task completion. In the previous closed loop analysis only the human impedance is considered. However, under the realistic assumption of a bounded external force the stability results are not touched.

C Experimental Setup

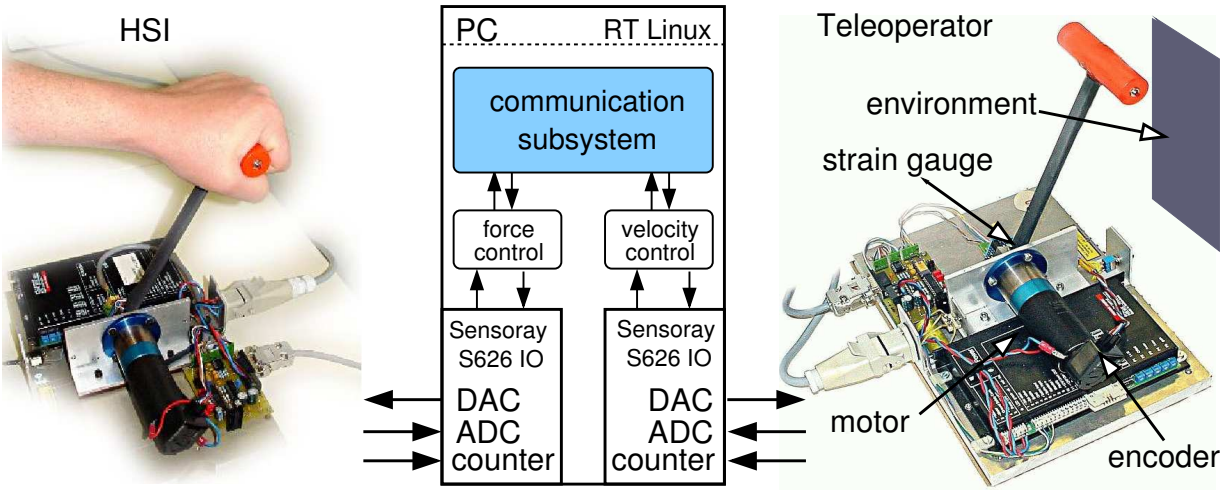

Figure C.1: Experimental system architecture.

The experimental setup consists of two identical single degree of freedom force feedback paddles connected to a PC. At the teleoperator side environments of different dynamics (wooden board, rubber foam) can be mounted such that different contact situations and of course free space motion can be evaluated.

The original design of the paddles can be found in [7]. The paddle DC motor torque is controlled by the PWM amplifier, which operates in current control with the reference given by a voltage from the D/A converter output of the I/O board. The force applied to the paddle lever, attached at the motor axis, is measured through the bending of the lever by a strain gauge bridge, that is attached at the bottom of the lever with the strain being amplified and converted by an A/D converter of the I/O board. The position[1] of the lever, measured by an optic pulse incremental encoder on the motor axis is processed by a quadrature encoder on the I/O board. The control loops and the model of the communication subsystem are composed of MATLAB/SIMULINK blocksets; standalone real-time code for RT Linux is automatically generated from the SIMULINK model. All experiments are performed with a sample time $T_A = 0.001$s.

The HSI is force controlled, the teleoperator is PI velocity controlled. For the experiments conducted in Chapter 3 the communication subsystem consists of a bilateral communication line with constant time delay, and the wave variable transformation. This model is extented by a random packet loss and the data reconstruction strategy with energy supervision for the experiments in Chapter 4. The time-varying delay together with the packet processing strategy is represented by the accordingly adjusted constant time

[1] The terms of position and force are understood in a generalized sense, i.e position is also used as synonym for angle, force as a synonym for torque.

delay and additional packet loss. The communication subsystem for the experiments in Chapter 5 consist of the deadband controller, a constant time delay and the data reconstruction. All communication related effects are emulated in the forward and the backward path with equal parameters. The parameters are listed in the according chapters.

Remark C.1 Further experiments with two degree-of-freedom (DoF) telepresence systems, over real Internet or over a real-time-network network emulator have been conducted in the course of this thesis, but are omitted here due to their mainly demonstrational character. In order to emulate the packet switched communication network in real-time, in [51, 57] including time-varying time delay and packet loss the network emulator NS2 is used instead of a SIMULINK model.

In [77] a two DoF haptic telepresence system is developed based on two identical Scara-robots. Impedance matching architectures, see Appendix A for details, are evaluated using this experimental system in [78, 79]. A tele-assembly experiment over the real Internet between Munich (Germany) and Berlin (Germany), see Fig. C.2 is conducted in [58, 133] in order to show the validity of the position feedforward architecture, see Appendix A and [27] for details. In this two DoF experiment the two force feedback paddles described above are used as HSI, an antropomorphic robotic arm with native 7 DoF reduced to two DoF in this experiment as teleoperator, see [133] and references therein for details on the teleoperator.

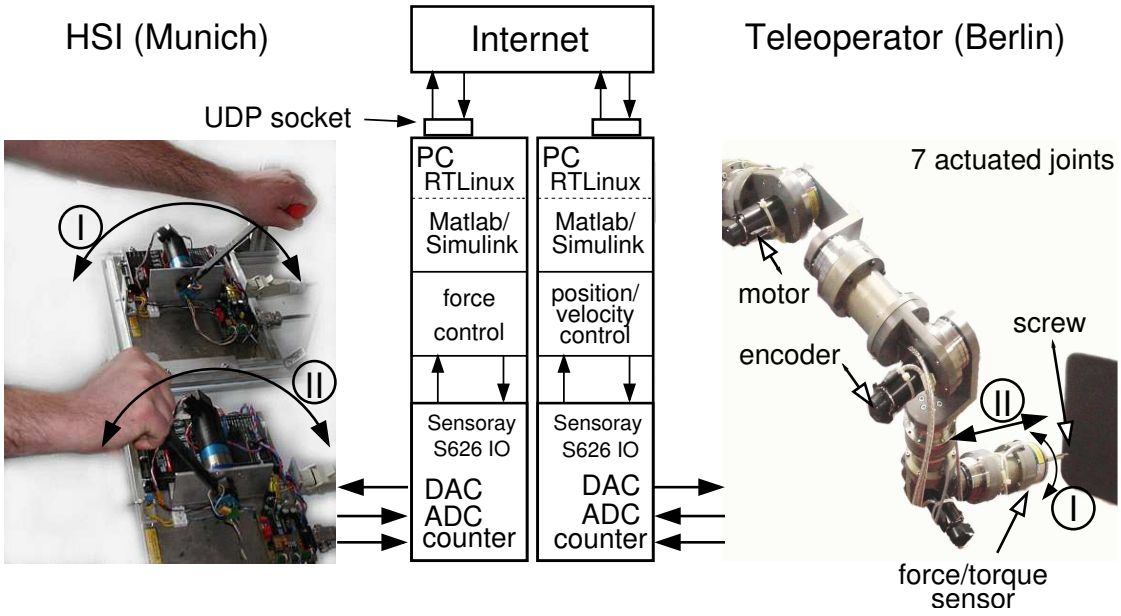

Figure C.2: Demonstration scenario: tele-assembly over the Internet.

Bibliography

[1] R.J. Anderson and M.W. Spong. Bilateral Control of Teleoperators with Time Delay. *IEEE Transactions on Automatic Control*, 34(5):494–501, 1989.

[2] R.J. Anderson and M.W. Spong. Asymptotic Stability for Force Reflecting Teleoperators with Time Delay. *International Journal of Robotic Research*, 11:135–149, 1992.

[3] P. Arcara. *Control of Haptic and Robotic Telemanipulation Systems*. PhD thesis, Universita degli Studi di Bologna, 2001.

[4] P. Arcara and C. Melchiorri. Control Schemes for Teleoperation with Time Delay: A Comparative Study. *Robotics and Autonomous Systems*, 38(1):49–64, 2002.

[5] K.J. Aström and B. Bernhardsson. Comparison of Riemann and Lebesgue Sampling for First Order Stochastic Systems. In *Proceedings of the 41nd IEEE Conference on Decision and Control CDC'02*, pages 2011–2016, Las Vegas (NV), US, 2002.

[6] M. Franceschetti K. Poolla M. I. Jordan B. Sinopoli, L. Schenato and S.S. Sastry. Kalman Filtering with Intermittent Observations. In *Proceedings of the 42nd IEEE Conference on Decision and Control CDC'03*, pages 701–708, Maui (HW), US, 2003.

[7] H. Baier, M. Buss, F. Freyberger, J. Hoogen, P. Kammermeier, and G. Schmidt. Distributed PC-Based Haptic, Visual and Acoustic Telepresence System—Experiments in Virtual and Remote Environments. In *Proceedings of the IEEE Virtual Reality Conference VR'99*, pages 118–125, Houston (TX), US, 1999.

[8] H. Baier, M. Buss, and G. Schmidt. Control Mode Switching for Teledrilling Based on a Hybrid System Model. In *Proceedings of the IEEE/ASME International Conference on Advanced Intelligent Mechatronics AIM'97*, Tokyo, Japan, Paper No. 50, 1997.

[9] H. Baier, M. Buss, and G. Schmidt. Stabilität und Modusumschaltung von Regelkreisen in Teleaktionssystemen. *at—Automatisierungstechnik*, 48(2):51–59, Februar 2000.

[10] H. Baier, F. Freyberger, and G. Schmidt. Interaktives Stereo-Telesehen – ein Baustein wirklichkeitsnaher Telepräsenz. *at—Automatisierungstechnik*, 49(7):295–303, 2001.

[11] H. Baier and G. Schmidt. Transparency and Stability of Bilateral Kinesthetic Teleoperation with Time-Delayed Communication. *Journal of Intelligent and Robotic Systems*, 40:1–22, 2004.

[12] F. Baker, R. Guerin, and D. Kandlur. Specification of Committed Rate Quality of Service. *draft-ietf-intserv-commit-rate-svc-00.txt*, June 1996.

[13] A. Bauer. *Transparenzgrad für Haptische Telepräsenz*. Bachelor thesis supervised by S. Hirche, Institute of Automatic Control Engineering, Technische Universität München, 2004.

[14] G.L. Beauregard and M. A. Srinivasan. The Manual Resolution of Viscosity and Mass. *ASME Dynamic Systems and Control Division*, 1:657–662, 1995.

[15] B. Berestesky, N. Chopra, and M. W. Spong. Discrete Time Passivity in Bilateral Teleoperation over the Internet. In *Proceedings of the IEEE International Conference on Robotics and Automation ICRA'04*, pages 4557–4564, New Orleans, US, 2004.

[16] S. Blake, D. Black, M. Carlson, E. Davies, Z. Wang, and W. Weiss. An Architecture for Differentiated Services. *IETF RFC 2475*, December 1998.

[17] R. Braden, D. Clark, and S. Shenker. Integrated Services in the Internet Architecture: an Overview. *IETF RFC 1633*, July 1994.

[18] H. Brandtstädter, J. Schneider, and F. Freyberger. Hardware and Software Components for a New Internet-Based Multimodal Tele-Control Experiment with Haptic Sensation. In *Proceedings of the EuroHaptics'2004 Conference*, pages 426–427, Munich, Germany, 2004.

[19] Bronstein, Semendjajew, Musiol, and Mühlig. *Taschenbuch der Mathematik*. Harry Deutsch, 1995.

[20] T.L. Brooks. Telerobotic response requirements. In *Proceedings of the IEEE International Conference on Systems, Man, and Cybernetics*, pages 113–120, Los Angeles (CA), US, 1990.

[21] J.M. Brown and J.E. Colgate. Factors affecting the z-width of a haptic display. In *Proceedings of the IEEE International Conference on Robotics and Automation*, pages 3205–10, San Diego, CA, 1994.

[22] G.C. Burdea. *Force and Touch Feedback for Virtual Reality*. John Wiley, 1996.

[23] M. Buss and G. Schmidt. Control Problems in Multi-Modal Telepresence Systems. In P.M. Frank, editor, *Advances in Control: Highlights of the 5th European Control Conference ECC'99 in Karlsruhe, Germany*, pages 65–101. Springer, 1999.

[24] M.C. Cavosoglu, A. Sherman, and F. Tendick. Design of Bilateral Teleoperation Controllers for Haptic Exploration and Telemanipulation in Soft Environments. *IEEE Transactions on Robotics and Automation*, 18(4):641–647, October 2002.

[25] C. Cetinkaya and E.W. Knightly. Egress Admission Control. In *Proceedings of the 19th Annual Joint Conference of the IEEE Computer and Communications Society INFOCOM*, pages pp.686–695, Tel Aviv, Israel, 2000.

[26] C.-C. Chen. *Quality-of-Service Control for Networked Control Systems*. Master thesis supervised by S. Hirche, Institute of Automatic Control Engineering, Technische Universität München, 2005.

[27] N. Chopra, M.W. Spong, S. Hirche, and M. Buss. Bilateral Teleoperation over Internet: the Time Varying Delay Problem. In *Proceedings of the American Control Conference*, pages 155–160, Denver (CO), US, 2003.

[28] N. Chopra, M.W. Spong, R. Ortega, and N.E. Barabanov. On Position Tracking in Bilateral Teleoperation. In *Proceedings the American Control Conference ACC 2004*, Boston (MA), US, 2004.

[29] D. Clark. Adding Service Discrimination to the Internet. In L.W. McKnight and J.P. Bailey, editors, *Internet Economics*. The MIT Press, 1997.

[30] D.D. Clark and W. Fang. Explicit Allocation of Best Effort Packet Delivery Service. *IEEE/ACM Transactions on Networking*, 6(4):pp. 362–373, August 1998.

[31] J. E. Colgate, M. C. Stanley, and G. G. Schenkel. Dynamic Range of Achievable Impedances in Force-Reflecting Interfaces. In *Proc. SPIE Vol. 2057, Telemanipulator Technology and Space Telerobotics, Won S. Kim; Ed.*, pages 199–210, December 1993.

[32] J.E. Colgate and N. Hogan. Robust Stability of Dynamically Interacting Systems. *International Journal of Control*, 48(1):65–88, 1988.

[33] H. Das, H. Zak, W.S. Kim, A.K. Bejczy, and P.S. Schenker. Operator Performance with Alternative Manual Control Modes in Teleoperation. *Presence*, 1(2):201–217, 1992.

[34] C. A. Desoer and M. Vidyasagar. *Feedback Systems: Input-Output Properties*. Academic Press, 1975.

[35] A. Eusebi and C. Melchiorri. Force Reflecting Telemanipulators with Time Delay: Stability Analysis and Control Design. *IEEE Transactions on Robotics and Automation*, 14(4):635–640, 1998.

[36] W.R. Ferrell. Remote Manipulation with Transmission Delay. *IEEE Transactions on Human Factors*, 6:24–32, 1965.

[37] W.R. Ferrell. Delayed Force Feedback. *IEEE Transactions on Human Factors*, 8:449–455, 1966.

[38] G.A. Gescheider. *Psychophysics: The Fundamentals*. Lawrence Erlbaum and Associates, 3rd Edition, Hillsdale.

[39] K. Goldberg, M. Mascha, S. Gentner, N. Rothenberg, C. Sutter, and J. Wiegley. Beyond the Web: Manipulating the Physical World via the WWW. *Computer Networks and ISDN Systems Journal*, 28(1), 1995.

[40] D. Gracanin, Y. Zhou, L. DaSilva, and V. Tech. Quality or Service for Networked Virtual Environments. *IEEE Comunications Magazine*, 42(4):pp.42–48, September 2004.

[41] G.S. Guthart and J.K. Salisbury. The Intuitive™ Telesurgery System: Overview and Application. In *Proceedings of the IEEE International Conference on Robotics and Automation*, pages 618–621, San Francisco, CA, 2000.

[42] B. Hannaford. Stability and Performance Tradeoffs in Bi-Lateral Telemanipulation. In *Proceedings of the IEEE International Conference on Robotics and Automation*, pages 1764–1767, Scottsdale (AZ), US, 1989.

[43] B. Hannaford and J.-H. Ryu. Time-Domain Passivity Control of Haptic Interfaces. *IEEE Transactions on Robotics and Automation*, 18(1):1–10, February 2002.

[44] K. Hashtrudi-Zaad and S.E. Salcudean. On the Use of Local Force Feedback for Transparent Teleoperation. In *Proceedings of the IEEE International Conference on Robotics and Automation*, pages 1863–1869, Detroit (MI), US, 1999.

[45] K. Hashtrudi-Zaad and S.E. Salcudean. Analysis and Evaluation of Stability and Performance Robustness for Teleoperation Control Architectures. In *Proceedings of the IEEE International Conference on Robotics and Automation*, pages 3107–3113, San Francisco (CA), US, 2000.

[46] K. Hashtrudi-Zaad and S.E. Salcudean. Analysis of Control Architectures for Teleoperation Systems with Impedance/Admittance Master and Slave Manipulators. *International Journal of Robotics Research*, 20(6):419–445, 2001.

[47] R.A. Heinlein. *Waldo and Magic.* Ballantine Books, 1990.

[48] P. Hinterseer, S. Hirche, E. Steinbach, and Buss M. A Novel, Psychophysically Motivated Transmission Approach for Haptic Data Streams in Telepresence and Teleaction Systems. In *Proceedings of the IEEE International Conference on Acoustics, Speech, and Signal Processing, ICASSP'2005*, Philadelphia (PA), US, 2005.

[49] S. Hirche and M. Buss. Haptic Internet-Telepresence. In G. Hommel and H. Sheng, editors, *The Internet Challenge: Technology and Applications, Berlin, Germany*, pages 63–72. Kluwer, 2002.

[50] S. Hirche and M. Buss. Passive Position Controlled Telepresence System with Time Delay. In *Proceedings of the American Control Conference*, pages 168–173, Denver (CO), US, 2003.

[51] S. Hirche and M. Buss. Study of Teleoperation Using Realtime Communication Network Emulation. In *Proceedings of the IEEE/ASME International Conference on Advanced Intelligent Mechatronics AIM2003*, pages 586–591, Kobe, Japan, 2003.

[52] S. Hirche and M. Buss. Packet Loss Effects in Passive Telepresence Systems. In *Proceedings of the 43rd IEEE Conference on Decision and Control*, pages 4010–4015, Nassau, Bahamas, 2004.

[53] S. Hirche and M. Buss. Telepresence Control in Packet Switched Communication Networks. In *Proceedings of the IEEE International Conference on Control Applications*, pages 236–241, Taipei, Taiwan, 2004.

[54] S. Hirche and M. Buss. Transparency Aspects of Haptic Telepresence over the Internet. In *Proceedings of the IEEE International Conference on Control Applications*, pages 328–333, Toronto, Canada, 2005.

[55] S. Hirche, P. Hinterseer, E. Steinbach, and M. Buss. Network Traffic Reduction in Haptic Telepresence Systems by Deadband Control. In *Proceedings IFAC World Congress, International Federation of Automatic Control*, Prague, Czech Republic, 2005.

[56] S. Hirche, P. Hinterseer, E. Steinbach, and M. Buss. Towards Deadband Control in Networked Teleoperation Systems. In *Proceedings IFAC World Congress, International Federation of Automatic Control*, Prague, Czech Republic, 2005.

[57] S. Hirche, B. Stanczyk, and M. Buss. Transparent Exploration of Remote Environments by Internet Telepresence. In *Proceedings of the International Workshop on High-Fidelity Telepresence and Teleaction, jointly with the IEEE conference HUMANOIDS'2003*, Munich, Germany, 2003.

[58] S. Hirche, B. Stanczyk, and M. Buss. Haptic Tele-Assembly over the Internet. In *Proceedings of the EuroHaptics'2004 Conference*, pages 417–421, Munich, Germany, 2004.

[59] G. Hirzinger. ROTEX–The First Robot in Space. In *Proceedings of the ICAR International Conference on Advanced Robotics*, pages 9–33, Tokyo, Japan, 1993.

[60] N. Hogan. Controlling Impedance at the Man/Machine Interface. In *Proceedings of the IEEE International Conference on Robotics and Automation*, pages 1626–1631, Scottsdale (AZ), US, 1989.

[61] R. Isermann. *Identifikation dynamischer Systeme 1.* Springer, 1992.

[62] H. Ishii and T. Basar. An Analysis on Quantization Effects in H^∞ Parameter Identification. In *Proceedings of the International Conference on Control Applications*, pages 468–473, Taipei,Taiwan, 2004.

[63] H. Ishii and B. Francis. *Limited Data Rate in Control Systems with Networks*, volume 275. Springer, Lecture Notes in Control and Information Sciences, 2002.

[64] L. A. Jones and I. W. Hunter. Human Operator Perception of Mechanical Variables and Their Effects on Tracking Performance. *ASME Advances in Robotics*, 42:49–53, 1992.

[65] L.A. Jones. Matching Forces: Constant Errors and Differential Thresholds. *Perception*, 18:681–687, 1989.

[66] L.A. Jones and I.W. Hunter. A Perceptual Analysis of Stiffness. *Experimental Brain Research*, 79:150–156, 1990.

[67] L.A. Jones and I.W. Hunter. A Perceptual Analysis of Viscosity. *Experimental Brain Research*, 94(2):343–351, 1993.

[68] H.K. Khalil. *Nonlinear Systems*. Prentice Hall, 1996.

[69] W.S. Kim. Shared Compliant Control: a Stability Analysis and Experiments. In *Proceedings of the IEEE International Conference on Systems, Man, and Cybernetics*, pages 620–623, Los Angeles (CA), US, 1990.

[70] W.S. Kim. Development of New Force Reflecting Control Schemes and an Application to a Teleoperation Training Simulator. In *Proceedings of the IEEE/RSJ International Conference on Intelligent Robots and Systems IROS*, pages 1412–1419, Nice, France, 1992.

[71] W.S. Kim, B. Hannaford, and A.K. Bejczy. Force Reflection and Shared Compliant Control in Operating Telemanipulators with Time Delay. *IEEE Transactions on Robotics and Automation*, 8(2):176–185, 1992.

[72] K. Klank. *Hybride Regelung eines Haptischen Telepräsenzsystems in Verschiedenen Kontaktsituationen*. Diploma thesis supervised by S. Hirche, Institute of Automatic Control Engineering, Technische Universität München, 2004.

[73] K. Kosuge, H. Murayama, and K. Takeo. Bilateral Feedback Control of Telemanipulators via Computer Network. In *Proceedings of the IEEE/RSJ International Conference on Intelligent Robots and Systems IROS*, pages 1380–1385, Osaka, Japan, 1996.

[74] P. Kremer. *Paketverlust in Haptischen Telepräsenzsystemen mit Quality-of-Service Kommunikation*. Studienarbeit supervised by S. Hirche, Institute of Automatic Control Engineering, Technische Universität München, 2004.

[75] A. Kron. *Beiträge zur bimanuellen und mehrfingrigen haptischen Informationsvermittlung in Telepräsenzsystemen*. PhD thesis, Technische Universität München, Institute of Automatic Control Engineering, 2004.

[76] A. Kron, G. Schmidt, B. Petzold, M. F. Zäh, P. Hinterseer, and E. Steinbach. Disposal of Explosive Ordnances by Use of a Bimanual Haptic Telepresence System. pages 1968–1973, New Orleans (LA), US, April 2004.

[77] M. Kuschel. *Konstruktion eines SCARA-Roboters zur Erforschung von Regelungsstrategien in der Telepräsenz*. Studienarbeit supervised by S. Hirche, Control Systems Group, Faculty of Electrical Engineering and Computer Science, Technical University Berlin, 2004.

[78] M. Kuschel. *Performance Oriented Control of Haptic Telepresence Systems*. Diploma thesis supervised by S. Hirche, Institute of Automatic Control Engineering, Technische Universität München, 2004.

[79] M. Kuschel, S. Hirche, and M. Buss. Communication Induced Disturbances in Haptic Telepresence Systems. In *Proceedings IFAC World Congress, International Federation of Automatic Control*, Prague, Czech Republic, 2005.

[80] C.A. Lawn and B. Hannaford. Performance Testing of Passive Communication and Control in Teleoperation with Time Delay. In *Proceedings of the IEEE International Conference on Robotics and Automation*, pages 776–783, Atlanta (GA), US, 1993.

[81] D.A. Lawrence. Stability and Transparency in Bilateral Teleoperation. *IEEE Transactions on Robotics and Automation*, 9(5):624–637, October 1993.

[82] D.A. Lawrence and D.J. Chapel. Performance Trade-Offs for Hand Controller Design. In *Proceedings of the IEEE International Conference on Robotics and Automation*, pages 3211–3216, San Diego (CA), US, 1994.

[83] D. Lee and P. Li. Passive Coordination Control for Nonlinear Bilateral Teleoperated Manipulators. In *Proceedings of the IEEE International Conference on Robotics and Automation*, pages 3278–3283, Washington (DC), US, 2002.

[84] H.K. Lee and M.J. Chung. Adaptive Control of a Master-Slave System for Transparent Teleoperation. *Journal of Robotic Systems*, 15(8):465–475, 1998.

[85] G.M.H. Leung and B.A. Francis. Bilateral Control of Teleoperators with Time Delay Through a Digital Communication Channel. In *Proceedings of the 30th Annual Allerton Conference on Communication, Control and Computation*, pages 692–701, Illinois, US, 1992.

[86] G.M.H. Leung, B.A. Francis, and A. Apkarian. Bilateral Controller for Teleoperators with Time Delay via μ-Synthesis. *IEEE Transactions on Robotics and Automation*, 11(1):105–116, 1993.

[87] F.-L. Lian, J. Yook, P. G. Otanez, D. M. Tilbury, and J. R. Moyne. Design of Sampling and Transmission Rates for Achieving Control and Communication Performance in Networked Agent Systems. In *Proceedings of the American Control Conference*, pages 3329–3334, Denver (CO), US, 2003.

[88] Q. Ling and M.D. Lemmon. Robust Performance of Soft Real-time Networked Control Systems with Data Dropout. In *Proceedings of the 41st IEEE Conference on Decision and Control CDC'02*, pages 1225–1230, Las Vegas (NV), US, 2002.

[89] F.B. Lllewellyn. Some Fundamental Properties of Transmission Systems. *Proceedings of the IRE*, 40:271–283, 1952.

[90] R. Lozano, N. Chopra, and M. Spong. Passivation of Force Reflecting Bilateral Teleoperators with Time Varying Delay. In *Proceedings of the 8. Mechatronics Forum*, pages 954–962, Enschede, Netherlands, 2002.

[91] A. Mankin, F. Baker, B. Braden, S. Bradner, M. O'Dell, A. Romanow, A. Weinrib, and L. Zhang. RSVP Version 1: Applicability Statement, Some Guidelines on Deployment. *IETF RFC 2208*, September 1997.

[92] T. Matiakis, S. Hirche, and M. Buss. Applying the Scattering Transformation in Network Control Systems. In *Proceedings of the IEEE Conference on Control Applications CCA'05*, pages 705–710, Toronto, Canada, 2005.

[93] M.L. McLaughlin, J.P. Hespanha, and G.S. Sukhatme. *Touch in Virtual Environments: Haptics and the Design of Interactive Systems*. Prentice Hall PTR, 2002.

[94] D. Mills. Internet Delay Experiments. *RFC-889, M/A-COM Linkabit*, December 1983.

[95] D. Minoli and E. Minoli. *Delivering Voice over IP Networks*. Wiley, 2002.

[96] M. Minsky. Telepresence. *Omni*, June 1980.

[97] S. Munir. *Internet-Based Teleoperation*. PhD thesis, Georgia Institute of Technology, George W. Woodruff School of Engineering, 2001.

[98] S. Munir and W.J. Book. Wave-Based Teleoperation with Prediction. In *Proceedings of the American Control Conference ACC*, pages 4605–4611, Arlington (VA), US, 2001.

[99] S. Munir and W.J. Book. Internet Based Teleoperation using Wave Variable with Prediction. *ASME/IEEE Transactions on Mechatronics*, 7(2):124–133, 2002.

[100] S. Munir and W.J. Book. Control Technique and Programming Issues for Time Delayed Internet Based Teleoperation. *Journal of Dynamic System Measurement and Control-transactions of the ASME*, 125(2):205–214, 2003.

[101] K. Nichols, S. Blake, F. Baker, and D. L. Black. Definition of the Differentiated Services Field (DS Field) in the IPv4 and IPv6 Headers. *IETF RFC 2474*, December 1998.

[102] K. Nichols, V. Jacobson, and L. Zhang. A Two-Bit Differentiated Services Architecture for the Internet. *IETF RFC 2638*, July 1999.

[103] G. Niemeyer. *Using Wave Variables in Time Delayed Force Reflecting Teleoperation*. PhD thesis, MIT, Department of Aeronautics and Astronautics, September 1996.

[104] G. Niemeyer and J. E. Slotine. Designing Force Reflecting Teleoperators with Large Time Delays to Appear as Virtual Tool. In *Proceedings of the IEEE International Conference on Robotics and Automation*, pages 2212–2218, Albuquerque (NM), US, 1997.

[105] G. Niemeyer and J. E. Slotine. Using Wave Variables for System Analysis and Robot Control. In *Proceedings of the IEEE International Conference on Robotics and Automation*, pages 1619–1625, Albuquerque (NM), US, 1997.

[106] G. Niemeyer and J. E. Slotine. Towards Force-Reflecting Teleoperation Over the Internet. In *Proceedings of the IEEE International Conference on Robotics and Automation*, pages 1909–1915, Leuven, Belgium, 1998.

[107] G. Niemeyer and J.-J.E. Slotine. Stable Adaptive Teleoperation. *IEEE Journal of Oceanic Engineering*, 16(1):152–162, January 1991.

[108] G. Niemeyer and J.-J.E. Slotine. Telemanipulation with Time Delays. *International Journal of Robotic Research*, 23(9):873–890, September 2004.

[109] J. Nilsson. *Real-Time Control Systems with Delay*. PhD thesis, Department of Automatic Control, Lund Institute of Technology, 1998.

[110] R. Oboe and P. Fiorini. Internet-Based Telerobotics: Problems and Approaches. In *Proceedings of the International Conference on Advanced Robotics ICAR 97*, pages 765–770, Monterey (CA), US, 1997.

[111] R. Oboe and P. Fiorini. Issues on Internet-Based Teleoperation. In *Proceedings of the Symposium on Robot Control SYROCO 97*, pages 611–617, Nantes, France, 1997.

[112] R. Oboe and P. Fiorini. A Design and Control Environment for Internet-Based Telerobotics. *International Journal of Robotic Research*, 17(4):433–449, 1998.

[113] P. G. Otanez, J. R. Moyne, and D. M. Tilbury. Using Deadbands to Reduce Communication in Networked Control Systems. In *Proceedings of the American Control Conference*, Anchorage (AK), US, 2002.

[114] J.H. Park and H.C. Cho. Sliding-Mode Controller for Bilateral Teleoperation with Varying Time Delay. In *Proceedings of the IEEE International Conference on Advanced Intelligent Mechatronics AIM1999*, pages 311–316, Atlanta (GA), US, 1999.

[115] L.F. Penin. Teleoperation with Time Delay - a Survey and its Issue in Space Robotics. In *Proceedings of the 6. ESA Workshop on Adv. Space Tech. for Robotics and Automation*, Noordwijk, The Netherlands, 2000.

[116] D. E. Quevedo, G. C. Goodwin, and J. S. Welsh. Design Issues arising in a Networked Control System Architecture. In *Proceedings of the International Conference on Control Applications*, pages 450–455, Taipei,Taiwan, 2004.

[117] R.Adams and B. Hannaford. A Two-Port Framework for the Design of Unconditionally Stable Haptic Interfaces,. In *Proceedings of the International Workshop on Intelligent Robots and Systems IROS*, pages 1254–59, Victoria, Canada, 1998.

[118] G.J. Raju, G.C. Verghese, and T.B. Sheridan. Design Issues in 2-Port Network Models of Bilateral Remote Teleoperation. In *Proceedings of the IEEE International Conference on Robotics and Automation*, pages 1317–1321, Scottsdale (AZ), US, 1989.

[119] H.E. Ross and A.J. Benson. The Weber Fraction for the Moment of Inertia. *Fechner Day 86, International Society for Psychophysics*, pages 71–76, 1986.

[120] H.E. Ross and E.E. Brodie. Weber Fractions for Weight and Mass as a Function of Stimulus Intensity. *Q.J. of Exp. Psych. [A]*, 39:77–88, 1987.

[121] S. Sahu, P. Nain, D. Towsley, C. Diot, and V. Firoiu. On Achievable Service Differentiation with Token Bucket Marking for TCP. In *Proceedings of the ACM SIGMETRICS*, Santa Clara (CA), US, 2000.

[122] S.E. Salcudean. Control for Teleoperation and Haptic Interfaces. In B. Siciliano and K.P. Valavanis, editors, *Lecture Notes in Control and Information Sciences 230: Control Problems in Robotics and Automation*, pages 51–66. Springer, London, 1998.

[123] H. Sanneck, L. Le, and A. Wolisz. Intra-Flow Loss Recovery and Control for VoIP. In *Proceedings of ACM Multimedia*, Ottawa, Canada, 2001.

[124] R. Schuster. *Evaluation of Qualify-of-Service-Parameter Control in Haptic Telepresence Systems*. Bachelor thesis supervised by S. Hirche, Institute of Automatic Control Engineering, Technische Universität München, 2005.

[125] C. Secchi, S. Stramigioli, and C. Fantuzzi. Dealing with Unreliabilities in Digital Passive Geometric Telemanipulation. In *Proceedings of the IEEE/RSJ International Conference on Intelligent Robots and Systems IROS*, Las Vegas (NV), US, 2003.

[126] C. Secchi, S. Stramigioli, and C. Fantuzzi. Digital Passive Geometric Telemanipulation. In *Proceedings of the IEEE International Conference on Robotics and Automation ICRA'03*, Taipei, Taiwan, 2003.

[127] S. Shenker and J. Wroclawski. General Characterization Parameters for Integrated Service Network Elements. *IETF RFC 2215*, September 1997.

[128] T.B. Sheridan. Telerobotics. *Automatica*, 25(4):487–507, 1989.

[129] T.B. Sheridan. *Telerobotics, Automation, and Human Supervisory Control*. MIT Press, Cambridge, Massachusetts, 1992.

[130] T.B. Sheridan. Space Teleoperation Through Time Delay: Review and Prognosis. *IEEE Transactions on Robotics and Automation*, 9(5):592–606, 1993.

[131] M. Sitti and H. Hashimoto. Tele-Nanorobotics using Atomic Force Microscope. In *Proceedings of the IEEE/RSJ International Conference on Intelligent Robots and Systems IROS*, pages 1739–1746, Victoria, Canada, 1998.

[132] J.-J.E. Slotine and W. Li. *Applied Nonlinear Control*. Prentice Hall, 1991.

[133] B. Stanczyk, S. Hirche, and M. Buss. Telemanipulation over the Internet: a Tele-Assembly Experiment. In *Proceedings of the IEEE International Conference on Mechatronics and Robotics, MechRob2004*, pages 315–320, Aachen, Germany, 2004.

[134] Kay M. Stanney. *Handbook of Virtual Environments*. Lawrence Erlbaum Associates, 2002.

[135] S. Stramigioli. *Modeling and IPC Control of Interactive Mechanical Systems: a coordinate free approach*. Springer, London, 2001.

[136] S. Stramigioli. About the Use of Port Concepts for Passive Geometric Telemanipulation with Time Varying Delays. In *Proceedings of the 8. Mechatronics Forum*, pages 944–953, Enschede, The Netherlands, 2002.

[137] S. Stramigioli, C. Secchi, A.J. van der Schaft, and C. Fantuzzi. A Novel Theory for Sample Data System Passivity. In *Proceedings of the IEEE/RSJ International Conference on Intelligent Robots and Systems IROS*, pages 1936–1941, Lausanne, Switzerland, 2002.

[138] S. Stramigioli, A.J. van der Schaft, B. Maschke, and C. Melchiorri. Geometric Scattering in Robotic Telemanipulation. *IEEE Transactions on Robotics and Automation*, 18:4, 2002.

[139] Durlach N.I. Beauregard G.L. Tan, H. Z. and M. A. Srinivasan. Manual Discrimination of Compliance Using Active Pinch Grasp: The Role of Force and Work Cues. *Perception and Psychophysics*, 57:495–510, 1995.

[140] H. Z. Tan, N.I. Durlach, Y. Shao, and M. Wei. Manual Resolution Compliance When Work and Force Cues are Minimized. *ASME Advances in Robotics*, 42:13–18, 1992.

[141] Srinivasan M. A. Eberman B. Tan, H. Z. and B. Cheng. Human Factors for the Design of Force-Reflecting Haptic Interfaces. *ASME Dynamic Systems and Control Division*, 1:353–359, 1994.

[142] P.L. Tang and C.W. de Silva. Ethernet-based Predictive Control of an Industrial Hydraulic Machine. In *Proceedings of the 42nd IEEE Conference on Decision and Control CDC'03*, pages 695–700, Maui (HW), US, 2003.

[143] N.A. Tanner and G. Niemeyer. Practical Limitations of Wave Variable Controller in Teleoperation. In *Proceedings of the IEEE Conference on Robotics, Automation, and Mechatronics*, pages 25–30, New Orleans (LA), US, 2004.

[144] N.A. Tanner and G. Niemeyer. Improving Perception in Time Delayed Teloperation. In *Proceedings of the IEEE International Conference on Robotics and Automation*, pages 356–361, Barcelona, Spain, 2005.

[145] Y. Tipsuwan and M.Y. Chow. Control Methodologies in Networked Control Sytems. *Control Engineering Practice*, 11:1099–1111, 2003.

[146] M. Ueberle, N. Mock, and M. Buss. ViSHaRD10, a Novel Hyper-Redundant Haptic Interface. In *Proceedings of the 12th International Symposium on Haptic Interfaces for Virtual Environment and Teleoperator Systems, in conjunction with IEEE Virtual Reality 2004 conference*, Chicago (IL), US, 2004.

[147] M. Ueberle, N. Mock, A. Peer, and M. Buss. Design, Control, and Performance Evaluation of a Hyper-Redundant Haptic Device. *IEEE Transactions on Visualization and Computer Graphics,* Special Issue on Haptics, Virtual and Augmented Reality, 2005, *under review.*

[148] A.J. van der Schaft. *L2-Gain and Passivity Techniques in Nonlinear Control.* Springer, Communication and Control Engineering Series, 2000.

[149] J. Vertut, A. Micaelli, P. Marchal, and J. Guittet. Short Transmission Delay on a Force Reflective Bilateral Manipulator. In *Proceedings of the 4th Rom-An-Sy*, pages 269–274, Zaborow, Poland, 1981.

[150] G.C. Walsh, Hong Ye, and L. Bushnell. Stability Analysis of Networked Control systems. In *Proceedings of the American Control Conference*, pages 2876–2880, San Diego (CA), US, 1999.

[151] Q.P. Wang, D.L. Tan, N. Xi, and Y.C. Wang. The Control Oriented QoS: Analysis and Prediction. In *Proceedings of the IEEE International Conference on Robotics and Automation*, pages 1897–1902, Seoul, Korea, 2001.

[152] Q.P. Wang, D.L. Tan, N. Xi, and Y.C. Wang. Improving Efficiency of Internet Based Teleoperation using Network QoS. In *Proceedings of the IEEE International Conference on Robotics and Automation*, pages 2707–2712, Washington (DC), US, 2002.

[153] X. Wang, P.X. Liu, D. Wang, B. Chebbi, and M. Meng. Design of Bilateral Teleoperators for Soft Environments with Adaptive Environmental Impedance Estimation. In *Proceedings of the IEEE International Conference on Robotics and Automation*, pages 1139–1144, Barcelona, Spain, 2005.

[154] E. H. Weber. *Die Lehre vom Tastsinn und Gemeingefühl, auf Versuche gegründet.* Vieweg, Braunschweig, 1851.

[155] Z. Wei, M. Branicky, and S. Phillips. Stability of Networked Control Systems. *IEEE Control Systems Magazine*, 21(1):84–99, February 2001.

[156] P. P. White. RSVP and Integrated Services in the Internet: A Tutorial. *IEEE Communications Magazine*, pages 100–106, May 1997.

[157] J.C. Willems. Dissipative Dynamical Systems, Part 1: General Theory. *Archive for Rational Mechanics and Analysis*, 45:321–351, 1972.

[158] J. Wroclawski. Specification of the Control-Load Network Element Service. *IETF RFC 2211*, September 1997.

[159] N. Xi and T.J. Tarn. Action Synchronization and Control of Internet Based Telerobotic Systems. In *Proceedings of the IEEE International Conference on Robotics and Automation*, pages 219–224, Detroit (MI), US, 1999.

[160] Y. Yokokohji, T. Imaida, and T. Yoshikawa. Bilateral Control with Energy Balance Monitoring under Time-Varying Communication Delay. In *Proceedings of the IEEE International Conference on Robotics and Automation*, pages 2684–2689, San Francisco (CA), US, 2000.

[161] Y. Yokokohji, T. Tsujioka, and T. Yoshikawa. Bilateral Control with Time-Varying Delay including Communication Blackout. In *Proceedings of the 10th Symposium on Haptic Interfaces for Virtual Environment and Teleoperator Systems*, Orlando (FL), US, 2002.

[162] Y. Yokokohji and T. Yoshikawa. Bilateral Control of Master-Slave Manipulators for Ideal Kinesthetic Coupling Formulation and Experiment. *IEEE Transactions on Robotics and Automation*, 10(5):605–619, 1994.

[163] W.H. Zhu and S.E. Salcudean. Stability Guaranteed Teleoperation: An Adaptive Motion/Force Control Approach. *IEEE Transactions on Robotics and Automation*, 8(2):176–185, 1992.

[164] W.H. Zhu and S.E. Salcudean. Teleoperation with Adaptive Motion/Force Control. In *Proceedings of the IEEE International Conference on Robotics and Automation*, pages 231–237, Detroit (MI), US, 1999.